Examining the effect of immunity on infection dynamics at the host, population, and multi-population levels

by

Bryan T. Mayer

A dissertation submitted in partial fulfillment
of the requirements for the degree of
Doctor of Philosophy
(Epidemiological Science)
in The University of Michigan
2013

Doctoral Committee:

Associate Professor Joseph N. S. Eisenberg, Chair
Associate Professor Allison E. Aiello
Associate Professor Edward L. Ionides
Professor James S. Koopman

For my parents, John and Pam. Thanks for your continuous support and encouragement.

ACKNOWLEDGEMENTS

I want to thank my committee and advisors for their contributions to this work. Thanks to Joe and Jim for accepting me as an epidemiology PhD student, funding me, and introducing me to dynamic models. I thank Joe specifically for being my mentor through these years and helping me develop as a researcher, writer, and scientist. I thank Jim for his enthusiasm and perspective in helping me develop as a scientist, and particularly for getting me involved in polio eradication research. I thank Ed for collaborating with me on my projects; his knowledge and input were crucial to my research. I thank Allison for her insight into the public health aspects of my research and generating excellent discussions at our committee gatherings.

I thank the Center for Advancing Microbial Risk Assessment (CAMRA) for funding most of my PhD career. I thank Professor Ana Baylin for hiring me as a GSI, it was a pleasure working with her and being a part of her course. I thank the collective group of students who put together a nice LaTeX template for me to use. I would also like to thank Michigan State faculty members who inspired me along the way: Ronald Fintushel for suggesting I become a math major; Robert Shelton for his contributions to my development as a writer; and Joel Shapiro for his patience and supporting my decision to pursue a graduate degree in Biostatistics. I am thankful for the MSU basketball program for providing a much needed distraction every March and April.

Last but certainly not least, thanks to my friends and family, who were invaluable to the completion of my dissertation. I am indebted to my academic peers and friends who spent their time listening to my research, discussing my ideas, editing my work

(edit club), and doing fun things too: Doug, Erin, Ethan, Ian, Grant, Ludi, Maria, and Meghan. I would also like to thank my amazing friends for being there for me for as long as I can remember, I'm not sure where I would be without them: Gabe, Nathan, Scott, and Steve. I would like to thank Pinery and the Pinery people for being my summer getaway. I thank my musical friends for helping to enrich my life: Danielle, Eric, Erin, John, JP, and Megan (and Jameson). I thank my grandparents for the periodic greeting cards, "goody bags," and their love. I thank my Uncles Curt and Steve for their support along the way. I thank my sister, Laurie; I am sorry I forgot to acknowledge her at my defense and I am sure she is sorry about her yawn.

My biggest thanks goes to my parents, John and Pam, and my partner, Erin, for their endless support and love. My parents' infinite encouragement always pushed me further. Erin's contributions (and patience) regarding my research, writing, and life cannot be properly enumerated and is a testament to the amazing human being that she is. Thanks again to everyone I've encountered along the way for inspiring and shaping me.

TABLE OF CONTENTS

LIST OF FIGURES

Figure

LIST OF TABLES

Table

LIST OF APPENDICES

Appendix

LIST OF ABBREVIATIONS

AFP acute flaccid paralysis

cVDPV circulating vaccine-derived polioviruses

GPEI Global Polio Eradication Initiative

IAH independent action hypothesis

IPV inactivated polio vaccine

MLE maximum likelihood estimate

mOPV monovalent oral polio vaccine

OPV oral polio vaccine

SIAs supplementary immunization activities

SIR susceptible-infected-recovered

SIRS susceptible-infected-recovered-susceptible

SIS susceptible-infected-susceptible

tOPV trivalent oral polio vaccine

WPV wild polio virus

ABSTRACT

Examining the effect of immunity on infection dynamics at the host, population, and multi-population levels

by

Bryan T. Mayer

Chair: Joseph N. S. Eisenberg

Dynamic modeling is an important tool for informing public health decisions. In this dissertation, we explored the role of host immunity in infection transmission models at the host, population, and multi-population level. We applied these models to two pathogen systems: 1) anthrax infection at the host level and 2) polio transmission at the population and multi-population level.

At the host level, dose-response models are used to characterize the risk of infection given a pathogen exposure and are one of the primary tools for risk assessments. These models are generally static assuming invariant risk over time. However, if the temporal response of the immune system to pathogen exposures is of the same time scale as the temporal patterns of exposure then delivering a dose over a short time span may result in a higher risk than if that same dose was delivered over a longer time span. To explore the implications of such an immune response, we developed a dose-response model that incorporates the immune response to pathogen exposures and thereby allows risk calculations to be dependent on exposure patterns that vary over time. We then applied our model to an anthrax system using survival analysis.

Our analysis indicated that the risk of anthrax is invariant to exposure patterns. Although the anthrax data set did not reveal a dose timing pattern of risk, more variable exposure data is needed to fully evaluate this process. We recommend that future dose-response experiments incorporate variable temporal patterns of exposure to assess if risk of infection is affected by temporally variant exposures.

At the population level, transmission models elucidate dynamic infection processes and provide a framework to analyze intervention effectiveness. In the context of polio eradication, childhood vaccination with oral polio vaccine (OPV) has been the key intervention to achieve elimination. Final eradication, however, has been elusive and a better understanding of polio transmission dynamics is important to elucidate underlying difficulties. It is possible that waning immunity may play an important role in polio persistence. We developed a model of polio transmission that incorporates vaccine strain transmission and waning immunity to assess the successes and failures of the polio eradication campaign. We demonstrated that short-term success through vaccination policy is possible under diverse transmission conditions. However, long-term success may be difficult due to reinfection transmission dynamics attributable to waning immunity. Increased vaccine strain transmission mitigates the influence of reinfection by boosting immunity but cannot necessarily be relied upon due to risk of disease caused by circulating OPV. Therefore, for highly transmissive regions, additional interventions may be appropriate such as boosters in older populations or improved sanitary conditions.

Another reason that may make final eradication difficult is that at the multi-population level, vaccination policies may have effects across population groups. Therefore, we extended our polio transmission model to include migration across populations. Our analysis demonstrated that if vaccination coverage lapses in one population, it may be detrimental to the vaccination programs in neighboring populations. This is exemplified when migration comes from populations with high trans-

mission levels. Thus eradication strategies should account for the induced immunity of the disease, particularly where coverage of migratory populations may be crucial to achieving elimination in the remaining endemic regions. This work demonstrated that the eradication campaign is a global effort and success depends on properly targeting connected populations.

CHAPTER I

Introduction

1.1 Background and Motivation

Traditional transmission models have incorporated the role of host immunity in infectious disease transmission in a variety of ways. However, many of these approaches make simplifying assumptions regarding the nature of these processes. For example, a susceptible-infected-recovered (SIR) model assumes that all infected individuals recover into a recovered state described by complete immunity to future infections. However, immunity is seldom complete or lifelong. An individual's immune response may vary over time, where their immunity is strong initially after infection but wanes over time. Furthermore, host immunity describes a complex system important at various stages of the infection process. At the time of exposure, the immune system aims to prevent a pathogen from replicating and initiating infection. When infection occurs, the immune system then works to remove the pathogen determining how contagious individuals are and how long infection lasts. Additionally, the effectiveness of these defenses may vary depending on past exposures. Population contact with pathogens is a complicated process where characterizing meaningful exposures requires understanding the interaction between pathogens and the immune system. These host immunity properties are important at the population level where infectious contacts occur between individuals. Those with higher immunity levels will partici-

pate less in population transmission where they are less likely to get infected and will have a faster resolution of infection. To take advantage of these properties, interventions are designed induce immunity and reduce population transmission. However, in the context of connected populations, the intervention policies in one population may affect another. We aim to understanding how host immunity affects infection dynamics across these resolutions: the host, population, and multi-population levels.

Initially, we focus on the effect of immunity on risk of infection at the host level. The ability of the immune system to prevent a pathogen from initiating infection may depend on the nature of the exposure. For example, a large, immediate exposure through a sneeze may elicit a different risk of infection than an equivalent exposure inhaled slowly over time from contaminated air. If the immune response is more efficient at eliminating small quantities of pathogens, the large, immediate exposure might elicit a higher risk of infection. Therefore, the dynamic nature of the immune system may be an important factor determining risk of infection, specifically where different routes of transmissions result in varying temporal exposure patterns. To account for this, we developed a dynamic dose-response model incorporating the immune response in chapter II. We applied our model to a risk assessment framework in the anthrax disease system.

To incorporate host immunity into population models, we considered immunity as it affects susceptibility to infection, and how it affects contagiousness and duration if an infection occurs. Host immunity varies depending on the time since last infection. In contrast to the SIR model framework, complete immunity is not permanent but the first level in a series of stages where immunity is waning over time. We applied this framework to a polio transmission system. Polio eradication is in its final stage; and at this stage, immunity and cross population dynamics may play an important role in transmission dynamics. In chapter III, we developed a polio transmission model incorporating waning immunity and vaccine transmission. In chapter IV, we extended

this polio transmission model to include migration across heterogeneous populations. Here, elimination success may be affected by migration due to the interaction of waning immunity and varying vaccination policy across populations.

1.2 Dynamic modeling of infectious diseases with immunity

1.2.1 Dose-response modeling at the host level

1.2.1.1 Contemporary dose-response models

In chapter II, we developed a dose-response model in the anthrax disease system. The role of dose-response models is to characterize the risk of infection given a pathogen exposure. Dose-response models are used extensively in risk assessment where risk of infection can be readily calculated for different exposure scenarios [1–3]. Currently, these models are also implemented in environmental transmission models where pathogens exposures mediated through the environment are assigned probabilities based on dose-response models [4].

The classic dose-response models used for microbial risk assessment are the exponential and beta-poisson distributional models [2]. These models were developed under the independent action hypothesis (IAH) assumption that any individual pathogen unit has a non-zero independent risk of initiating infection. The development of exponential model is the most simplistic realization of the IAH. It is derived by assuming that pathogens from an exposure arrive as a Poisson process with an expected value equivalent to the total measured dose size. Further, each pathogen has an independent survival risk, k. The integration of the joint probability of pathogen arrival and pathogen survival (assumed to be independent distributions) at given expected dose size yields an exponential distribution with risk parameter, k [2]. Using any single input dose and a known k risk parameter, a probability of infection can then be calculated. Furthermore, the exponential model allows risk extrapolations

(with mechanistic justification) for very small dose sizes which are difficult to elucidate experimentally. Low dose exposures are relevant to a variety of scenarios and risk due to single pathogens has been directly observed for influenza Type A and intravenous salmonella [5–7].

In the exponential model, we assume that the risk parameter k is a fixed value. This assumption is relaxed in the beta-Poisson model, where the risk is assumed to be a distribution that represents variability in the population. To derive this model, k is assumed to have the beta distribution. By integrating the joint pathogen arrival and survival distributions as before, we find a mixture distribution that represents the beta-Poisson dose-response model. By allowing non-constant risk per pathogen, this two parameter statistical distribution is more flexible at the extremes and can elicit dose-risk curves that are less steep than the usual exponential models. These models, however, were developed in a static framework where the risk of infection is independent of the timing of doses.

1.2.1.2 Limitations of static, time-independent dose-response models

The beta-Poisson and exponential models are time-independent models, limiting their ability to account for the dynamic effects of the immune system. Particularly, in the exponential model, infection risk from each pathogen is independent of the time course they are given, *i.e.*, the overall risk for a total pathogen level is constant for every exposure pattern. To illustrate the implications of this assumption, consider an extreme example of an exposure of 50 pathogens instantaneously versus 50 exposures of a single pathogen separated by a week each. In the exponential model, the overall risk calculated would be equivalent for each scenario. This approach assumes the effect of host clearance mechanisms on the elimination of pathogens is a constant process. However, this may not be true. For example, the immune system might be very efficient at eliminating low doses of pathogen but less efficient as the total

pathogen level increases. This would allow higher doses to persist longer in the host than a series of smaller doses and thus correspond to higher potential for infection to initiate.

Few studies have taken into account the importance of exposure patterns and dose-timing. This trend, however, is slowly changing first by incorporating modeling time post inoculation [8–10]; however, still lacking are risk data where subjects are exposed to varying exposure patterns in experimental settings. To justify and analyze these experiments, dose-response models will need to account for time-dependent risk. The dynamic dose-response model we developed in chapter II provides framework to design and analyze experiments utilizing time-dependent exposure patterns.

A more biologically motivated dose-response model was previously proposed by Pujol *et al.* in 2009 [10]. In this model, innate immune effector particles and pathogens are modeled in a stochastic competition framework capturing both the growth of pathogens and diminishing immune response. The model we presented in chapter II is computationally less intensive than the model in Pujol *et al.* and therefore more suitable for integration into a transmission model.

1.2.2 Transmission modeling at the single and multiple population level

1.2.2.1 Overview of polio transmission model

In chapters III and IV, we develop a transmission model that assesses the population dynamics of polio transmission under varying conditions. Our model was designed to incorporate specific characteristics of polio transmission and the eradication campaign. These factors include waning immunity, vaccination programs with multiple boosters per year, the transmission of OPV, and the interaction of multiple populations. The background for the transmission model framework is described in sections 1.2.2.2–1.2.2.5 and the specific construction of the polio transmission model is described in chapters III and IV.

1.2.2.2 Transmission model framework assumptions

We utilized a deterministic, compartmental model framework. Compartmental transmission models are structured systems that allow for the dynamics of disease transmission to be mathematically explored over time using differential equations. The important assumptions of deterministic, continuous model are that the population size is infinite and that population distributions are continuous. These assumptions represent simplistic realizations of transmission systems but allow for clear interpretation and flexibility in structures. The use of transmission models to simulate real world systems allows epidemiologists to assess the effect of potential interventions.

Classic transmission models can take fairly simplistic forms [11]. For example, a susceptible-infected-susceptible (SIS) model is a two compartment model where populations are either infected or susceptible. In this model, infection does not result in immunity. This assumption may be appropriate if the disease confers no immunity. Immunity can be added to the framework by employing a SIR structure where infection resolves into a recovered state where there is full immunity. This extension may be appropriate for short-term epidemic analysis or for diseases that induce long-term immunity (*e.g.,* smallpox).

1.2.2.3 Model selection for waning immunity

In polio transmission, immunity to infection is not permanent [12–14], so we employ a model structure that accommodates for partial and temporary immunity in the susceptible population. When immunity is not life-long, reinfection dynamics become an important component of transmission. This is especially relevant in the context of interventions. An analysis of reinfection dynamics indicate a distinct reinfection threshold at certain R_0 levels [15]. When transmission conditions are below this threshold, interventions are particularly effective. However, above this threshold, interventions become less effective and reinfection dynamics induce rebound epidemics.

Our transmission structure is based on assumptions that are somewhere between the two most extreme assumptions regarding immunity: 1) that infection results in no immunity (SIS model) or 2) infection results in full and permanent immunity (SIR model). One simple way to relax the assumption of full immunity is to use a susceptible-infected-recovered-susceptible (SIRS) model where recovered individuals eventually become susceptible again. This implies that a given individual has either complete immunity or complete susceptibility to infection. Given knowledge about adaptive immunity, this may be a oversimplification of the underlying biology that could affect model inferences. In chapters III and IV, we expand the SIRS model to include partial levels of immunity between recovered and fully susceptible. Specifically, in chapter III, we developed a framework for employing waning immunity in transmission modeling.

1.2.2.4 Model selection for vaccination and vaccine transmission

Because vaccination is the most important intervention for reducing polio transmission, we included a vaccination rate into our transmission model. The implementation of vaccination rates in transmission models has been extensively studied [11]. Generally, vaccination rates (particularly childhood vaccination) are modeled such that a proportion of new births are immediately vaccinated. Under waning immunity framework, employing birthrate vaccination may reduce prevalence to low levels but sustained transmission remains possible as population immunity wanes over time [16]. Therefore, for vaccination to be successful without permanent immunity, boosting may be required. In the polio eradication campaign, children may be vaccinated many times per year [17]. To allow for boosting, we applied the vaccination rate directly on an age-structured susceptible population to allow for multiple vaccinations per child.

Because it is a live virus, OPV is transmissible through the same routes as wild po-

liovirus [18]. OPV, therefore, can vaccinate populations and boost immunity through transmission processes. To incorporate vaccine strain transmission, we employ a model structure including infection due to OPV in chapters III and IV. Because the infection course of OPV is similar to wild polio virus (WPV) but attenuated in terms of duration and shedding [18], we utilized a similar transmission structure for both OPV and WPV.

1.2.2.5 Multiple population models

The effect of vaccination programs is not necessarily isolated to a single population. Populations are in constant flux and thus the policies in one region may affect the policies in another depending on their relationship. In chapter III we introduced key components of polio transmission: the waning of immunity and the transmission of OPV. Under conditions of waning immunity and vaccine transmission, the effect of migration on vaccination success may be affected by populations with partial immunity or OPV infection. We therefore expand the single population polio transmission model to multiple populations in chapter IV.

There are many formulations of spatially connected, multiple population transmission models [11]. In classical metapopulation models, the interaction between populations is constructed where the populations influence each other but are separated. This is generally realized by using a weighted force of infection where the connected populations are coupled depending on their spatial or social relationship. The abstract assumption regarding population interaction is relaxed in mechanistic metapopulation models [19, 20]. In these models, explicit population movement is modeled where a proportion of each population migrates to the other population where it remains temporarily contributing to the transmission process before returning. Keeling & Rohani [19] explored parameter conditions under which the classical and mechanistic metapopulaton models are equivalent. Specifically, they derived the

equivalence between the coupling parameters of the "phenomenological" model and the movement parameters of the mechanistic model demonstrating the relationship is disease dependent.

Multi-population models have been used to study the effect of vaccination across populations [21–25]. The interaction between connected populations have potentially important effects on vaccination programs in each subpopulation. Specifically, optimal overall vaccination strategies depend on the relationship between connected populations. May & Anderson [21] relaxed the assumption of homogeneous population mixing by allowing heterogeneous populations to interact in a classical metapopulation framework. They demonstrated that, when heterogeneous mixing is assumed between connected populations, lower total vaccination rates are required to reach elimination when the subpopulations with the highest contact rates are the focus of intervention. However, an extension of this model showed that targeting populations with the highest levels of interaction may be more important as demonstrated by regional difficulties in smallpox eradication [22]. A recent transmission model utilizing explicit migration and vaccination intervention indicated that in an SIR model with fully coupled migration, vaccination rates in one population could be used to benefit the other [25].

In the polio endemic regions, migration is an important demographic feature. The types of migration in Afghanistan, Pakistan, and Nigeria vary (*e.g.*, rural/urban, seasonal, refugees, etc.) but vaccination rates are lower in migratory populations [26–28]. Recent success in India has been partially attributed to stronger focus on migratory families [29] where lower vaccination rates were previously observed in rural migrants in northern India [30]. A general population migration structure relevant to polio transmission is depicted in figure 1.1.

To assess the effect of under-vaccinated migratory populations on a given population, the model presented in chapter IV utilizes unidirectional migration. In figure

1.1, this would be described by having no return arrow to the source population and instant integration of migrants into the destination population. Unidirectional population movement implies that vaccination or transmission conditions in the destination population cannot affect the source population. This might describe rural-urban migration where migrants are unlikely to return to their home regions. This approach can also be interpreted abstractly, where the source population represents an aggregate of migratory populations that come from different transmission or vaccination conditions. In either interpretation, we would not expect policies in the destination population to affect people in the source population.

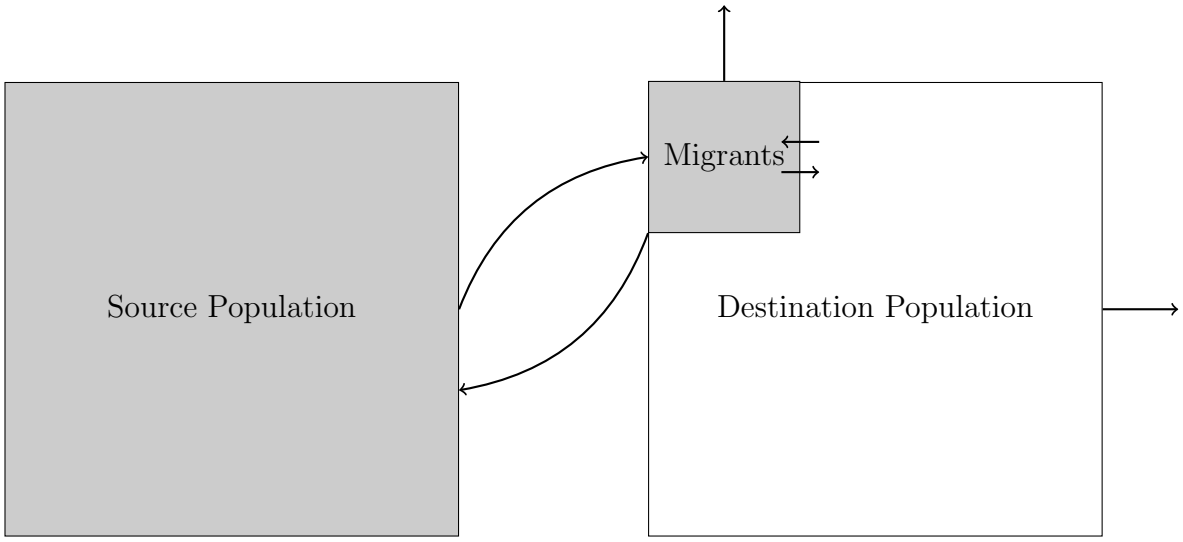

Figure 1.1: A general population migration structure. Individuals from a source population explicitly move to a destination population, where they could stay but remain separated, migrate to another population, integrate with the destination population, or return home. Transmission depends on the relationship between the migrants and the destination population and how the pathogen is transmitted. For example, a refugee model might be structured such that migrants and the destination population are partitioned and transmission occurs through preferential mixing. A rural/urban migration model might be structured such that populations from source rural areas migrate and then integrate quickly into the urban destination population where return rates are low.

1.3 Immunity and pathogen background

1.3.1 Background on biology of the immune system

Our analysis focused on the efficiency of the immune system in preventing infection and attenuating future infections. While certain aspects of the immune system were not specifically modeled, it is important to understand the underlying biology of the human immune system and immune response. The human immune system is a biological system designed to detect and prevent disease [31]. It targets a wide range of pathogenic organisms, viruses, and tumor cells. The immune system is generally broken into two categories, the innate and adaptive immune system. The innate immune system is considered the first line of defense characterized as fast but not very specific. The adaptive immune system is much slower to respond but is much more specific to the type of infection. However, components from both work together in response to potential infection or disease. The immune system is characterized by its ability to discriminate between host cells and foreign cells, maintain memory of past infections, and coordinate specific responses to specific pathogens.

In chapter II, we built a dynamic dose-response model incorporating the effects of the innate immune system. Furthermore, the innate immune response is important to the anthrax infection process. The innate immune system is characterized by very a fast but non-specific response [32] drive by three important cell types: macrophages, dendritic cells, and natural killer (NK) cells. Macrophages circulate in the peripheral blood system and function by ingesting pathogenic agents and then chemically eliminating them [31]. To identify potential threats, macrophage and dendritic cells carry receptors called pattern recognition receptors. These cells are crucial for recognition, memory, and continued protection against encountered antigens [32].

In chapters III and IV, our analysis focused on polio transmission and vaccination in the context of waning immunity. Immunity against polio infection is mostly de-

scribed by the adaptive system, which is characterized by a highly specified but slow response to infection. One important job of the innate immune system is to hold off infection long enough so the adaptive immune response can be activated. The cells of the adaptive immune system are lymphocytes; specifically T cells and B cells.

Plasma cells (mature B cells) are lymphocytes primarily associated with the humoral immune response with the primary job of secreting antibodies [31]. Antibodies combine with other immune effectors to more efficiently eliminate an infection. The effect of antibodies on pathogenic particles and cells is the defining feature of the humoral immune system. The classic pathway complement system is characterized by immunoglobulins aiding immune cells in the elimination of pathogenic cells through phagocytosis or direct lysis. Antibody classes IgG and IgM bind to antigenic structures and form complexes that are more easily eliminated by immune cells. IgA, an antibody associated with mucosal immunity, does not strongly induce the complement system but prevents pathogens from replicating.

The immune system response varies by type of pathogen encountered where some responses are more efficient than others. In the context of anthrax and polio, there are differences in how the immune system responds and how it contributes to disease. Anthrax symptoms stem from damage caused to cells by the use of exo-toxins and encapsulation [33]. Poliovirus replicates at the naso-pharyngeal exposure site and eventually travels to the gastrointestinal tract causing sub-clinical infection [34]. Both pathogens are able to disseminate. Poliovirus causes poliomyelitis when it invades the nervous system while *B. anthracis* can cause severe disease at infection site and through dissemination in the lymph system.

1.3.2 Biological characteristics of *Bacillus anthracis* and disease

1.3.2.1 Background on anthrax

Bacillus anthracis and anthrax were the focus of the dose-response model built in Chapter II. Anthrax is a disease that manifests differently depending on the location of exposure. Infection can occur on the skin, in the respiratory system, or in the gastrointestinal tract. The causative agent of anthrax is the spore-forming bacteria *Bacillus anthracis*. *B. anthracis* is a very resilient pathogenic bacteria that can live in soil and generally infects herbivores. Human exposure of anthrax generally occurs upon contact with spores in the environment. Spores are not generally transmitted person to person [33, 35].

Bacillus anthracis is a gram positive, spore-forming, rod-shaped bacterium that can cause extracellular infection in animal hosts. It is the most lethal and pathogenic species of the *Bacillus* family. Spore formation in aerobic bacteria is a unique characteristic of the *Bacillus* family[36]. The endospores created by the bacteria are highly resistant to harsh environmental conditions and may persist for very long periods of time (decades) in soil. Spore formation occurs when harsh environmental cues and oxygen are detected. *B. anthracis* is also capable of producing a poly-glutamate capsule to resist phagocytosis from macrophages [33].

A spore may remain in the lungs for weeks before infection occurs [37]. *B. anthracis* releases two powerful and lethal exo-toxins, lethal toxin and edema toxin, which contribute to severe damage to the lungs tissue and cells. Symptoms begin to manifest as the classic flu-like symptoms such as malaise and fever. Disease may then quickly progress to respiratory distress, cyanosis, massive edema, and potentially death [36]. Dissemination of the bacteria into the lymph system may also lead to bacteremia and toxemia which is characteristic of severe and potentially fatal disease. Due to the lethality of the toxins, proper antibiotic may still be ineffective in

prevention of respiratory failure and ultimately death [33].

1.3.2.2 Process of infection and immune response for anthrax infection

While the sites of infection result in different symptoms, the process of infections for cutaneous anthrax and inhalation anthrax are similar. Pathogenesis in the lungs results in lung tissue damage and symptoms of pneumonia while pathogenesis for skin infection is described by the progression of the lesion [33]. In an exposed host, the bacterial spores begin germinating in both extracellular locations and within macrophages. Replicating bacteria excrete toxins and form capsules that primarily affect macrophages. The use of a polyglutamate capsule prevents macrophages from using phagocytosis to destroy the pathogen and it is just one of its methods for evading immune response .

The major source of anthrax symptoms are caused by cell damage due to exotoxins. To be pathogenic, the edema factor and lethal factor must combine with the protective antigen to form the respective toxins. Protective antigen creates channels on host cell membranes and thus allows the lethal factor and edema factor to enter the cell and cause damage. Lethal toxin causes protein degradation in macrophages, which leads to apoptosis and necrosis within 2 hours [35]. Action of the toxin on the surrounding tissue will also lead to necrosis. It is also believed that the two toxins work together in inhibiting cytokine release from macrophages [38]. Specifically, both inhibit the release of TNF-α which greatly hinders the ability of the innate immune system to mount a defense against the infection. Furthermore, edema toxin is shown to inhibit the cytokine IL-12 which is crucial to both innate recruitment and activation of Th1 cells to mediate an adaptive response [38]. Edema toxin works by increasing intracellular cyclic AMP (cAMP)[39]. In macrophages, this disrupts the release of a variety of cytokines and results in an inflammatory response described by over swelling, or edema. The use of these two toxins on macrophages explains why the

immune system rarely develops an effective adaptive response.

A major complication of anthrax infection is the dissemination of the pathogen into the lymph system and then throughout the body. When macrophages ingest anthrax spores they generally are able to eliminate the spore using phagocytosis. In some instances, the macrophage is lysed and the bacteria escape to replicate. However, in another possibility, the spores survive, germinate, and then replicate in a vegetative form in the macrophages [40]. Once transported to a lymph node, the bacteria are capable of releasing toxin and lysing the macrophage. The bacteria may then infect the lymph node and use the lymph system to spread throughout the body where the toxins can cause systematic damage resulting in very severe or fatal disease.

1.3.2.3 Public health threat of anthrax attacks

In Chapter II, we constructed a dose-response model and analyzed anthrax infection data. Because anthrax is not transmitted person-to-person, it is not generally considered a natural infectious disease threat. Before the 2001 release, no case had occurred in the United States in 25 years and the last major world outbreak occurred in 1979 due to a major contamination leak event from a Soviet Union biological weapons plant [41]. Due to its high virulence as a pneumonic disease, anthrax use as a weapon represents a public health concern. Disease may manifest quickly and present as severe respiratory distress potentially leading to death [36]. Furthermore, proper antibiotic use may still be ineffective in prevention of respiratory failure and ultimately death [33]. As a public health concern, the factors to consider to prepare for and to handle anthrax exposure include risk assessment, cost analysis of treatment prophylaxis, vaccination, and cleanup [42]. In 2001, for example, the decontamination along the trail of exposure totaled over $20 million.

Risk assessment is an important tool to prepare for potential bioterrorism threats [3]. Dose-response models are a key component of these risk assessments because

they quantify differing exposure scenarios into an infection risk calculation. Our dose-response model presented in chapter II accounts for temporally variable exposure patterns whereas previous dose-response models generally use simple exposure assumptions to calculate risk. The model is able to account for varying exposure patterns by incorporating immune system dynamics. Our dynamic dose-response model is thus a versatile tool that can implemented in more complicated risk assessments where exposure patterns may be important.

1.3.3 Poliovirus infection and poliomyelitis

1.3.3.1 Epidemiology of poliovirus

In chapters III and IV, we focused on the study of poliovirus and its transmission. Poliomyletis is a viral disease caused by three subtypes of poliovirus, a human enterovirus [43]. Polio transmission occurs through the fecal-oral and oral-oral route. Thus polio is able to transmit extensively in regions with poor sanitation.

Poliovirus is a subtype of enteric viruses which are known to survive in the environment; experiments have shown that poliovirus persists in food, water, soil, and on fomites for prolonged periods of times, ranging from days to weeks [44]. Therefore, human interaction with the environment may be an important component of the transmission process. Because poliovirus is excreted through gastrointestinal routes, proper sanitation measures may reduce exposure through environmental sources.

Poliovirus causes poliomyelitis, a generally asymptomatic gastrointestinal disease [43]. Non-specific symptoms occur in less than 10% of infections. However, a rare and serious complication can occur if poliovirus infection enters the central nervous system and causes neurological disease. In these cases, less than 1% of infections, acute flaccid paralysis (AFP) may occur. AFP is a seriously debilitating illness that can be permanent. Of the poliovirus subtypes, type 1 infection has the highest rate of AFP occurrence.

Poliovirus transmission is controlled worldwide using vaccination. Only three nations, Afghanistan, Nigeria, and Pakistan, still have sustained endemicity while infrequent outbreaks occur in neighboring regions [45]. The use of vaccination has substantially reduced cases of poliomyelitis globally where eradication may soon become a reality [46].

1.3.3.2 Poliovirus infection and immunity

Poliovirus, of genus *enterovirus*, is a positive-sense RNA virus that primarily infects humans [34]. Infection occurs when poliovirus enters the body, generally through the nasopharyngeal route and binds to a specific poliovirus receptor (PVR) on a host cell. Poliovirus is able to then rapidly replicate and spread via bloodstream or lymph system to its primary replication site in the gastrointestinal tract. The virus can replicate and be excreted from the gastrointestinal tract for several weeks. During acute viremia, the virus may potentially enter the central nervous systems and cause aseptic meningitis or AFP through a process called retrograde axonal transport.

Immunity to poliovirus is maintained through antibody secretion. Mucosal immunity is generated through IgA production which may prevent or attenuate infection of the GI tract [34]. Induced serum IgG may prevent future poliovirus viremia. While immunity to paralysis may be lifelong, immunity to infection may wane over time [12–14, 47].

Two vaccine are currently in use: inactivated polio vaccine (inactivated polio vaccine (IPV)) and oral polio vaccine (OPV). Both vaccines induce immunity to paralysis [17] but OPV induces higher protection against future infections [14, 48, 49]. Both OPV and IPV generate serum IgG conversion, likely associated with preventing paralysis, but only OPV induces GI mucosal immunity through IgA production [34]. That is, OPV is more useful to prevent future infection but both vaccines are suitable to prevent against poliomyelitis complications. Therefore, the choice of vaccine depends

on the goal of the intervention. To reduce transmission in endemic nations and regions that are still at risk for infection, OPV is generally employed. The drawback, however, is that OPV strains can be transmitted and cause disease. Therefore, under conditions where polio has been eliminated and infection is unlikely, IPV is employed.

To induce immunity for all three subtypes of WPV, a trivalent oral polio vaccine (tOPV) has been in use during the eradication campaign [48]. The tOPV induced the highest immunity against type 2 WPV [34], which has been eradicated, so recent efforts in India have focused on monovalent oral polio vaccine (mOPV) types 1 and 3 to target the remaining strains [29]. As an attenuated live vaccine, OPV is transmissible which allows for natural population boosting [18]. However, circulating vaccine-derived polioviruses (cVDPV) can also cause paralytic disease and thus cessation of OPV is an important final step in eradication.

1.3.3.3 Global polio eradication

In 1988, the Global Polio Eradication Initiative (GPEI) began a campaign to rid the world of polio. Since the induction of the initiative, there has been global success with significant reduction in transmission worldwide, eradication of type 2 WPV, and elimination of all poliovirus subtypes from all but three nations [46]. However, the final stages of polio eradication have been characterized by prolonged difficulty in reaching the final goal of eradication. Recently achieved success in India has been bittersweet as transmission continues in Afghanistan, Pakistan, and Nigeria. In 2011, an Independent Monitoring Board (IMB) review of the campaign indicted the GPEI with blunt commentary regarding its ineffectiveness in the final stages [50]. The GPEI has since responded and hopes to see improvement by the end of 2012.

Polio eradication has proven difficult in poorer areas of the world, specifically, Afghanistan, Nigeria, Pakistan, and northern areas of India [17]. Although India has managed recent elimination success, polio persists in the other three countries.

While the GPEI works to achieve elimination, previously eliminated nations have experienced periodic outbreaks when coverage slips, specifically in countries bordering Nigeria and Pakistan [45]. To reduce the risk of future outbreaks due to importation, it is of great public health significance to reach eradication as soon as possible.

Previous failure in India has been attributed to many causes, including lack of sanitation, improper vaccination of children, and high transmission conditions [29]. Further, reduced IgG seroconversion rates indicated that competing enteric infections were preventing OPV from inducing an immune response [17]. Despite these conditions, India managed elimination success through a highly vitalized campaign that updated vaccine selection, drastically increased vaccination children rates, and targeted previously hard to reach populations [29]. Persistence in Afghanistan, Nigeria, and Pakistan has been attributed to many causes including population aversion to vaccination [51, 52], failure of governance to adequately ensure vaccination [53] and continuous transmission across borders [46, 54].

After over 20 years of effort to eradicate polio, it may become difficult to sustain these high level public health efforts. Currently, it costs $1 billion per year and intense public health efforts to maintain the status quo [50]. The transmission model analyses presented in Chapters III and IV aim to elucidate the current underlying difficulties in eradication, highlight how success has occurred, inform alternative intervention strategies, and provide a framework for evaluating future eradication efforts.

1.4 Specific Aims

Aim 1

Rationale: Dose-response models are utilized to translate a pathogen exposure into a risk of infection or disease. Currently, these models are primarily focused on single exposure events that are intrinsically time-independent processes. However, in real world scenarios, exposure events could be described in a variety of patterns depending

on routes of transmission.

Hypothesis: Depending on the dose received, the host immune system can be overwhelmed and therefore repeated inoculations over time affect the probability of any single pathogen initiating the infection process.

Implementation: We developed a dose-response model that is a function of the dose-pattern received and is dependent on the clearance rate of the immune system. Furthermore, combined with previous data, a statistical method was developed to analyze time series data where infection events are occurring amid inoculation events.

Aim 2

Rationale: The GPEI has experienced worldwide success through the use of childhood vaccination programs to eliminate polio transmission. However, several countries and regions, characterized by poor vaccination coverage and high transmission conditions, still experience transmission. Because polio immunity wanes over time, reinfection dynamics may play an important role in sustained transmission.

Hypothesis: Failure of polio eradication programs in transmissive regions occurs due to waning immunity and low transmission of the live OPV. Reinfection in older populations with waned immunity helps sustain transmission despite adequate vaccination coverage in children.

Implementation: A transmission model was built incorporating waning immunity allowing previously infected populations to be reinfected by wild polio. Further, the model incorporates transmission of OPV. Prevalence outcomes were then explored in this model for varying levels of transmission (R_0), vaccination rates, transmission levels of OPV, and waning immunity rates.

Aim 3

Rationale: The polio eradication campaign is a global effort to eradicate polio. Po-

liomyelitis incidence has been significantly reduced using childhood vaccination as implemented through the cooperation of the GPEI and national public health programs. The final endemic regions are characterized by poor vaccination coverage, mobile populations, and moderate to high transmission conditions. Because transmission occurs across borders, populations are interdependent entities with respect to vaccination effectiveness.

Hypothesis: Migration can affect vaccination programs due to differing vaccination policies and transmission conditions across populations.

Implementation: This model was a modification of a previous transmission model of polio that implements both the effects of waning immunity and age based vaccination programs. Specifically, we developed a transmission model incorporating migration between populations to explore how differing vaccination implementation affect prevalence levels in neighboring populations.

CHAPTER II

A dynamic dose-response model to account for exposure patterns in risk assessment: a case study in inhalation anthrax

2.1 Abstract

The most commonly used dose-response models implicitly assume that accumulation of dose is a time-independent process where each pathogen has a fixed risk of initiating infection. Immune particle neutralization of pathogens, however, may create strong time-dependence; *i.e.*, temporally clustered pathogens have a better chance of overwhelming the immune particles than pathogen exposures that occur at lower levels for longer periods of time. In environmental transmission systems, we expect different routes of transmission to elicit different dose-timing patterns and thus potentially different realizations of risk. We present a dose-response model that captures time dependence in a manner that incorporates the dynamics of initial immune response. We then demonstrate the parameter estimation of our model in a dose-response survival analysis using empirical time series data of inhalational anthrax in monkeys in which we find slight dose-timing effects. Future dose-response experiments should include varying the time pattern of exposure in addition to varying the total doses delivered. Ultimately, the dynamic dose-response paradigm presented here

will improve modeling of environmental transmission systems where different systems have different time patterns of exposure.

2.2 Introduction

Dose response functions are central to microbial risk assessments. In transmission systems, dose-response modeling is important in evaluating risk given an environmental pathogen exposure. Exposure occurs when susceptible individuals contact a pathogen source, usually an environmental reservoir or an infected individual. These exposure events can be characterized by the frequency and magnitude of pathogens that reach a susceptible host. The route of transmission, exposure behaviors, and physical aspects of the system will cause the dose-timing patterns of pathogen exposure to vary. For example, in influenza transmission, a direct pathogen exposure from a sneeze may be characterized as a large bolus exposure event while aerosolized exposure may be constant over a long period of time but exposure consists of a smaller number of pathogens at any given time.

Biologically, the immune system may handle varying exposure patterns with varying efficiency. Pathogen inoculations that occur very close together may carry a comparable risk of infection to an equivalent total dose occurring at a point in time if the immune response is slow compared to the period of exposure for the repeated doses. Longer periods between pathogen exposures, however, may allow the immune system to eliminate the pathogen and recover between each inoculation. The rates at which the immune system responds and clears the pathogen are clearly important in determining the accumulation of multiple inoculations. For these extreme instances, short versus long inoculation intervals, we can conclude that inoculations either accumulate as a sum or should be considered as separate events. However, it becomes unclear how accumulation of pathogen levels within the host may vary for patterns that occur on a time scale where the innate immune system has begun to respond

but failed to clear all the pathogens.

Immune response is variable depending on many factors such as pathogen type, location of pathogen, and prior exposure. We specifically focus on the dynamics of the initial immune response. This includes the innate immune response, natural host barriers (*e.g.*, mucosal clearance), and potentially standing elements of the acquired immune response. It is possible, however, that given long enough time frames of exposures that the adaptive immune response will also act as an initial response to future inoculations. Our hypothesis is that these initial host protections are not constant in nature, and that repeated inoculations affect the probability of any single pathogen initiating the infection process.

The classic dose-response models used for microbial risk assessment are the exponential and beta-poisson distributional models [2]. These models calculate the risk of infection for a single dose value. Parameters for these models are empirically informed using animal dosing experiments in which varying single bolus pathogen doses are given to animals and infection or disease is monitored [1, 5]. In environmental infection transmission systems where the environment is not just a source but is a medium of pathogen transport between individuals, these models are justified for the extreme scenarios of very closely spaced or very distantly spaced exposures described above. In these scenarios, the probability of infection can be calculated independently for each dosing event. However, for other exposure patterns, total within host pathogen level at a given inoculation time is dependent on remaining pathogen levels from past inoculations. In these cases the state of the system (*i.e.*, the number of living pathogens and the number of immune elements available to fight them) after any defined interval is dependent on the clearance rate of pathogens and the destruction and recruitment rate of standing immune elements. Here we define standing elements as those elements existing or that would have appeared on their own in the absence of new immune element generation due to an acquired immune response.

The exponential and beta-poisson models make implicit assumptions about how multiple pathogens interact to cause infection. Under the independent action hypothesis (IAH), any individual pathogen is capable of initiating infection with some independent probability [2]. The traditional dose-response models operate under this paradigm. This hypothesis, however, is generally considered only under single inoculation scenarios. We contend that, even though a single pathogen is capable of initiating infection, the infectivity of a pathogen may depend on the state of the immune system, which in turn is affected by prior inoculations. This is in contrast to the IAH that pathogen risk probability is independent of other pathogens. It also deviates from a threshold model in that the risk of infection given any inoculation size is still never zero.

One aim for this model will be future integration into transmission models. Particularly, in transmission models, when we specifically consider pathogen exposure from the environment, we must translate an exposure event into a probability of infection. This could be done using the exponential or beta-poisson models but these models potentially ignore exposure dynamics associated with different routes of exposures, as discussed in the exposure scenarios above. Although a more biologically motivated dose-response model was previously proposed [10], we present here a model that is computationally less intensive and therefore more suitable for integration into a transmission model. In Pujol *et al.* [10], innate immune effector particles and pathogens are modeled in a stochastic competition model capturing both the growth of pathogens and diminishing immune response. In our model, we aim to capture these dynamics with a simple model that does not explicitly model the immune dynamics. This satisfies the goals of dose-response at the transmission or population level by allowing utilization of an exposure pattern (history of inoculations) into the calculation of the probability of infection. Our model provides a framework to realistically relax the assumption of dose independence in a biologically plausible yet

computationally efficient manner that implicitly incorporates the dynamics of the immune system. Furthermore, we present a statistical method to analyze such time series data where infection events are occurring amid inoculation events. Experimental data to inform a time-dependent dose-response model are extremely rare, but there are data from a 1966 study on inhalation anthrax in monkeys that incorporates varying exposure patterns and time to death data [55]. Even though this study was not specifically designed to study varying risk by exposure patterns, our analysis provides direction for more informative future dose-response experiments that will incorporate time-dependent dosing patterns.

2.3 Methods

2.3.1 Overview

The methods section will describe the construction of our time-dependent dose-response model followed by its application to time-series anthrax dose-response data. The first three sections describe the development of the model in a general framework focusing on the clearance of pathogens within a host and the probability of infection take-off during the clearance time frame. Section 2.3.2 mathematically describes the within host-pathogen level at any given time after a point source inoculation and then section 2.3.3 extrapolates this process to multiple inoculations. Section 2.3.4 describes the development of a hazard for infection at a given time post-inoculation. At this point, enough information is provided to use this time-dependent dose-response model to make risk calculations given a parameterization. Particularly, it could be used in a transmission model setting to translate multiple exposure events into an infection risk calculation. The last three sections pertain to analyzing data. Section 2.3.5 uses the hazard to develop a likelihood statistic suitable for analyzing time-series dose-response data. To further analyze the data we have, we must make further

assumptions concerning the data which are described in detail in Section 2.3.6. Section 2.3.7 describes our exploration of the results from section 2.3.6 in more controlled experimental settings.

2.3.2 Time Dependent Pathogen Clearance

Our model aims to describe the clearance of pathogen until either the pathogen is eliminated or the pathogen establishes infection. To capture the dose-timing region between the extremes discussed above, a model should reflect decreasing ability of the immune system to inactivate pathogens as pathogens accumulate and immune elements are consumed. The differential equation in equation (2.1) illustrates such a model, where t represents time and $P(t)$ is a function representing the total within host pathogen level at a given time. The parameter γ roughly approximates a net per-pathogen clearance rate. The pathogen clearance rate is also affected by a shaping parameter, α, which elicits different inoculation accumulation effects depending on its value.

$$\frac{\mathrm{d}P}{\mathrm{d}t} = -\gamma P^{-\alpha} \tag{2.1}$$

To keep this model biologically plausible we consider the domain of γ to be in the interval $(0, \infty)$ and the domain of α to be in the interval $[0, 1]$. When $\alpha = 1$, γ becomes the per capita rate of decay of within host pathogen and the decay curve takes the exponential shape. In this case, the pathogens die-out is a linear function of the total number of pathogens P, *i.e.*, the immune system is equally effective in eliminating one pathogen regardless of the current number of pathogens in the system. The state of the immune system, therefore, is irrelevant since its efficacy to eliminate pathogens is constant. When α is less than one, this per capita change, γ,

is attenuated by the factor, $1/P^{1-\alpha}$. That is, the effectiveness of the immune system is dependent on the total number of within host pathogens. As α decreases and approaches zero, the shape of decay becomes more linear and slower for a fixed γ. Therefore, the parameter α can also be biologically described as the degree to which the immune system can be overwhelmed by pathogen level. For a single inoculation, the decay curve is illustrated in Figure 2.1. Given a total dose of 100 pathogens, the curve represents the total within host pathogen level at any given time over the course of clearance for varying values of α over two fixed values of γ.

By considering a negative differential equation, we are modeling under the assumption that the total within host pathogen level, or the infection hazard, is strictly decreasing. Biologically, our assumption is that after an inoculation, on average, the rate of pathogen reproduction is less than the rate of pathogen clearance. If this inequality reverses, that is pathogen reproduction becomes greater than pathogen clearance on average, this would correspond to the pathogen establishing infection. This assumption may not be suitable for all pathogens depending on biological traits, particularly the pathogens ability to replicate within our time scale of interest.

2.3.3 Dose Clearance and Multiple Dosing

We propose to use this function to calculate an effective dose for risk assessments when multiple inoculations occur within a biologically relevant time frame. To do this, we must first evaluate the solution to equation (2.1) with initial condition given at time 0, $d = P(0)$, where d is a single inoculation given at time 0.

$$P(t,d) = \begin{cases} d \cdot \mathrm{e}^{-t\gamma}, & \alpha = 1 \\ (t\gamma(\alpha-1) + d^{1-\alpha})^{\frac{1}{1-\alpha}}, & \alpha \in [0,1) \\ 0, & t_e \leq t \end{cases} \tag{2.2}$$

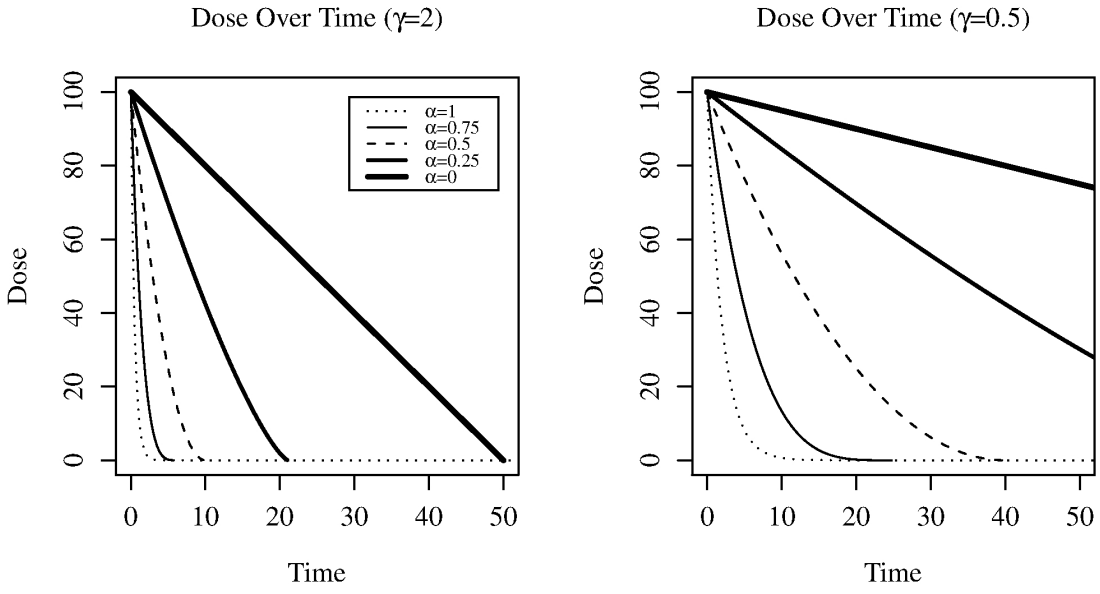

Figure 2.1: Shape and rate of within host dose decay by levels of α and γ. While the shape of decay is dependent only on α , the rate of decay is a dependent on both α and γ.

To ensure that $P(t, d) > 0$, we implement the last constraint in equation (2.2), where $P(t, d)$ is absorbed at 0 after t_e, the time of extinction for a given inoculation. The closed form solution for the time of extinction for a single inoculation is given by equation (2.3). Note that even though t_e is unbounded when $\alpha = 1$, the dose function (an exponential decay function) takes on small values fairly quickly for a fixed γ as t increases, as illustrated in Figure 2.1.

$$t_e = \begin{cases} \dfrac{d^{1-\alpha}}{\gamma(1-\alpha)}, & \alpha < 1 \\ \infty, & \alpha = 1 \end{cases} \tag{2.3}$$

In multiple exposure scenarios, the input doses for this model are represented by a sequence of inoculations such as those illustrated in the top two graphs((a) and (b)) in Figure 2.2. Each inoculation, d_i, is received instantaneously at a designated time, t_i.

Formally, we map a one to one correspondence between a sequence of n inoculations, $\{d_i\}_{i=1}^n$, and a sequence of n inoculation times, $\{t_i\}_{i=1}^n$. In a study, we observe subjects in real time (or close to) and record a corresponding final observation time, T. This final observation time, T, can occur in any interval between inoculations, $t_i \leq T \leq t_i+1$ or after the final inoculation time, $t_n < T$. Further, for a subject j, the total inoculations experienced before an infection event or censoring may be less than n, so we can denote the subject specific sequence size to be n_j with corresponding final observation time, T_j.

Now that multiple dosing situations have been introduced, we can consider evaluation of equation (2.2) for multiple inoculations. Since past inoculations may still be present at the time of a new inoculation, the dose function must incorporate the sequence of all past inoculations up to time, t. We can picture the multiple dose time function as a series of decay curves with discontinuity jumps occurring at each inoculation point, illustrated in the bottom two graphs((c) and (d)) of Figure 2.2. Particularly, the total within host pathogen level at any inoculation time, t_i, is the sum of the current inoculation, d_i, and the remaining within host pathogens, p_i. The remaining pathogen level is described in equation (2.4) recursively using equation (2.2). When $\alpha = 1$, the remaining pathogen level can be defined as an independent accumulation of previous inoculations, this is derived in the appendix, section A.2.

$$p_i = \begin{cases} 0, & i = 1 \\ P(t_i - t_{i-1}, p_{i-1} + d_{i-1}), & i > 1 \\ \sum_{j=1}^{i-1} d_j \mathrm{e}^{-\gamma(t_i - t_j)}, & i > 1 \cap \alpha = 1 \end{cases} \tag{2.4}$$

Since equation (2.4) describes the points of discontinuity at inoculation times, we can use it to reconstruct equation (2.2) to utilize multiple dose arguments. The

following function is the multiple dose function

$$P(t, \{d_i\}_{i=1}^{k}) = \begin{cases} p_k + d_k, & t = t_k \\ P(t - t_k, p_k + d_k), & t_k \leq t \leq t_{k+1} \end{cases} \tag{2.5}$$

This function can be interpreted as the total within host pathogen level at a given time, t, given all past inoculation up to that time. The function is jump discontinuous in that it decreases and is absorbed at 0 (by construction in equation (2.2)) but has point increases at inoculation times, t_i by an inoculation value, d_i. Note that, given a time sufficiently greater than the time of the last inoculation, this equation approaches zero under the same conditions as equation (2.2). The time to extinction, t_e, after inoculation time t_i, can still be calculated using equation (2.3) but with input dose, $p_i + d_i$, instead of d_i. When $\alpha = 1$, the function approaches zero quickly with decreasing error as $t \gg t_k$ since the true convergence time is in the limit, $t \to \infty$, discussed in detail in the appendix, section A.2.

2.3.4 Dose-Response Risk from Multiple Dose Function

We consider an effective dose to be any value calculated from equation (2.2) that could contribute to an infection hazard at any given time. To evaluate the accumulated effective dose in a given host, we integrate equation (2.2), over a time period of interest. For a single inoculation, the closed form solution for the effective dose from inoculation to extinction is

$$\int_0^{t_e} P(t, d)\, \mathrm{d}t = \frac{d^{2-\alpha}}{\gamma(2-\alpha)} \tag{2.6}$$

When there are multiple inoculations, the accumulated effective dose is a sum of

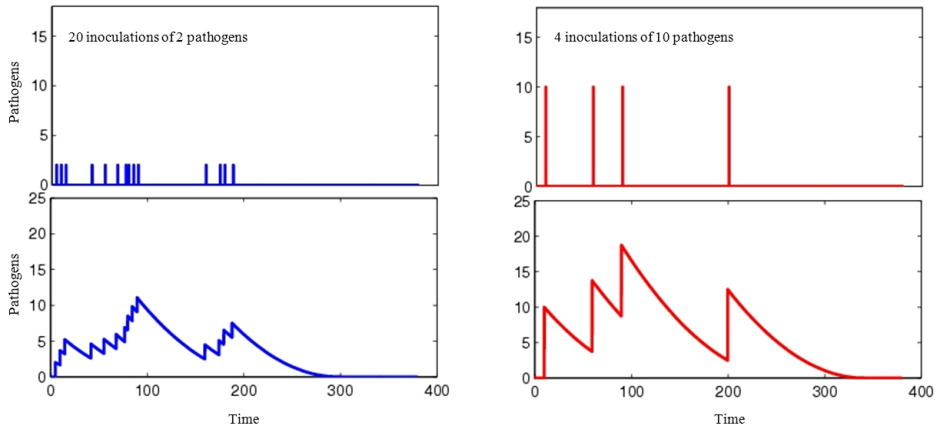

Figure 2.2: Example of two different inoculation patterns (above) and the time-evolution of pathogen numbers within the host (below). The models parameters are e $\alpha = 0.5$ and $\gamma = 0.05$. The patterns of inoculation correspond to two different multiple inoculation scenarios: 20 inoculation events of 2 pathogens each (left), and 4 inoculation events of 10 pathogens each (right). Although the total inoculated dose (40 pathogens) and the time of exposure (200 minutes) is the same, it is visually evident that pathogens from the four inoculation events persist longer in the immune system.

integrals over the continuous sections of the multiple dose function. This is seen in equation (2.7), for any time, T, before the final within host pathogen extinction. If $T = t_k$, or the upper bound of the integral is equivalent to an inoculation time, the last term of equation (2.7) is zero.

$$\int_0^T P(t, \{d_i\}_{i=1}^k)\mathrm{d}t = \sum_{i=1}^{k-1}\left[\int_0^{t_{i+1}-t_i} P(t, p_i + d_i)\mathrm{d}t\right] + \int_0^{T-t_k} P(t, p_k + d_k)\mathrm{d}t \quad (2.7)$$

To evaluate the accumulated effective dose through final pathogen extinction, we simply replace the final term of equation (2.7) with equation (2.6) with $p_n + d_n$ (the initial pathogen level at the final inoculation) substituted for d. For $\alpha = 1$ and $T \gg t_n$, we can still substitute in equation (2.6) with small error, this is discussed in greater detail in the appendix, section A.2.

To consider how α determines the importance of dose timing, consider an entire dose course over an exposure pattern, for example, the top two graphs in figure 2.2, where we have two distinct exposure patterns of 40 pathogens given over 200 minutes. The accumulated effective dose over this time can be calculated using the integral given in equation (2.7). When $\alpha = 1$, the accumulation of inoculations is an independent process, as illustrated in equation (2.4) due to the exponential memoryless property. Because of this property, the total effective dose over the exposure period is the sum of the inoculations divided by γ. This solution holds for all potential dosing patterns evaluated through effective extinction $T \gg t_n$ when $\alpha = 1$, discussed further in the appendix, section A.2.

When $\alpha < 1$, however, the pathogen clearance rate depends on the within host pathogen level. Under these conditions, the total effective dose is dependent on the timing of given inoculations. For $\alpha = 0.5$, the accumulated effective dose (the area under the curve) differs across dosing patterns despite the sums of the inoculations

both totaling 40 pathogens (see the bottom two graphs of figure 2). Although the total inoculated dose (40 pathogens) and the time of exposure (200 minutes) is the same, it is visually evident that pathogens from the four inoculation events persist longer.

The goal of our model is to analyze decaying hazard post inoculation, until either the pathogen is cleared or the pathogen takes hold and initiates infection prior to clearance. We now introduce the risk of infection due to a single pathogen per unit time that is present in the immune system, s. This formulation is a one-hit model of infection; *i.e.*, a single pathogen unit is capable of initiating infection. This phenomenon has been shown empirically for pathogens such as influenza A [7] and intravenous salmonella exposure [6]. However, unlike the exponential formulation of a one hit model, each hit does not have identical and independent risk. Instead, risks are dependent upon prior hits and thus α and γ also contribute to the calculation of the risk.

For an instantaneous risk associated to a single pathogen, s, and the current number of pathogens within the host, P, we can calculate the force of infection, *i.e.* the probability of a susceptible individuals becoming infected, $sP(t)\mathrm{d}t$. This is evaluated at each time step. For multiple inoculations, we insert our multiple dose function. We can interpret this as a hazard function, $\lambda(T)$, given in equation (2.8).

$$\lambda(T)\mathrm{d}t = sP(T, \{d_i\}_{i=1}^{k})\mathrm{d}t \tag{2.8}$$

By integrating and exponentiating the hazard over an interval time up to time, T, we can calculate the survival function, or the probability of not being infected by time, T, given as follows

$$S(T) = \mathrm{e}^{-s\int_0^T P(T,\{d_i\}_{i=1}^k)\mathrm{d}t} = 1 - \Pr(\text{Infection by Time, } T) \tag{2.9}$$

We now have a corresponding risk of $1 - S(T)$, which matches the familiar functional form of the exponential dose-response model. If we consider $T \gg t_n$, then this risk corresponds to the risk of an entire exposure pattern. When $\alpha = 1$ and there is a single inoculation event and clearance, the single pathogen risk parameter, k, from the exponential model is equivalent to the ratio s/γ. Furthermore, continuing to assume complete pathogen clearance, this equivalence holds for all exposure patterns when $\alpha = 1$. This relationship is lost when $\alpha < 1$ as pathogen clearance, and thus risk, becomes dependent on the size and timing of inoculations. That is, when $\alpha < 1$, the equivalence of the exponential function and our cumulative dose risk function is dependent on the inoculation size. Mathematical explorations of the relationship between the exponential model and our model when $\alpha = 1$ are discussed in the appendix, section A.2.

2.3.5 Likelihood statistic and parameter estimation from data

By multiplying the hazard and survival function we can calculate the probability density for infection at a final observation time, T, standard in a survival analysis. This is given in equation (2.10).

$$f(T) = S(T)\lambda(T) \tag{2.10}$$

To estimate the model parameters using time-dependent exposure data including time of infection, we propose a likelihood statistic derived from survival analysis framework. The likelihood is formulated depending on a subject j's infection status given by Δ_j. This is illustrated in equation (2.11) where we consider each subject to

be independent. If $\Delta_j = 1$ (infection occurs), then the likelihood is calculated from the probability of infection at time, T_j, given by the density function $f(T_j)$. If $\Delta_j = 0$ (no infection or censoring), then the likelihood is calculated from the probability of survival up to time, T_j. To estimate parameters, we propose a maximum likelihood approach, that is, we find the best parameter values that maximize the likelihood values.

$$\prod_j L(T_j) = \prod_j S(T_j)^{(1-\Delta_j)} f(T_j)^{\Delta_j} \tag{2.11}$$

By taking the negative log of the likelihood and substituting in equation (2.10), we simplify the equation (2.11) to equation (2.12).

$$-\sum_j \log L(T_j) = \sum_j s \int_0^{T_j} P(T, \{d_i\}_{i=1}^{n_j}) \mathrm{d}t - \Delta_j \log \lambda(T_j) \tag{2.12}$$

When evaluating time-dependent dose-response data, finding exact times of infection will generally be difficult if not impossible. We may know a time interval in which the process of infection began but not an exact time. For these scenarios we can adjust the likelihood formulation such that interval censoring can be incorporated. This adjustment is discussed in detail in the appendix, section A.3.

2.3.6 Case study: inhalational anthrax data

Inhalation anthrax mortality data in monkeys were published by Brachman *et al.* [55] from an observational animal study conducted in a wool sorting mill in South Carolina in 1966. Cynomogus monkeys were placed in a laboratory trailer and air was ventilated into the trailer from the wool sorting mill. Air was periodically sampled to measure the anthrax concentration. A daily inhaled dose was estimated using these data and an estimated monkey respiration rate. We considered these inhaled spores

as pathogens capable of initiating infection.

The experiment was conducted during five distinct time intervals and three of these were reported. During the third and fourth runs, the monkeys were continuously exposed to contaminated air during working hours. Air was intermittently sampled daily. These were the only two runs we were able to use to evaluate our model. As air was ventilated in from the wool sorting mill, exposure was based on the natural concentrations in the mill and therefore was not controlled by the researchers. For our purposes, dose levels were estimated from figures provided in the paper in which a single total daily exposure was recorded. We assumed that on days when exposures were recorded that single equivalent sized inoculation occurred at the beginning of each hour for the entire day. Monkeys health was monitored over the exposure period and for a brief time after the terminal exposure. The experimenters checked in on the monkeys three times per day. Autopsies were conducted immediately after a death was discovered. Deaths due to non-anthrax causes also occurred and were recorded. All monkeys were sacrificed shortly after the exposure period to determine anthrax infection status.

During the third run, 32 monkeys were exposed for 47 days during which time 10 deaths due to anthrax infection were recorded. On the 50th day, all the remaining live monkeys were sacrificed. At this time, two more monkeys were found to be infected bringing the infection total to 12 with observed risk to be 44%. During the fourth run, 31 monkeys were exposed for 41 days during which time 10 deaths due to anthrax infection were recorded. The remaining live monkeys were sacrificed on the 51st day. No additional monkeys were found to be infected and the observed risk was thus 23%. Figure 2.3 is a graphical depiction of these data.

By the end of the study, monkeys had become infected, died of other causes, or survived (did not become infected) over the duration of exposure. Survived subjects were sacrificed several days after the final inoculation which technically elicits a right

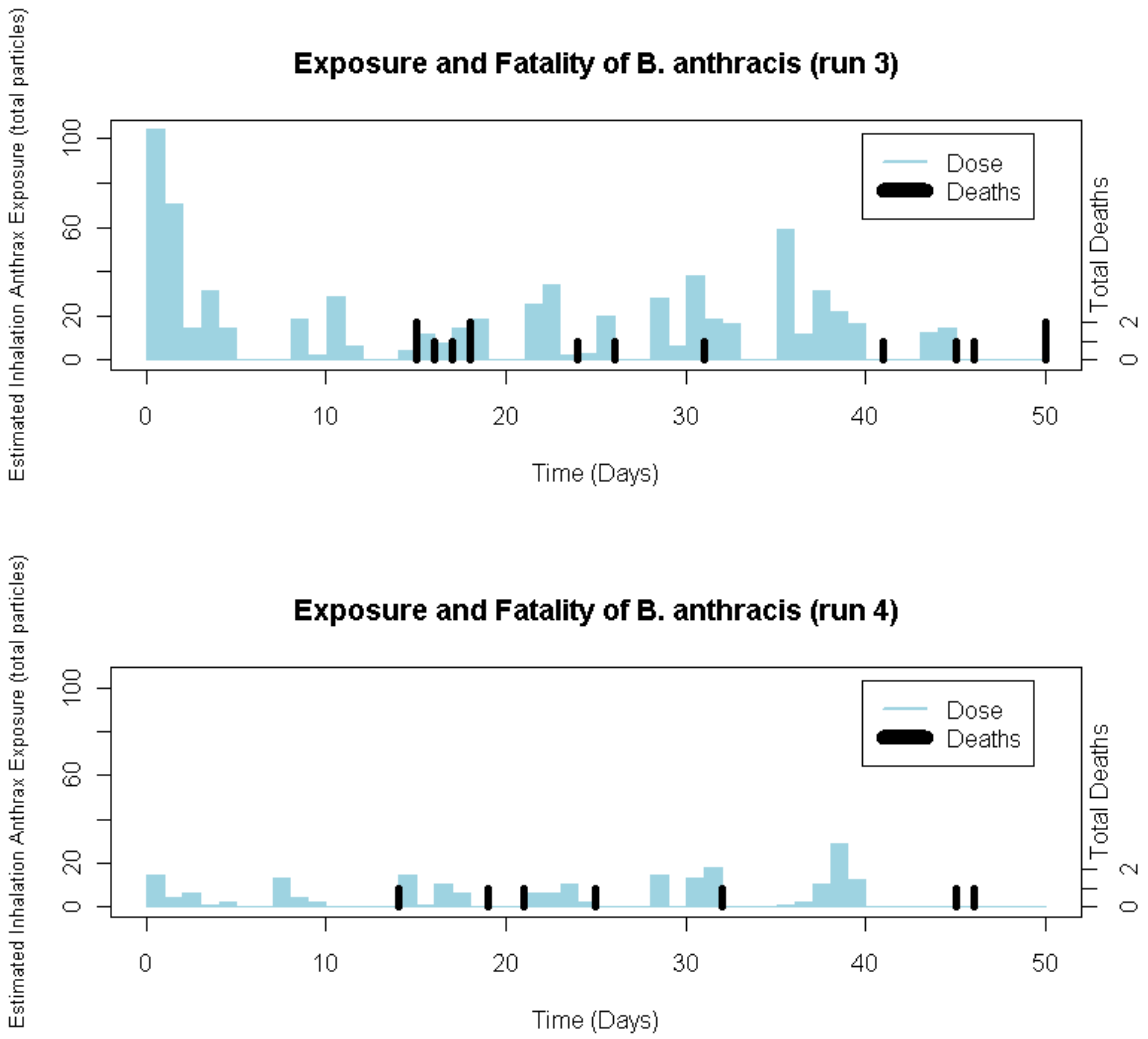

Figure 2.3: Exposure (left axis and represented by lighter bars with width of 1 day) and mortality (right axis and represented by black thin bars) results from the third and fourth runs of the anthrax dataset. Exposure is assumed to be given uniformly once every hour on days when exposures were recorded. In the third run, 12/32 monkeys died from anthrax, and in the fourth run, 10/31 monkeys died from anthrax.

censoring. We assume that autopsies that were negative for anthrax are conclusive in that subjects would never have become infected. That is, we assume all non-infected sacrificed monkeys survived the entire dose course. We also assume that anthrax has a case-fatality rate of 100% in monkeys (*i.e.*, no monkey survived infection). A small set of subjects in these data died of causes not related to anthrax. We assume these censored subjects died from reasons that were completely random and unrelated to anthrax exposure and therefore evaluate their survival up to their final observed time, T_j. For subjects who were infected, only day of death was observed.

Since we were interested only in time to infection take-off, we considered a fixed population lag period, τ, which is the time between infection take-off (when the course of ongoing infection is assured to be progressive) and time of death. Given the observed time of death, T_j, the predicted time to infection is $T_j - \tau$. We do not aim to dynamically model any processes during the lag time, τ, and thus treated it as a constant parameter. A previous study [56] showed that time between symptoms and death is on the scale of several hours for Cynomologus monkeys so we do not think symptom onset would aid in finding the total lag period.

This lag period, τ, was treated as a population parameter but it is likely individually probabilistic in nature. Based on the Vasconcelos study that this lag is variable, a variety of τ values were initially implemented. However, the Vasconcelos experiments used significantly higher dosing in bolus (the ID_50) and potentially a different strain of the *Bacillus anthracis*, and therefore lag times may not be comparable. Further, an experiment on several other pathogens showed relatively invariant latency periods for inoculations less than the ID_50 [57].

To come up with a lag time estimates, we considered a previous study [58] that used lag time distributions with median lag times of 1-3 days. However, their lag period described the period from spore germination to symptoms. Anthrax infection occurs after germination in macrophages [40, 59]. The biology and persistence of

spores from time of exposure to infection is not well understood, but elimination of spores is mediated by epithelial cells and macrophages [60]. While epithelial cells are capable of eliminating anthrax spores alone[60], spores are also readily phagocytized by alveolar macrophages where they germinate. While, the macrophage is capable of eliminating the bacillus, *B. anthracis* toxins and defense mechanisms inhibit this ability as it attempts to use the macrophage to reach the regional lymph system where it can initiate infection as an extracellular pathogen [59]. This process implies that germination is an important step in the infection process but that it occurs before infection takes off. We therefore expect the lag period described in our model to be less than that described in Brookmeyer et al.[58] and used a period from 1 to 4 days. Treating τ as a nuisance parameter, we fixed it to a discrete uniform distribution; it was then integrated out of the likelihood using conditional expectation. Further discussion can be found in the appendix, section A.3.

Model fitting was done by profiling over α while optimizing the parameters s and γ (in unit per hours) to minimize the negative log likelihood based on the Brachman experimental data for run 3 and run 4. By profiling over a fixed α, we are also analyzing these data under different assumptions concerning accumulation of doses in terms of differing dose timing. Inference was done by fitting a spline curve through the values of the negative log likelihood for each value creating a smooth depiction of the log likelihood space. Using the minimum value of the spline (the overall maximum likelihood estimate (MLE) fit), we defined a critical cut-off using the likelihood ratio test [61]. That is, at the 95% significance level, the confidence interval of α falls in the range of the minimum log likelihood $\pm\frac{1}{2} \times \chi^2(0.95, \text{d.f.}=1)$.

To evaluate consistency of our model with some past anthrax models, we calculated risks over a range of single dose values. This can be done for $\alpha = 1$, reducing our model to an exponential model, in which the exponential risk parameter k is equivalent to the ratio of s over γ. For parameterizations involving $\alpha < 1$ in which

dose-timing patterns impact risk and the exponential model is no longer valid, our model is only comparable to past models under single inoculation scenarios. Risks for range of single dose values were calculated using equations (2.6) and (2.9).

Integrals were estimated using the adaptive Simpson quadrature method in MATLAB. Optimization was done using minimax search algorithm in MATLAB. Spline fitting was done using the default spline function in MATLAB.

2.3.7 Dosing experiment design

To explore the models ability to discern between different exposure patterns and to illustrate the results from the Brachman data optimization, exposure patterns were created representing two extremes; one large bolus and one evenly distributed set of smaller inoculations given once daily over 15 days. The sum of the inoculations is equivalent for both patterns at a value of 15,000 as it corresponds to the sum of the total dose in run 3. Using the parameter MLEs from the model, risks were calculated for each dosing pattern for a fixed α and corresponding MLE γ and s values. The varying values of α illustrate potential expected results from an animal experiment that incorporated dose timing.

2.4 Results

Figure 2.4 shows the results of the optimization profile over α using data from the Brachman inhalational anthrax study runs 3 and 4. The likelihood space is a fairly smooth decreasing curve in the optimized log likelihood space over as seen in figure 2.4a. A smoothed spline was fit through the points and the 95% lower limit was connected to the upper boundary of by a horizontal line. The optimal parameter fit occurred when $\hat{\alpha}$=0.90 with respective MLE values for $\hat{s}$ and $\hat{\gamma}$ at 1.81×10^{-7}/h and 0.0097/h. For these overall MLE fits, the predicted risk for run 3 and run 4 is 50% and 16% compared to the observed attack rates of 44% and 23%, respectively.

The 95% CI for α was (0.51, 1) where 1 is a bound due to our imposed constraints on values of α. It is mathematically and statistically possible to extend α beyond our imposed upper limit constraint but the biological interpretation of our model becomes less intuitive. For $\alpha > 1$, bolus exposures patterns have lower risks than evenly distributed exposure patterns when total dose is fixed. Results for $\alpha > 1$ are discussed in the appendix, section A.4.

Plotting of the MLE $\hat{s}$ and $\hat{\gamma}$ values over the significant region of α can be seen in figure 2.4b,c. The MLE values of γ are log linearly correlated with α. Recall that the shape and rate of within host pathogen decay depends on both these parameters and, therefore, this relationship is not unexpected as the optimization is trying to find a relatively stable clearance curve and there are likely many sets of α and γ that could elicit such a curve. When given multiple exposure patterns of the same total dose, we would expect the α parameter to determine the importance of dose timing effects, *i.e.*, whether the risk will differ between these exposure patterns. Therefore, without data containing more exposure patterns, it is difficult to independently estimate both α and γ. The MLE values of s are relatively insensitive for changing values of α. The data thus provide us with a consistent estimate of the instantaneous per pathogen infectivity parameter, s, for a given clearance pattern.

The attack rates for varying single doses were calculated using our MLE parameterization and equations (2.6) and (2.9). We compare our MLE results to another parameterization of our model and two previously analyzed anthrax dose-response models by creating a risk curve over a large range of bolus dose values, all illustrated in Figure 2.5. We consider results for $\alpha = 1$, equating this parameterization of our model to the exponential model where $k = s/\gamma = 3.95 \times 10^{-5}$. The other two models were a previous analysis of the Brachman data assuming each day was an independent trial using an exponential dose-response model [62] and a separate analysis of anthrax infection in Rhesus monkeys, specifically developed to model anthrax clear-

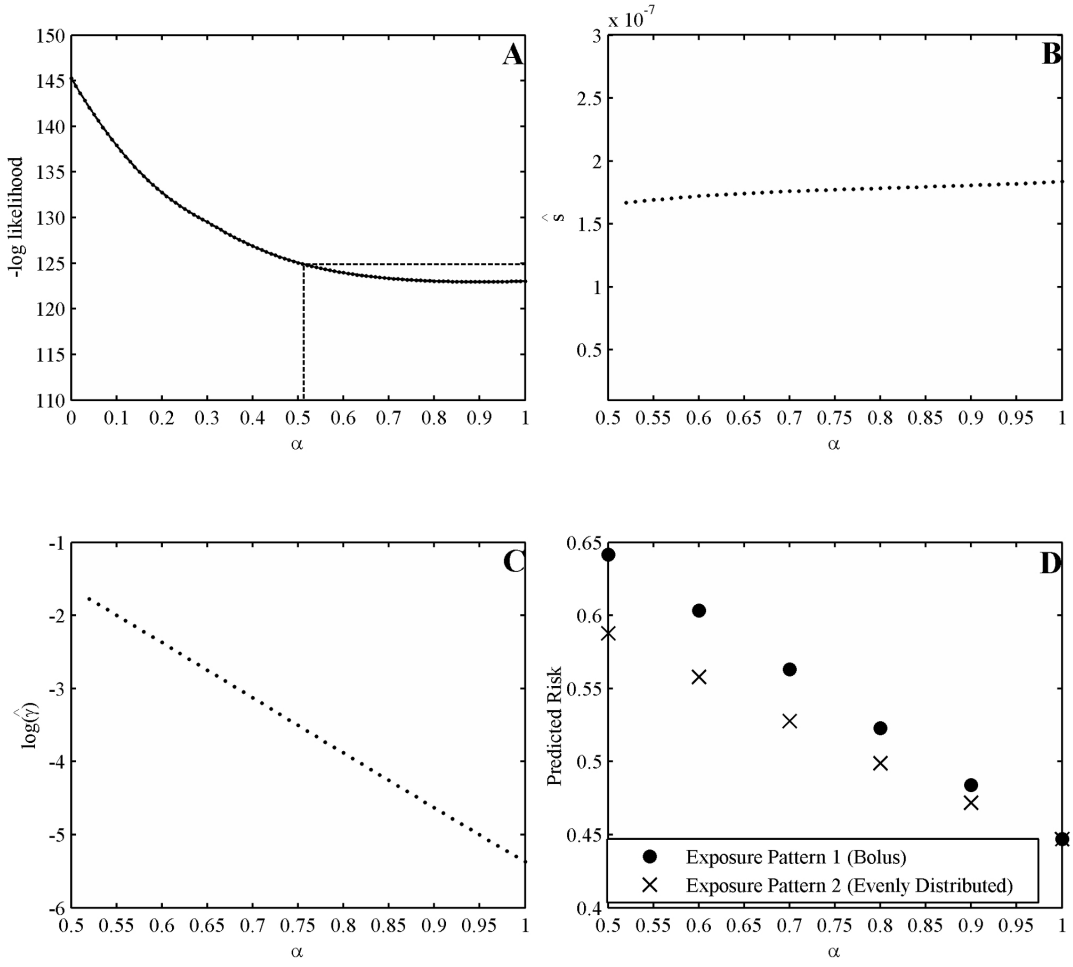

Figure 2.4: Results from the Brachman inhalational anthrax data analysis. A.) Results from optimization profile over α. A spline curve was fit to determine the minimum negative log likelihood (maximum likelihood estimate (MLE) $\hat{\alpha} = 0.90$) and to determine the 95% confidence interval (CI) (0.51, 1) using the log likelihood ratio test. B.) Optimized s values for values of α within its 95% CI. C) Optimized $\log(\gamma)$ values for values of α within its 95% CI. The minimum γ value in this range is 0.0046 h^{-1} and the maximum is 0.17 h^{-1}. D) Predicted risks for two exposure patterns using MLE values profiled over α. Two exposure scenarios were used, one bolus (circles) and one evenly distributed (crosses) exposure pattern, both with the same total dose of 15,000. Parameter sets used for these calculations were (α=0.50, s=1.65 $\times 10^{-7} h^{-1}$, γ=0.20 h^{-1}); (α=0.60, s=1.72$\times 10^{-7}$ h^{-1}, γ=0.093 h^{-1}); (α=0.70, s=1.76$\times 10^{-7} h^{-1}$,γ=0.044 h^{-1}); (α=0.80, s=1.78$\times 10^{-7} h^{-1}$, γ=0.021 h^{-1}); (α=0.90, s=1.81$\times 10^{-7} h^{-1}$, γ=0.0097 h^{-1}); and (α=1.00, s=1.84$\times 10^{-7} h^{-1}$, γ= 0.0046 h^{-1}).

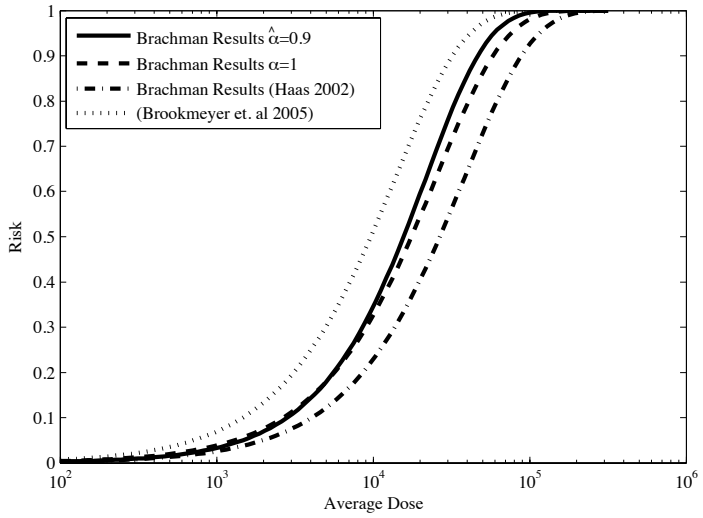

Figure 2.5: Comparison of our best fit results with other anthrax models when modeling risk for a single bolus dose. To calculate this risk when $\alpha = 0.9$, equations (2.6) and (2.9) were used in combination with MLE values, $\hat{s}$=$1.81\times10^{-7}\text{h}^{-1}$ and $\hat{\gamma}$=0.001h^{-1} (solid line). When $\alpha = 1$, our model is equivalent to an exponential model with $k = s/\gamma = 3.95 \times 10^{-5}$ (dashed line). Previous exponential modeling of Brachman data assuming each day as an independent dosing event yielded k=2.4×10^{-5}[62] (dash-dotted line). A model of anthrax outbreak in Rhesus monkeys which included clearance rate and hazard rate yielded an attack rate formula equivalent to an exponential model with k=7.17×10^{-5}[58] (dotted line).

ance rates[58]. This model is similar to our model when $\alpha = 1$, and produced a clearance rate and hazard rate of 0.0029/hr and 2.08×10^{-7}/h.

Next, we calculated the corresponding risks for the exposure patterns given in section 2.3.7. We chose the corresponding MLE parameter sets for several α values ranging from 0.5 to 1. Figure 2.4d depicts the predicted risks over this α range, comparing the bolus exposure to the evenly distributed exposure pattern. We can see that as α approaches 1, the gap between the predicted risks decreases. The largest gap presented occurs at $\alpha = 0.5$ where the bolus exposure has a risk of 64% and the distributed exposure has a risk of 59%. When $\alpha = 0.9$, the bolus risk is 47% and the distributed exposure has a risk of 46% indicating dose-timing effects that are small.

2.5 Discussion

2.5.1 Plausibility of our model as a dose-response model

Using a simple function that expresses cumulative dose dependence on the pathogen elimination rate, we are able to realistically relax the assumption that the risk of each pathogen dose is independent of the time of arrival of other pathogen doses. Further, through a survival analysis, we have presented a method for analyzing dose-response time series data of exposure and infection events. As a case study, we presented an analysis of inhalational anthrax infection in Cynomologus monkeys in an industrial setting [55]. Our optimization found the best fitting parameters for these data as follows: α=0.9, γ=0.0097/hr, and $s = 1.81 \times 10^{-7}$/h. This result indicates that there are very slight dose-timing effects, as indicated by the risk difference of 1% from the simulated exposure experiments. This result also appears dependent on our lag time assumptions. The problem of non-identifiability between our clearance rate (γ) and lag period (τ) requires us to make some assumptions about the overall distribution of the lag period, a problem also found in a previous anthrax analysis[58], where they optimized a convolution of a time to germination likelihood and an exponential lag period. Our lag period describes a period beginning with infection takeoff, which occurs sometime after germination within macrophages [59], and ending in death. The point at which infection has taken off is not provided in the Brachman experiment and thus we must rely on an assumed lag period. To test sensitivity to lag period assumptions, we tried other distributions, such a larger range of lag period and a truncated exponential. If all times were weighted equally or if there were heavier weighting on longer lag periods (greater than 6 days), the MLE $\hat{\alpha}$ was estimated at 1. However, a distribution that weights faster lag periods more (such as the exponential with mean of about 2 days) resulted in MLE $\hat{\alpha}$ values between 0.9 and 1. While lag periods may be less variable and slower for doses under the ID_{50}[57], such as in

this dataset, future anthrax modeling for larger doses may require careful distribution selection consistent with experiments done with higher dose levels[56]. The fitted values of s and γ decrease slightly as the lag period decreases. This result implies that our estimate of within host pathogen persistence and risk depends on our lag period selection and therefore we may be incorrectly classifying periods where dose-timing is important as the lag period.

Although our model is unique in its implementation of multiple doses, we can compare it to other dose-response models when considering the risk from a single dose. As illustrated in figure 2.5, our model produced consistent results with other anthrax models. Particularly, the ID_{50} of all these models are all within an order of magnitude. A review of several anthrax dose-response models[63] found that risk models that were similar to exponential distributions were the most successful at modeling anthrax risk. Our analysis is consistent with this result. To truly check consistency among other analyses, however, requires more data and models implementing multiple dosing.

Our 95% CI of (0.51, 1) reflects imprecision in estimation of values. Our confidence interval calculation is limited in this example as we implemented an artificial upper bound on α that is biological instead of statistical. If we allow α values greater than 1, we find this interval to extend as far as 1.48, as discussed in the appendix, section A.4. If $\alpha > 1$, we would have a paradigm where bolus exposures have lower risks than smaller, distributed exposures of the same total dose.

The strong functional relationship of α and γ implies that they should not be estimated independently. Particularly, they share a decreasing log linear relationship (figure 2.4c), showing that γ values decrease when α values increase. That is, when clearance decreases in speed, the shape of the clearance curve becomes more curvilinear. This illustrates a range of potential clearance curves that describe the pathogen decay. The s parameter then provides us with an instantaneous per pathogen infection risk over the clearance time. When estimating the parameters for our model,

we suggest a profile optimization over α. Using this approach, inference can then be done to determine if α differs from 1 which would imply that risk estimation depends on dose-timing. When using the model to estimate exposure risks or infection timing, we assign the appropriately fitted γ value to a specified α value.

One limitation of our model due to its simplicity is the use of abstract parameters. The α and s parameters are not readily biologically interpretable from the results and the parameter γ is only interpretable in the special case of exponential clearance. We can still present expected clearance curves and describe expected behavior of the system with known parameters. For example, if we know we do not have exponential clearance ($\alpha < 1$), then bolus exposures correspond to the highest risk of infection. However, given two different pathogens with this property ($\alpha < 1$) but different α values, it is not clear what the differing values of α tell us specifically about each pathogen, especially if the other parameters vary also. Furthermore, extrapolating our results to human populations requires additional assumptions. For traditional dose-response experiments, we would need susceptibility of the host animal to be similar to humans. Additionally, for our model, we would also need the surrogates immune response to occur at a similar rate with similar effectiveness to the human population. Cynomolgus monkeys and humans have similar anthrax infection pathology[56] which implies that we may expect the dynamics and risk assessments to be similar given these exposure patterns, however, it is not clear how the parameter sets might differ.

Another limitation of our model is that it does not take into account the reproduction of pathogens within host tissue, *i.e.*, we only model pathogen clearance as a decreasing curve between inoculations. Ideally, a model of the infection process includes pathogen elimination by the immune system and the growth of the pathogen within the host. The persistence of pathogen would then be more realistically described as a stochastic process, with spikes both increasing and decreasing over clearance until either the pathogen level reaches zero or begins to reproduce to an

unbounded level, as presented in a previous model[10]. This model, however, requires additional parameters and is computationally intensive which makes its implementation into complex models of environmental infection transmission systems difficult. By ignoring pathogen growth during innate clearance but before the infection takes off, the overall shape of pathogen decrease described by our model will be different than the more realistic model that takes into account both processes. However, by relaxing the assumption that infection risk must be time-independent, our model is a step forward in dose-response risk assessment.

2.5.2 Experiments to inform time-dependent dose-response models

Our proposed exposure patterns illustrate simple experimental structures that would elicit varying risk due to dose-timing effects. It is important to note that our model is only one potential realization of time-dependence in dose-response models. Conducting the proposed experiments and observing a significant risk difference between exposure patterns might be enough to imply that risk depends on dose-timing. This discovery alone would illustrate how characterizing the risk of different routes of transmission is critical, and further, would have important ramifications on intervention policies.

To conduct such a time-dependent dose-response experiment, preliminary experiments would need to be conducted to find a viable dose; that is, doses that do not have risks near 0% or 100%. Further, these preliminary experiments need to give insight into the time scale of interest. We used doses spaced by days since our results pointed to clearance rates on the scale of days. For a pathogen like the influenza virus, we may expect dose timing effects to be on a shorter time scale. After preliminary experiments, dosing schemes similar to our proposed patterns should be implemented with fixed total doses. By using exposure patterns that differ so widely, we are better able to evaluate the impact of dose timing on the effectiveness of the immune sys-

tem. Simply observing varying risk by exposure pattern can provide enough insight to imply that risk depends on dose-timing. Simple analysis on differing risks would be sufficient to show dose-timing effects. One shortfall of these experiments is that they would likely require large subject sizes unless there are substantial dose timing effects. If we look at the predicted risks of our exposure patterns from our analysis when α=0.5, we would need 1550 subjects per pattern to find a statistically significant difference at the 0.05 level with 80% power using Fishers 2-sided exact test. Naturally, if there are stronger dose timing effects (risks differences are much higher), the necessary sample size drops. Other options would include designing experiments that are mechanistically specific to the pathogens of interest and monitoring the corresponding immune response. For anthrax, we may design an experiment monitoring macrophage loads over different dosing patterns and then analyzing the data with an anthrax-specific mechanistic model. This scenario would reduce the emphasis on elucidating risk differences and therefore may not require such large sample sizes.

By using a sufficient number of subjects, the time to infection distribution and overall risk would be stabilized for each dosing course and thus provide stable data to estimate our parameters. Further, using varying total doses is an additional method to introduce precision to parameter estimation in our model. There were many limitations in using the Brachman data to estimate our model parameters. The data had small sample size and only two exposure patterns. Furthermore, the exposure patterns are roughly similar for each run and the total doses differ. The estimation of α depends on the effect of dose-timing and thus would be best estimated by widely varying exposure patterns of fixed total dose.

2.5.3 Time-dependence in the dose-response model paradigm

Through the use of our model, we have shown that exposure timing can be used in the calculation of risk and estimation of infection times. This is a distinct advantage

over the risk calculation of classical dose-response models. In transmission systems, different routes of transmission lead to varying types of exposure patterns. We can now relax the assumption that the risk is invariant to different dose timing and thus varying exposure patterns. Even if our model predicts invariant risks to exposure patterns (exponential clearance), it allows us to estimate when infections would occur over an exposure course. Fundamentally, we are interested in whether dose-timing is an important factor in the calculation of risk. Our analysis shows that for anthrax, there may not be these effects on the time scale we examined, *i.e.*, the accumulation of inoculations is an independent process with respect to immune clearance when time intervals are one day at the minimum. There might be such time dependence across shorter times. Despite these findings, we still provide a reasonable estimate for the persistence of the pathogen in the host on the scale of days. We expect that the importance of dose-timing would be dependent on the infection process of a given pathogen. For other pathogens, such as non-respiratory bacteria or viruses, we may not expect these properties to remain constant, especially if the immune mechanisms of clearance differ biologically. For example, the *B. anthracis* bacillus uses macrophages as a transport to the lymph system in the course of the infection process [40]. This is a unique mode of infection that affects both immune effectiveness and clearance time scale that differs from infection processes of many other pathogens, *e.g.*, the influenza virus.

Infectious disease transmission systems are time-dependent processes generally involving many different types of environmental exposure routes. In influenza transmission, the virus can be transmitted in the air, through direct contact, and through fomite surfaces [64]. In anthrax bioterrorism scenarios, we may wish to consider the risks of large release versus a small steady release of spores. For an enteric disease, like cholera, norovirus, or pathogenic *E. coli*, competing routes such as contaminated food or water contribute to varying exposure patterns. Each of these transmission routes

could be characterized by distinct exposure patterns such as evenly distributed, small exposures (*e.g.*, breathing dispersed pathogen in air) or a large bolus exposure (*e.g.*, consuming a contaminated glass of water). Modeling these routes requires many assumptions, particularly when time-independent dose-response models are implemented to give a risk calculation for a given exposure pattern. If exposures occur in a time frame in which the immune system has begun to respond but has not cleared the pathogen, we may no longer have independent pathogen risk calculations. In this scenario, distinct exposure routes may elicit differing risk properties. To see these properties, dose-timing effects must be considered in dose-response experiments, such as we suggest, elucidating the time scale of clearance and the potential importance to risk calculations. We aim to develop a dose-response paradigm that readily includes time-dependence in both risk and infection time calculations.

2.6 Publication and acknowledgments

This work has been published by the Journal of the Royal Society Interface [65]. Contributing authors to this research were Bryan T. Mayer, James S. Koopman, Edward L. Ionides, Josep M. Pujol and Joseph N. S. Eisenberg.

CHAPTER III

Successes and shortcomings of polio eradication: A transmission modeling analysis

3.1 Abstract

Polio eradication is on the cusp of success with only a few regions still maintaining transmission. Improving our understanding of why some regions have been successful and others have not will help both with global eradication of polio and with development of more effective vaccination strategies for other pathogens. To examine past eradication efforts we constructed a transmission model for wild poliovirus incorporating waning immunity affecting both infection risk and transmissibility of any resulting infection, age-mediated vaccination rates, and transmission of OPV. The model produces results consistent with the four country categories defined by the Global Polio Eradication Program: elimination with no subsequent outbreaks; elimination with subsequent transient outbreaks; elimination with detected transmission for more than 12 months; and endemic polio transmission. Analysis of waning immunity rates and OPV transmissibility reveals that higher waning immunity rates make eradication harder due to increasing numbers of infectious adults and higher OPV transmission rates make eradication easier as adults become re-immunized. Given these dynamic properties, attention should be given to intervention strategies that

complement childhood vaccination. For example, improvement in sanitation can reduce the reproduction number in problematic regions, while adult vaccination can lower adult transmission.

3.2 Introduction

The use of vaccines is a major success story in the field of public health. On the verge of global eradication of polio, eliminating polio from the remaining few countries has proven difficult. Local elimination efforts have focused on both fine-tuning vaccine design and developing strategies to attain intensive coverage of children. Here we review the history of polio eradication through the lens of transmission system theory.

The Global Polio Eradication Initiative has classified countries into four categories based on their elimination success [45]. Countries in Category A have had successful elimination with no subsequent outbreaks. This is the largest group including, by continent, the Americas, Australia, Western Europe, and large portions of both Africa and Asia. India, after continual eradication difficulty, has been recently classified into Category A. Countries classified as Category B have documented successful elimination with subsequent transient outbreaks. These countries are African countries near Nigeria, and Euro-Asian nations near India, Pakistan, and Afghanistan. Countries classified as Category C, Angola, Chad, Democratic Republic of the Congo, and Sudan, have had documented successful elimination followed by subsequent outbreaks and transmission detected for more than 12 months after the first subsequent outbreak [45]. The last group of countries, comprising Category D, has endemic polio transmission. These countries are Afghanistan, Nigeria, and Pakistan. We undertake here a dynamic systems analysis that helps explain how countries got into these different categories and what determines how they move between these different categories.

Poliomyelitis is a disease caused by the poliovirus that is characterized by acute flaccid paralysis. Poliovirus is transmitted fecal-orally and primarily causes gastroin-

testinal infection with minor or no symptoms. These infected individuals excrete virus into the environment where poor sanitation and high population density allows the virus to persist and transmit.

While polio immunity against paralysis does not wane substantially, immunity affecting susceptibility to infection and contagiousness does. Evidence of increasing susceptibility with waning immunity comes from antibody patterns [12, 13, 47, 66–76] and the relationships between antibody levels and protection against infection [77, 78]. Evidence of increasing contagiousness with waning immunity comes from: 1) an oral polio vaccine OPV challenge study demonstrating that individuals with prior wild polio virus WPV infection 40-50 years earlier excrete as much virus as completely susceptible individuals [12]; 2) an OPV challenge study in elderly populations demonstrating the association of excretion among previously vaccinated adults with antibody levels [79]; and 3) recently immunized children that excreted significant quantities of WPV [49, 80].

The two types of vaccines in use are the live virus OPV and the IPV. Both vaccine types provide immunity to paralysis [18] but OPV provides higher protection against infection and greater reductions in excretion during infection [14, 48, 49]. As a live virus, OPV is transmissible through the same routes as wild poliovirus and thus has added effects of reaching unvaccinated populations and boosting immunity in those previously infected or vaccinated. Unfortunately, mutated derivatives of circulating OPV can also cause paralytic disease [18]. Consequently, cessation of OPV is an important final step in eradication.

Though elimination in some countries with good sanitation has been achieved using an early childhood routine vaccination schedule, the national level elimination programs in other countries involve supplementary immunization activities (SIAs) reaching all children 5 and under on national immunization days.

The regions where polio elimination has been most difficult are heterogeneous in

terms of population size, density, sanitation, and vaccination coverage. For example, in northern India, which has very dense and extensive populations with poor sanitation, successful elimination required more than 15 SIAs per year in some areas. In contrast, a 2010 outbreak in the Congo occurred under conditions of low population density and low exposure to poor sanitation, but low vaccination coverage in a subset of the population [45].

To better understand what determines success or failure under these diverse conditions, we examine a dynamic model across a diversity of transmission conditions, vaccination levels, vaccine effects and vaccine transmissibility. Our model does not aim to capture any specific country scenario but rather describe the general phenomena of polio elimination.

3.3 Methods

The structure for our transmission model is shown in figure 3.1. Appendix B contains a detailed background of the development and structure of our model. We constructed a deterministic, compartmental model that included different levels of immune status between the recovered state and the fully susceptible state. These are seen model equations (B.2)–(B.5) in section B.2. We included separate infection compartments for WPV and OPV, assuming no concurrent infection, as shown in equations (B.7). OPV transmission was modeled relative to wild polio transmission using parameters that reduced contagiousness and duration of infection while maintaining the same susceptibility as WPV, as shown in equations (B.1) and (B.7)). Model parameters are described in table 3.1 (and in more detail in table B.1). Age compartments allowed for age-specific vital dynamics and vaccination programs that target children. Aging was modeled as a pure delay process consistent with past aging models in pertussis and measles [81, 82], for additional detail see supplementary material B.3.

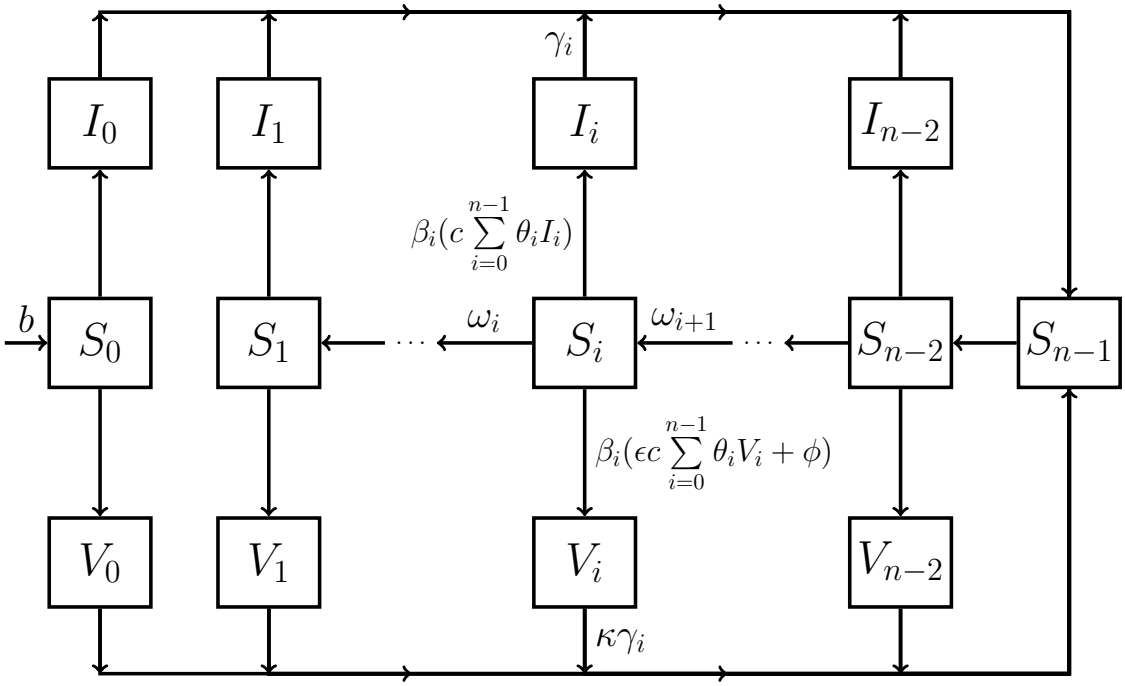

Figure 3.1: Graphical depiction of the transmission model without aging or vital dynamics (for details on vital dynamic implementation, see appendix B.3). The I compartments correspond to the wild poliovirus (WPV) infected population and the V compartments correspond to the oral polio vaccine (OPV) infected population. Each set of S, I, and V compartments are further broken down based on immunity stage, i, with n total immune stages. Individuals enter the population at rate, b, and have no immunity. The S_{n-1} state corresponds to full immunity and is achieved after infection caused by either OPV or WPV. Waning of immunity occurs as population transitions between S_i compartments, at rate ω_i, moving from higher immunity to lower immunity. We assume that complete loss of immunity is not possible. Levels of immunity are determined by immune stage, i, and affect susceptibility, β_i; contagiousness, θ_i; and recovery rate, γ_i. Force of infection is the product of the effective contact rate (a fully infectious contact given no immunity), c, and the linear combination of the relative contagiousness, θ_i, of each infected subpopulation times its density. Transmission of OPV is reduced compared to WPV by decreasing the contagiousness by factor ϵ and increasing the recovery rate from infection by factor κ. Infection due to OPV can also occur due to effective vaccination rate, ϕ. The parameters are also explained in table 3.1 and in greater detail in the appendix, section B.2.

Table 3.1: Polio transmission model parameters

Model Parameters	**Descriptions**	**Values**
i	Immune stage	1...n
j	Age group	1...m
n	Total immune stages	10
m	Total age groups	34
b	Birth rate into population (yr^{-1})	0.025[a]
c	Effective contact rate (yr^{-1})	40–200[b]
β_i	Relative susceptibility for immune stage, i	0–1[c,d]
θ_i	Relative contagiousness for immune stage, i	0–1[c,e]
γ_i	Relative recovery rate (yr^{-1}) for immune stage, i	10–40[c,f]
ω_i	Rate of immune stage change (yr^{-1})	0, 0.2, or 2[g]
ϕ_j	Effective vaccination rate (yr^{-1})	0–3
ϵ	Relative contagiousness OPV^h:WPV^h	0.15–0.45
κj	Relative recovery rate OPV^h:WPV^h	2.25–6.25
μ_j	Age-dependent death rates (yr^{-1})	[i]

[a]The birth rate, b, was set in relation to the death rate, μ_j, so that the population size is constant.

[b]The effective contact rate, c, was assigned using previously established R_0 values [18],along with our derived transmission model calculation of R_0 (table 3.2).

[c]Immunity response to susceptibility, contagiousness, and duration of contagiousness were assigned across their ranges of values using an exponential function (see section B.4 for more details).

[d]The immunity parameter for susceptibility, β_i, attenuates the infectivity of an effective contact on the susceptible population, where 1 defines no reduction (no immunity) and 0 defines no susceptibility (full immunity).

[e]The measure of contagiousness, θ_i, attenuates the force of infection due to the infected population, where 1 defines full contagiousness (no immunity) and 0 defines no contagiousness (full immunity).

[f]The recovery rate, γ_i, is defined according to observed ranges of shedding duration [14, 49].

[g]See section B.4 and table B.1

[h]Oral Polio Vaccine (OPV); Wild Polio Virus (WPV)

[i]See section B.3

Immunity reduces susceptibility to infection and also reduces contagiousness and duration of infection if there is reinfection. As immunity wanes (modeled as an underlying exponential process), susceptibility, contagiousness and duration of infection increase. As depicted by the S_0 compartment in figure 3.1, we assumed that individuals never fully lose immunity; i.e., only new members of the population, introduced at a fixed birthrate, were completely susceptible, shown in equations (B.2)–(B.3). Infection with WPV or OPV through either vaccination or OPV transmission resolves into full immunity, a short lived period where there is no susceptibility to reinfection, shown in figure 3.1 using flows from the infected populations (compartments I and V) into the susceptible compartment with highest immunity, S_{n-1}. As time since recovery increases (population flows across the S compartments in figure 3.1), susceptibility to reinfection increases and subsequent reinfection has increasing contagiousness and duration. After a reinfection, full immunity is regained. For more detail on the modeling of waning immunity see supplementary material, section B.4.

Unless otherwise stated, we assumed that susceptibility wanes to 50% compared to no immunity after 10 years. The immunity waning rates for contagiousness and duration were set to be equal to one-fourth the waning rate of susceptibility. An exploration of waning settings is shown in the appendix, section B.5.1. Initially, we fixed OPV transmissibility to 5% of WPV transmissibility. This value for OPV relative transmission was selected using criteria from Fine and Carneiro [18] such that circulating OPV, specifically for serotypes 1 and 3, would not sustain transmission. We then investigated a broader range of OPV transmission, including higher transmissibility consistent with serotype 2. Further, we investigated the effect of waning immunity by choosing values to examine the impact of waning on the dynamics for wide-ranging outcomes. The model parameters we varied for our analysis are shown in table 3.2.

To model vaccination we considered effective vaccination rates in contrast to actual

Table 3.2: Model factors varied in the analysis

Analysis Variable	**Description**	**Calculation**	**Range**[a]
Maximum R_0	Reproduction number in an immunologically naive population	c/γ_0	4–20[18]
OPV[b] transmissibility	Transmissibility relative to WPV[b] (%)	ϵ/κ	0–20[18]
Susceptiblity waning rate	Exponential waning rates (yr^{-1})[c]		0.04, 0.07, 0.1[d,e]
ϕ_j	Effective vaccination rates (yr^{-1}) in children (0-5 year olds)		0–3 [45, 48]

[a]Upper and lower bounds were selected as biologically plausible limits.
[b]Oral Polio Vaccine (OPV); Wild Polio Virus (WPV)
[c]See section B.4
[d]Waning rate values are not well defined and are, therefore, chosen to examine the impact of waning on the dynamics for wide-ranging outcomes. Additional values are explored in sections B.5.1 and B.5.3
[e]The susceptibility waning rates, 0.04, 0.07, and 0.1 per year correspond to losing 50% susceptibility after 17, 10, and 7 years, respectively.

vaccination rates. An effective vaccination rate corresponds to vaccination resulting in complete immunity. In reality, a dose of OPV may not induce an immune response and multiple OPV vaccinations are required to achieve full immunity [48]. The effective vaccination rate is thus less than the actual vaccination rate. Our major inferences did not change when we changed the model such that vaccines result in partial but increasing immunity from each vaccination. The pertinent analysis is presented in supplementary material section B.5.2.

We simulated polio transmission initially without vaccination until the model reached steady state dynamics. After achieving steady state, we introduced vaccination into the population. The target effective vaccination rate was achieved over an implementation time period where vaccine rates increased linearly from zero to the target level. The main analysis used a 2-year implementation time. Results for

10-year implementation are presented in supplementary material section B.5.3.

We numerically solved differential equations across a range of waning rates, relative oral polio vaccine transmissibility levels, effective vaccine rates, and the reproduction number, as shown in table 3.2. The reproduction number was calculated for a fully susceptible population with no vaccination and is approximately equivalent to the effective contact rate times the duration of infection. By monitoring prevalence levels over the course of a vaccination program we identified parameter ranges that correspond to difficulties in eradication across the countries described in table 3.3.

Modeling was conducted in Python using the SciPy module and figures were made in R using the lattice package.

3.4 Results

3.4.1 Explaining success in polio eradication efforts across country classifications

Figure 3.2 displays both short-term (3.2A) and long-term (3.2B) vaccination success across differing levels of R_0 and effective vaccination rates. We measured short-term success as the minimum prevalence in the first 50 years, such that the lower this minimum prevalence, the greater the short-term success. The ability to achieve low prevalence at any given time does not imply long-term success. We therefore measured long-term success as the final equilibrium prevalence. A low long-term prevalence is an indicator of stable elimination. Countries classified as Category A, based on the GPEI [45], generally have both short and long-term success. Countries classified as Category B and C are those countries with fragile short-term success, i.e., they achieved short-term success but have conditions for non-zero final prevalence. Category D countries have not achieved success in the short or long term.

The placement of countries onto figure 3.2 was based on country specific estimates

Table 3.3: Classification of countries in context of polio eradication initiative in 2012.

Country type	**Hygiene Status**[a]	**Examples**	**Eradication category**[b]	**R_0 ranges**[a]
Industrialized	Good	United States, Western Europe, Australia, etc.	A	4
Industrialized	Poor	South America, Russia	A	10
Developing	Poor	Egypt, Eastern Europe, Northern Africa, Middle Eastern Countries, etc.	A	12
Developing	Dense & poor	India	A	14–18
Developing	Poor	Horn of Africa (e.g., Congo, Uganda)	B	8–12
Developing	Poor	Central Asia (e.g., Tajikistan, Turkmenistan)	B	10–14
Developing	Poor	Angola, Chad, Democratic Republic of the Congo, and Sudan	C	8–12
Developing	Poor	Afghanistan, Nigeria, and Pakistan	B	14–18

[a]Country type, hygiene status, and R_0 values chosen from Fine & Carneiros polio transmission review [18].

[b]Country classification based on the Global Polio Eradication Initiative [45]. Category A corresponds to countries that have achieved eradication; category B describes countries that have achieved eradication but have transient epidemics; category C describes countries that have achieved eradication but have re-established transmission; and category D describes countries that have not achieved elimination.

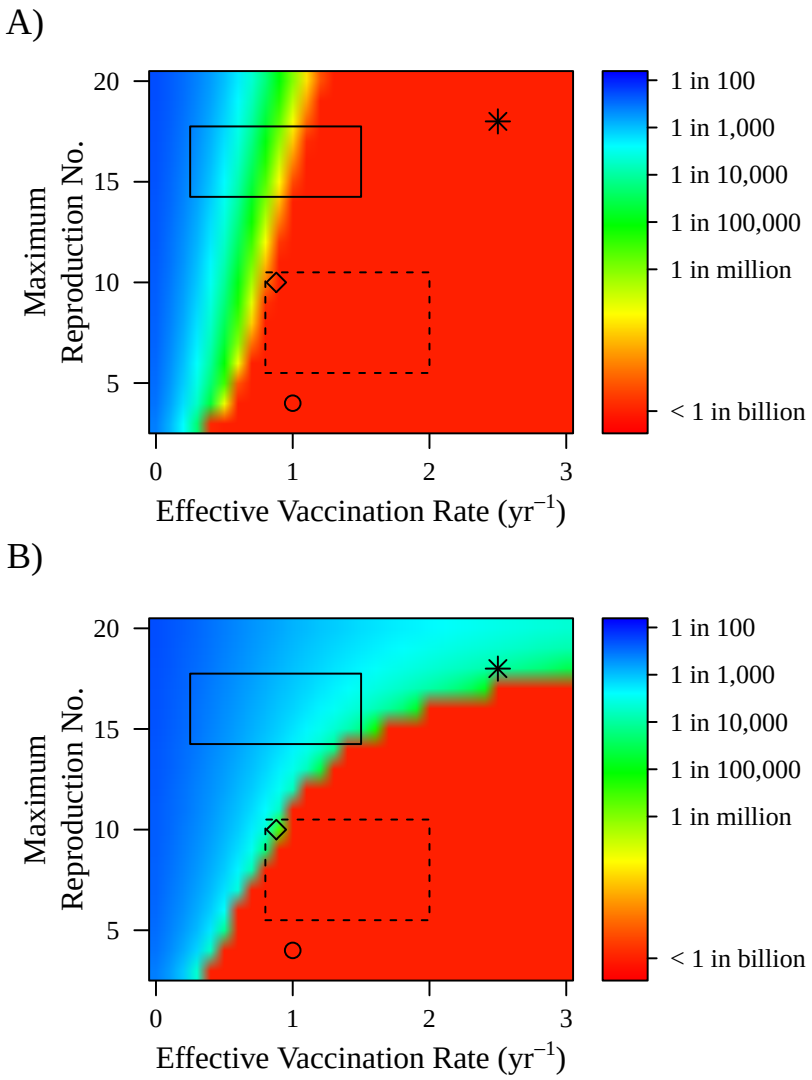

Figure 3.2: A) The minimum prevalence reached in the first 50 years due to the initial vaccine implementation (a measure of short-term success) and B) the final prevalence resulting from the vaccination program (a measure of long-term success), across R_0 and effective vaccination rates per year for all children under 5. OPV transmissibility is set to 5% of WPV transmissibility. Waning rates are set such that it takes 10 years to reduce susceptibility by 50%. The circle represents the United States, the asterisk represents regions of India (Uttar Pradesh and Bihar), and the diamond represents Xinjiang, China. The dashed rectangular box represents China and the solid rectangular box represents the endemic countries: Afghanistan, Pakistan, and Nigeria. Values for R_0 and effective vaccination rates were selected qualitatively and are discussed in the section 3.4.1. Divergence in prevalence levels between A) and B) does not necessarily predict future outbreaks or endemicity but indicate potential fragile short-term eliminations.

for R_0 and vaccination rates. R_0 values were selected using data from Fine & Carneiro [18]. We crudely selected effective vaccination rates for categories and countries using the Global Polio Eradication Initiative criteria [45] by considering enhancing factors such as SIAs deployment and mitigating factors such as poor coverage or take-rates. Category A countries comprise diverse conditions but generally have lower transmission conditions with adequate vaccination coverage. The United States is shown on figure 3.2 with a small, stable R_0 due to its low transmission conditions and a 100% vaccination rate to illustrate a consistent, effective vaccination program. In contrast, Bihar and Uttar Pradesh of India are presented in figure 3.2 as having very high transmission conditions and very high vaccination levels. The yearly vaccination rate of 2.5 was selected to represent full coverage plus at least one fully effective booster.

With a recent outbreak in Xinjiang, China is an example of how Category B and C conditions emerge from Category A countries. China is large nation with varying transmission conditions so we selected a range of R_0 values for figure 3.2 consistent with those presented for both types of industrialized nations in table 3.3. The outbreak in Xinjiang has been attributed to importation and falling vaccination rates [46] so we illustrate potential effective vaccination rates ranging from enhanced (greater than 1) to reduced (less than 1). While the 2011 outbreak was an isolated incident in China, its placement in figure 3.2 demonstrates that other Category A nations with a higher R_0 or lower vaccination coverage may be at increased risk to emerge as Category B or C countries due to importation.

The category D countries (Afghanistan, Nigeria, and Pakistan) are depicted with moderate transmission levels but poor coverage, consistent with the difficulty programs have had in adequately vaccinating their remaining endemic regions. Afghanistan and Pakistan are grouped together due to their linked transmission conditions through importation [45].

In figure 3.2A, the short-term success of the vaccination program show decreasing

prevalence as vaccination increases for a given R_0. For low values of R_0, low minimum prevalence levels (figure 3.2A) correspond to low final prevalence levels (figure 3.2B) suggesting stable elimination under these conditions. However, at higher levels of R_0 where we still see low minimum prevalence levels, we no longer see low long-term prevalence suggesting that the initial drop in prevalence due to vaccination is not maintained and the probability of resurgence is increased. A further exploration of model dynamics associated with the rebound epidemics is presented in the appendix B.5.4.

To better understand what causes the increasing divergence between figure 3.2A and 3.2B at increasing levels of R_0, we need to consider waning immunity and reinfection dynamics, where reinfection is defined as WPV infection that occurs after a first infection caused by WPV transmission, OPV transmission, or OPV vaccination [15]. At high R_0, when vaccination is implemented, the combination of vaccine effectiveness and immunity boosting through reinfection causes an immediate sharp decrease in prevalence. However, if the vaccine levels are not high enough to push prevalence to zero, the waning of immunity eventually increases the number of susceptible individuals providing a means for virus circulation through reinfection epidemics. On the other hand, when R_0 is low, the prevalence reduction after vaccination implementation is not highly dependent on immune boosting through reinfection. Therefore, for low levels of R_0, vaccination levels of children do not have to reach very high levels in order to get below the population threshold for transmission illustrated in figure 3.2B.

3.4.2 Role of OPV transmission

Increasing OPV transmission from 2.5 to 20% of WPV results in a large reduction in the vaccination rates required to reach low or zero prevalence at equilibrium (figure 3.3). The reduction in required vaccination levels is particularly evident for high R_0

levels. These increased levels of OPV transmission correspond to serotype 2 vaccination which is known to be much more transmissible than the serotypes 1 and 3 [18]. At high levels of vaccine transmission, immunity is boosted in those previously infected reducing the overall transmission potential. Results for reducing relative OPV transmission to 0% are shown in the appendix B.5.5.

3.4.3 Role of waning immunity

Figure 3.4 illustrates final prevalence for faster and slower waning immunity rates. If waning immunity is slow, for example, it takes 17 years to reach 50% susceptibility (left half of figure 3.4), reaching elimination prevalence levels requires much less vaccination coverage than if waning is faster, for example, it takes 10 (figure 3.3) or 7 years to reach 50% susceptibility (right half of figure 3.4) for given levels of R_0. Further, by exploring across OPV transmissibility levels for each of these waning levels, we observe the importance of the boosting that occurs from OPV transmission. Even when immunity waning is fast, if relative OPV transmission is 20% that of WPV transmission, eradication is still achievable at an R_0 of 20 for effective vaccination rates around 3 per year or higher. Since waning immunity can significantly reduce the long-term efficacy of vaccination, this analysis highlights a range where it is important to understand these underlying dynamics.

3.4.4 Reinfection contributions to transmission at endemic equilibrium

Figure 3.5 illustrates the proportion of the force of infection attributable to reinfection across varying levels of reproduction numbers and vaccination rates. Reinfections are infections of WPV that occur after previous infection due to an earlier WPV infection, OPV infection, or vaccination. For lower levels of OPV transmissibility when vaccination levels are greater than 1 per year and elimination is not reached, the proportion of the force of infection that are due to reinfections rises above 50%.

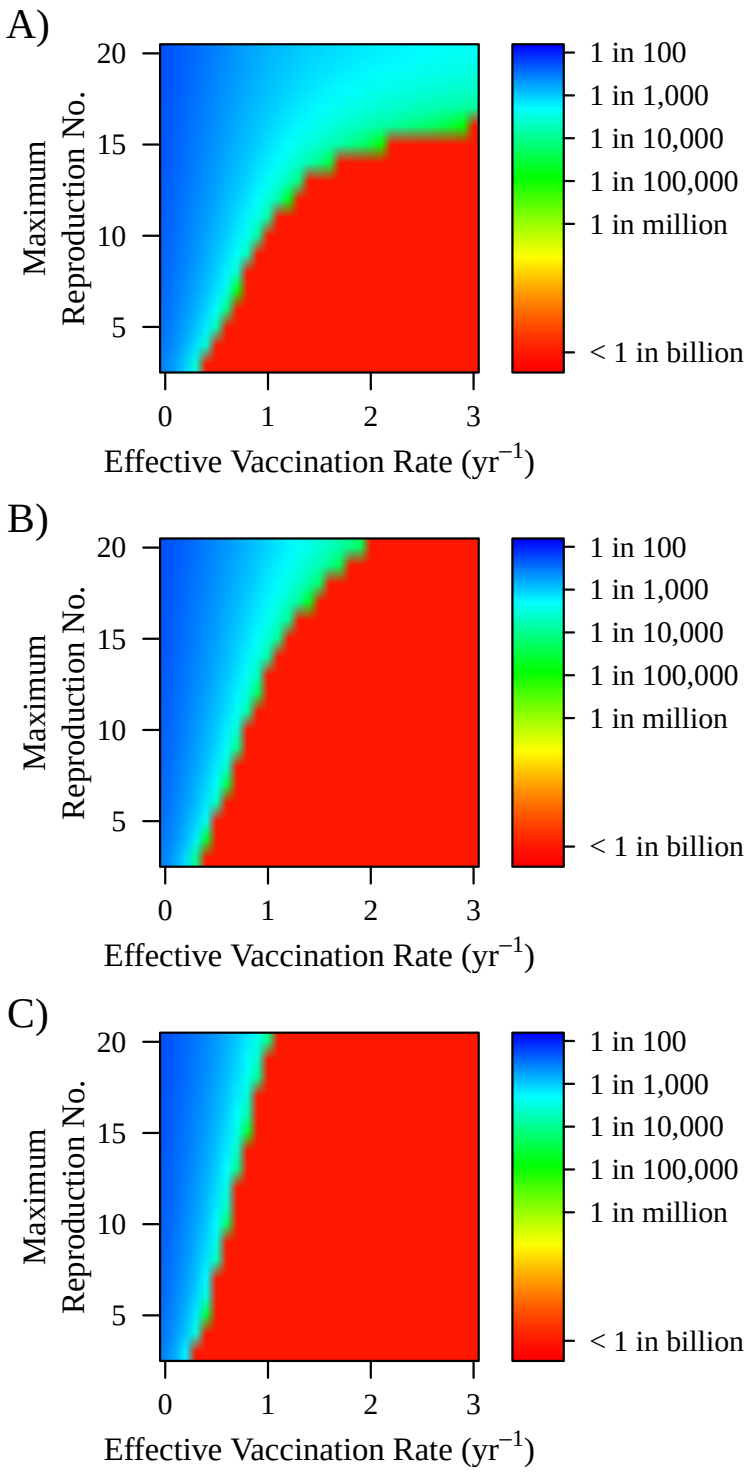

Figure 3.3: Final prevalence across vaccination rate and R_0 where oral polio vaccine (OPV) transmissibility relative to wild poliovirus (WPV) transmissibility is set to A) 2.5%, B) 10%, and C) 20% of OPV transmissibility. Waning rates are set such that it takes 10 years to reduce susceptibility by 50%, contagiousness of any resulting infection by 16% and duration of any resulting infection by 16%.

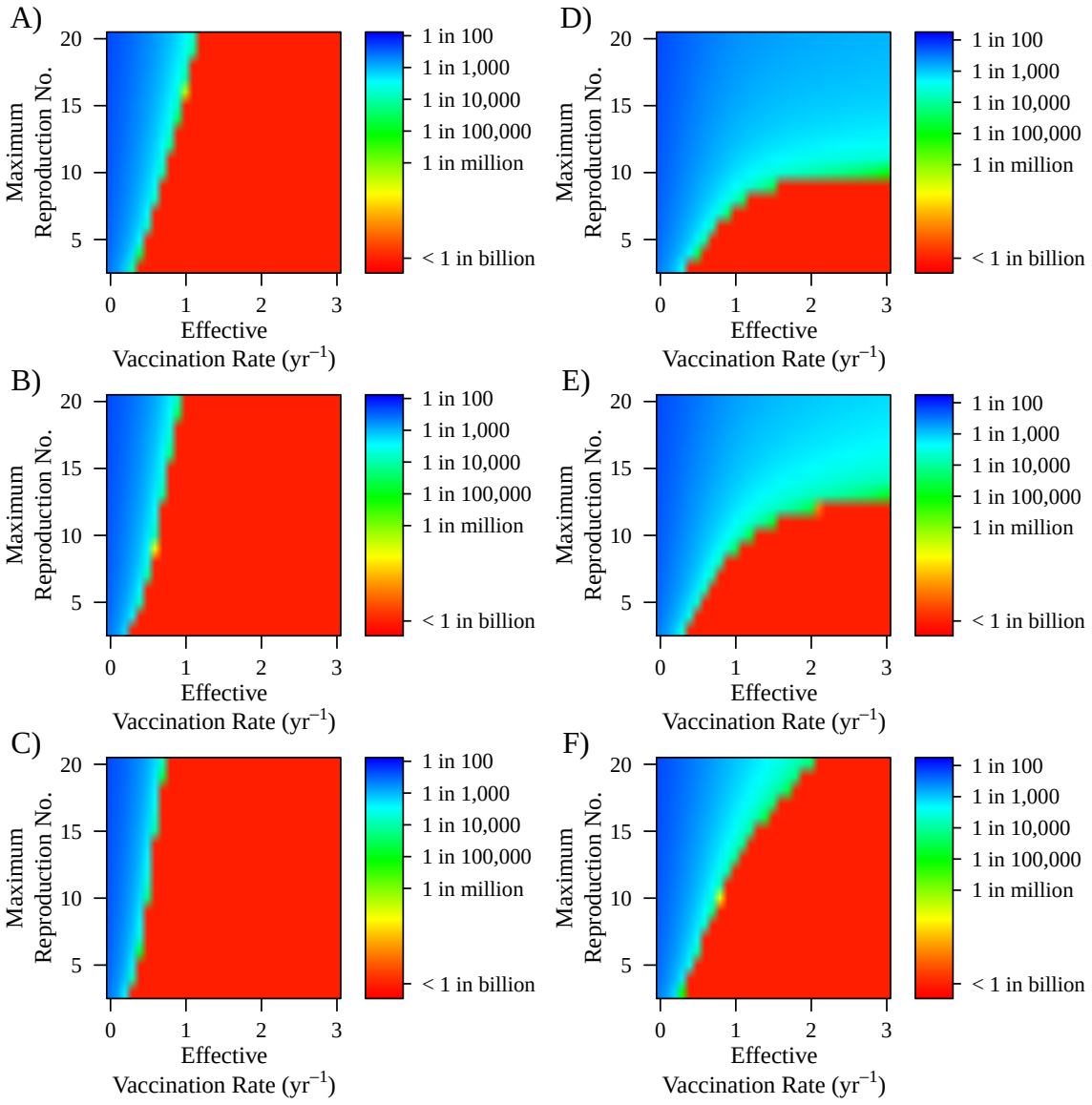

Figure 3.4: Final prevalence across vaccination and R_0 where by column, waning rates increase from slow (A, B, C: it takes 17 years to reach 50% susceptibility) to fast (D, E, F: it takes 7 years to reach 50% susceptibility); and by row, oral polio vaccine (OPV) transmissibility relative to wild poliovirus (WPV) transmissibility increases from 2.5% (A, D) to 10% (B, E) to 20% (C, F).

When relative OPV transmissibility reaches 20%, elimination occurs under conditions where at lower OPV transmissibility levels transmission was dominated by reinfection. OPV transmission prevents immunity from waning to the level where reinfection transmission is important. Specifically, in conjunction with figures 3.2 and 3.3, we can conclude that the final prevalence under high transmission conditions and high vaccination rates was maintained by reinfection transmission from aging populations experiencing waning immunity. This illustrates the importance of boosting immunity in populations with waned immunity.

3.5 Discussion

Global polio eradication is in its final stages. To ensure success, intensive efforts are needed in the few remaining countries. The analyses we have presented help demonstrate how reproduction numbers, transmissibility of OPV, immunity waning rates, and vaccination rates contribute to successes and failures. While our analytic approach cannot describe or predict the specific course of any nations elimination effort, it does help illustrate dynamics that should affect control decisions. Most importantly it reveals the fragility of elimination in high R_0 areas, how reinfection contributes to that fragility, and how high levels of OPV transmission counteract the fragility related to reinfection potential.

Worldwide eradication success has been achieved by targeting children. In countries with high levels of sanitation, the success was swift. In nations with poor sanitation, such as Egypt, India, and Bangladesh, success has been less swift, but has been possible. Supplementary immunization activities SIAs on national immunization days have been important for success under these more difficult conditions. SIAs revaccinate children many more times than routine immunization would. Since revaccinated children can excrete vaccine poliovirus [80], the resulting OPV transmission boosts immunity in unvaccinated children and in individuals whose waning

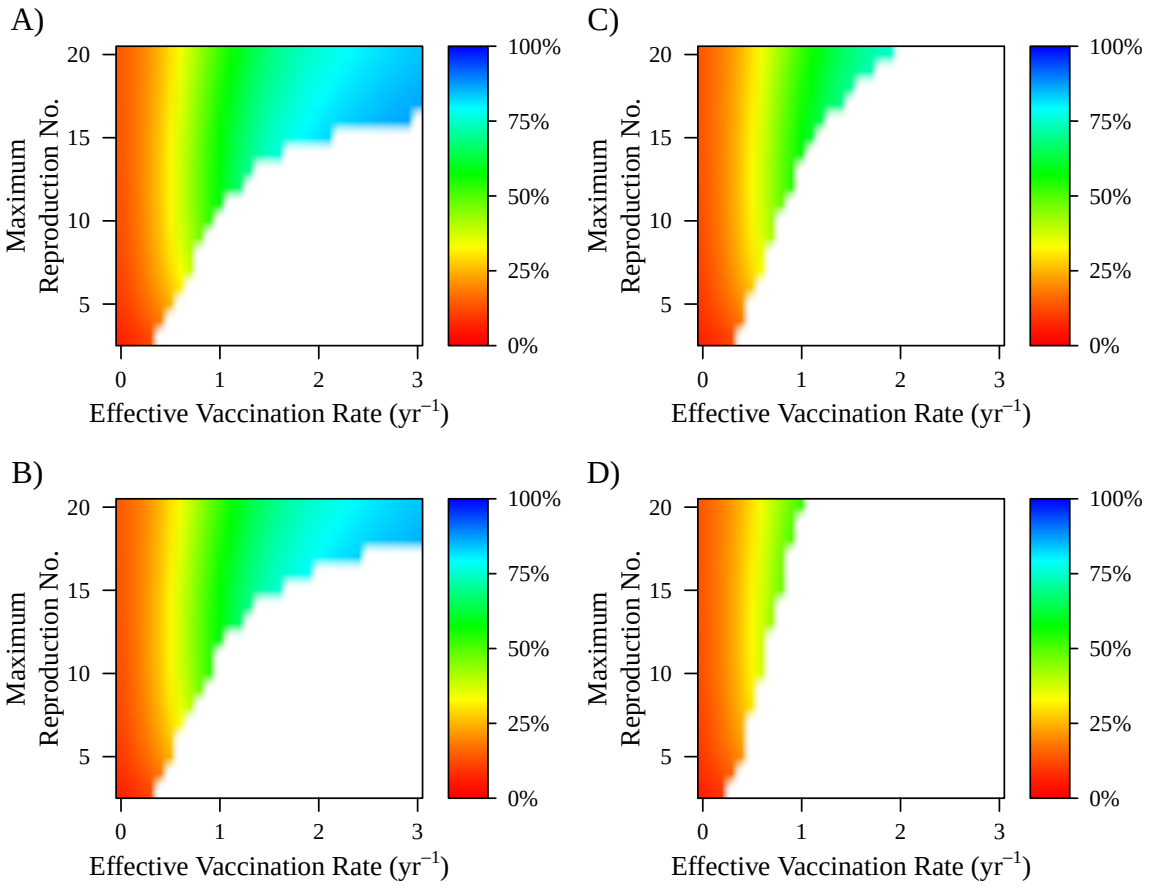

Figure 3.5: Depiction of proportion of the force of infection that are due to reinfections across vaccination rate and R_0 where oral polio vaccine (OPV) transmissibility relative to wild poliovirus (WPV) transmissibility is set to A) 2.5%, B) 5%, C) 10% and D) 20%. Reinfection is defined as WPV infection that occurs after an initial infection caused by an earlier WPV infection, vaccination, or infection due to OPV transmission. Waning rates are set such that it takes 10 years to reduce susceptibility by 50%, contagiousness of any resulting infection by 16% and duration of any resulting infection by 16%. In the white areas of the graph, there is not sustained transmission to calculate the force of infection (i.e., prevalence equals zero).

immunity might otherwise bring them to a state where they could be infected by and transmit WPV.

When OPV is highly transmissible, low levels of prevalence can be achieved in high transmission conditions with less than extreme vaccination coverage; this is true even for faster waning immunity and higher R_0. At high transmission (R_0) levels in figure 3.2B, the low levels of prevalence induced by the initial vaccine implementation have rebounded into considerably higher endemic equilibrium levels that are not observed when OPV transmissibility is high (figure 3.3C). When OPV transmissibility is low, under endemic conditions of high vaccination and high transmission, the force of infection is largely attributable to reinfection (figure 3.5). By increasing the transmissibility of the OPV strain, we eliminate transmission attributable to reinfection by effectively boosting populations with waned immunity. That is, asymptomatic adult populations with waned immunity may be important factors in transmission and their impact can be reduced by re-contracting vaccine strain poliovirus.

The final stages of eradication for WPV serotype 1 and 3 can be characterized by difficulties that did not affect the eradication of serotype 2. The increased efficacy of tOPV for WPV serotype 2 is clearly one important factor [45] accounting for the success in type 2 eradication, but our analysis illustrates that lower levels of vaccine strain transmission contribute to the difficulties in achieving eradication. When transmissibility of the vaccine strain is lower, as it is in poliovirus serotype 1 and 3 [18], vaccination strategies affecting the potential for reinfections to transmit should be considered. Besides focused SIAs, another strategy might be to add a single booster for adults in high transmission regions. Such a campaign would be costly and potentially difficult to implement but could contribute to success in regions where elimination remains in a fragile state. Furthermore, the importance of OPV transmission highlights the care that must be taken when ceasing OPV vaccination such as maintaining high quality surveillance. The potential for cVDPV needs to be

minimized in the final stages of eradication. Since IPV has been shown to induce mucosal immunity through boosting in previously OPV immunized populations [83, 84], IPV might be a candidate vaccine for boosters in older populations that could reduce cVDPV risks.

Our model of waning immunity uses a simple exponential process where OPV or WPV vaccination always results in complete immunity. It is possible that altering this assumption could affect our inferences about what is leading to success or failure in eradication efforts. If immunization can result in incomplete immunity then SIAs may experience success due to ensuring comprehensive coverage of under-immunized children. Furthermore, the evidence of waning of immunity through decrease in antibody levels, particularly in high transmission regions, could stem from nuances not addressed in our analysis. These include factors known to affect polio immunization such as malnutrition, concurrent enteric infections, and vaccine tolerance [83]. The extent to which these factors play a role deserves to be analyzed in future dynamic transmission system frameworks.

Because our model used a continuous, deterministic framework the continuous population assumption allows our transmission system to reach trivially low prevalence levels temporarily. In reality, when prevalence reaches very low levels, demographic stochasticity would lead to transmission cessation. Additionally, the deterministic nature of our model prevents us from modeling outbreaks in eliminated regions due to sporadic importation, a topic previously analyzed [85]. Nonetheless, our deterministic analysis shows how category A countries with high transmission conditions are still at risk for epidemics due to re-introduction of virus; i.e, we can discern problematic parameter regions where prevalence can reach very low levels due to initial vaccine implementation but maintain long-term prevalence (figure 3.2).

The polio vaccine has been a public health triumph since its first implementation over 50 years ago. Hoping to follow the success of the smallpox eradication program,

the polio eradication program has eliminated polio in most of the world, removing a terrible and debilitating disease from the memories of most living populations. With a handful of remaining endemic countries on the cusp of eradication, we are on the verge of a major public health victory. Our model highlights some of the potential challenges that have prevented success in the final phase of polio elimination. We hope that by better understanding the dynamics driving transmission we can improve the design of future public health initiatives to eradicate infectious diseases.

3.6 Publication and acknowledgments

This work has been accepted for publication by the American Journal of Epidemiology [86]. Contributing authors to this research were Bryan T. Mayer, Joseph N. S. Eisenberg, Christopher J. Henry, M. Gabriela M. Gomes, Edward L. Ionides, and James S. Koopman. We would like to thank the editors and reviewers for their contributions. We would also like to thank Rick Riolo and the Center for the Study of Complex Systems at the University of Michigan, Ann Arbor, for allowing us to use their computing resource; and Dr. Ethan Romero-Severson for his contributions to editing.

CHAPTER IV

Migration and polio eradication

4.1 Abstract

Reaching polio eradication has been difficult in the remaining endemic nations: Afghanistan, Nigeria, and Pakistan. Failure in these regions has been attributed to both "vaccine failure" and "failure to vaccinate." "Vaccine failure" corresponds to the difficulty of oral polio vaccine to properly induce immunity in certain populations. "Failure to vaccinate" describes conditions where vaccination implementation is poor. Vaccine implementation has been an issue in these endemic nations where governance has been poor, populations are mobile, and there is cultural aversion to vaccination. We developed a polio transmission model incorporating waning immunity and transmission of oral polio vaccine allowing for migration between populations. Through migration, we allow transmission conditions and vaccination policies of one region to affect vaccination effectiveness in another region. Our analysis demonstrated that migration from populations with poor vaccination implementation can mitigate the effectiveness of implementing vaccination campaigns and make reaching elimination more difficult. Where India achieved success by targeting hard to reach mobile populations, the remaining endemic regions could achieve success invoking similar strategies. Furthermore, success in these regions may be aided by complementary interventions such as improvement in sanitary conditions or vaccinating older populations.

4.2 Introduction

Persistent polio transmission in Afghanistan, Pakistan and Nigeria is the final challenge of global eradication. The recent epidemics in Niger, Tajikistan, the Republic of Congo, and China, however, underscore the tenuous nature of elimination. Polio importation and lapses in vaccination coverage can create susceptibility pockets where outbreaks can flourish highlighting the need to establish successful vaccination programs [46]. Two factors are critical for eradication: the biological efficacy of the intervention and effective implementation. These factors have been characterized as "vaccine failure" and "failure to vaccinate", respectively [52, 87]. In this paper, we explore how "failure to vaccinate" impedes polio elimination across regions through migration.

"Vaccine failure" can occur in several contexts: 1) the vaccine attenuates disease but not viral shedding, 2) the vaccine fails to induce immunity (i.e., low take-rates), or 3) induced immunity wanes over time. Both IPV and OPV provide immunity to paralysis but OPV induces higher protection against infection and greater reductions in excretion during infection [14, 17, 48, 49]. Therefore, to reduce polio transmission, OPV is used in transmissive regions. Failure to induce and maintain immunity is an important factor in polio eradication difficulty. Reduced take-rates have been observed in highly transmissive regions due to a variety of factors (*e.g.*, malnourishment, competing enteric infection, poor immune response) [48, 83, 87]. Duration of immunity is also limited where immunity to excretion induced by OPV has been shown to wane over time [14, 79, 80].

In India, elimination difficulty was largely attributed to "vaccine failure" [52, 53, 87] because OPV take-rates were lower than expected in high transmission regions [48, 83]. However, recent elimination in India shows success is possible under these conditions. To overcome vaccine efficacy limitations, vaccination implementation efforts were ramped up substantially to focus on under-vaccinated children,

undercovered villages, and hard to reach migratory populations [29]. The success of this strategy demonstrates the importance of "failure to vaccinate."

The concept of "failure to vaccinate" extends beyond the biological properties of the vaccine. The inability to properly vaccinate populations depends on demographics, politics, culture, and governance [52]. Further, vaccination implementation failure can occur at any population level ranging from villages to nations. Prior to the change in campaign strategy in India, lower vaccination rates were observed in rural migrants in northern India [30]. These mobile population were a major focus of the successful campaign [29]. Through their success, India potentially demonstrates the importance of vaccination implementation in undercovered subpopulations.

The remaining endemic nations of Afghanistan, Pakistan, and Nigeria face a combination of problems. Failure to achieve elimination in Pakistan and Nigeria has been attributed to both "vaccine failure" in high transmission conditions [87] and "failure to vaccinate" due to population aversion to vaccination [51, 52] and failure of governance to adequately ensure vaccination [53]. While the Global Polio Eradication Initiative made progress in Pakistan during 2012 [50], violence against health workers has created volatile security situations potentially impeding progress [45]. Failure to eliminate polio in Afghanistan has defied straightforward characterization. Recent reviews of the current status of polio eradication attribute failure in the southern region of Afghanistan to internal conflict and border migration with Pakistan [87]. However, Afghanistan has implemented a suitable vaccination program evidenced by success in northern regions [46, 52, 53]. Thus, it remains unclear whether persistent transmission in the southern regions can be attributed to higher transmission conditions, poor vaccination coverage, low vaccine efficacy, immigration from Pakistan, or some combination of these factors.

Migration is an important population feature of all of the remaining endemic regions. Genetic evidence has shown consistent transmission between Afghanistan and

Pakistan [54], where there is a long history of migration across a porous border [88]. Furthermore, Afghanistan and Pakistan have asynchronous vaccination campaigns where Afghanistan has had mild success in northern regions [46, 52, 53] but Pakistan has been inconsistent [46, 53] and recently plagued by violence against public health officials [45]. Nigeria has high levels of combined immigration and emigration [89] and is known to seed outbreaks in surrounding regions [45, 46]. Furthermore, these mobile populations tend to have poor vaccination coverage [26].

We have previously developed a polio transmission model incorporating components of "vaccine failure" through waning immunity in a single population framework where "failure to vaccinate" described reduced vaccination rates [86]. We demonstrated that achieving short-term success is possible even under high transmission conditions through initial vaccination. However, reaching elimination in the short-term may be the result of fragile stochastic die-out where long-term transmission is possible. When vaccination lapses, outbreaks must be handled or prevented by deploying mass vaccination campaigns requiring quality surveillance [85]. Migration connects regional populations and thus may enhance the detrimental effects of both "vaccine failure" and "failure to vaccinate."

The nature of global polio transmission has now fundamentally changed. Where at one time immunity from natural exposure and vaccination allowed us to reach elimination thresholds in most regions of the world, countries with eliminated transmission now rely on vaccination alone for continued population immunity [46]. While non-endemic countries remain at risk, maintaining elimination will be a continued and increasing cost on public health programs. Thus it is urgent to achieve elimination goals which is accomplished by understanding the difficulties in the remaining endemic nations. In this work, we expand our previous model of polio transmission to explore how "failure to vaccinate" in certain regions may impede elimination in other regions through migration.

4.3 Materials and methods

4.3.1 Migration model construction

Our polio migration model was constructed as a deterministic, compartmental transmission system accounting for 1) vaccine transmission, 2) waning immunity, 3) age, 4) varying vaccination rates, and 5) migration. The model presented here is an extension of the transmission model constructed in chapter III and thus topics 1) – 4) are covered in extensive detail in section 3.3 and appendix B.

To model migration, we considered two connected populations: a source population and a destination population. Each subpopulation was constructed with the same structure as the polio transmission model presented in chapter III. Here we focus on unidirectional migration as depicted in figure 4.1. Unidirectional migration is an atypical assumption in migration models (see section 1.2.2.5) but is a subset of multi-population models where the populations are not fully coupled. Our model is applicable to scenarios where the destination population cannot influence the source population. This could describe rural-urban migration where poor, rural migrants settle in developing urban areas, a scenario common in northern India [30], Pakistan [90], and Nigeria [26]. Furthermore, the model can be also be interpreted where the source population represents an abstract pool of migratory individuals coming from different transmission conditions with variable vaccination levels. In either case, vaccination rates and transmission conditions in the destination population do not influence source populations.

The rate of migration, α, was modeled as a log rate in contrast to an exponential rate because yearly population percent changes were more conventional and interpretable. For example, if α is 0.01, then that is interpreted as a migration rate of 1% per year. We assumed that migration is not differential by infection because polio tends to be asymptomatic. We assumed that the total overall population size was

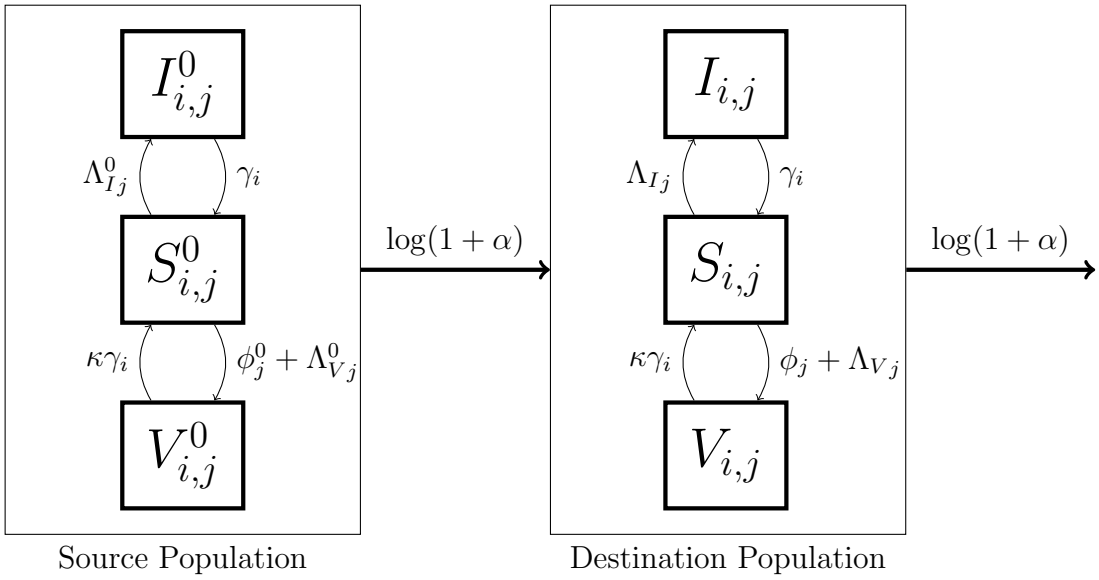

Figure 4.1: Two population migration model with one population migrating into another. Each subpopulation has susceptible, infected, and vaccinated populations. Subpopulations and rates with superscript zero denote heterogeneities between the two populations. For the forces of infection, Λ^0, the only parameter that was varied between the populations was the contact rate, c. Parameters and rates for polio transmission in each subpopulation are described in table 3.1. Parameters and rates specific to migration population are described in table 4.1.

fixed. Details on the model equations associated with migration are in appendix C.1.

4.3.2 Migration model analysis

The source and destination population differ by transmission conditions and vaccination rates. Parameters specific to the migration model are presented in table 4.1.

We assumed that birth rates, death rates, immunity waning rates, and OPV transmissibility were equivalent across the source and destination population. If birth and death rates were different between the populations, we expect that the populations would have different R_0 values. However, because the vital dynamic parameters are small relative to the contact rate and infection duration, the R_0 calculation (table

Table 4.1: Migration model parameters

Migration Parameters	**Descriptions**	**Values**	**Interpretation**
α	Migration rate (% yr^{-1})	0.001–10[a]	
c^0	Contact rate in source population (yr^{-1})	c	same[b]
		40	low
		100	medium
		200	high
ϕ_j^0	Vaccination rate in source population (yr^{-1})	0	no program
		0.75	suboptimal
		1	complete
		2	intensive

[a]Wide ranged used as a sensitivity analysis. See Appendix for more details on migration rates.
[b]The destination population contact rate, c. See table 3.1

3.2) is not sensitive to small changes in birth or death rates.

Waning rates and OPV transmissibility are functions of the vaccine. Vaccine efficacy varies across nations, specifically with respect to inducing immunity (take-rates) [83], and is partially captured by varying the effective vaccination rates between populations. However, we assumed that if a vaccination was successful (*i.e.*, resulted in induced immunity) then waning was the same across populations. We fixed the waning rate such that it takes 10 years to reach 50% susceptibility, consistent with the main results presented in our previous single population analysis [86]. Results for a wider range of waning rates is presented in appendix C.2.1. We modeled vaccine transmissibility relative to WPV and do not expect the relative relationship to vary across populations. We fixed OPV transmissibility to be 5% of WPV. This is similar to type 1 and 3 WPV [18], the remaining wild strains in endemic nations. Circulating vaccine-derived polio virus (cVDPV) in Nigeria closely represents type 2 strain (which has higher transmissibility), and therefore we presented a short analysis of higher OPV transmissibility in the appendix C.2.2.

To explore the effect of migration between interconnected populations, we varied the migration rate across five orders of magnitude ranging from 0.001% to 10% yr^{-1}. Current net migration rates for Afghanistan, Nigeria, and Pakistan range between -3 and 8 per 1000 persons per year [91]. Because we aim to infer the effect of migration on transmission dynamics in a given population, we use a wide rate range to capture outcomes ranging from very low to very high levels of migration.

The goal of our analysis was to assess how poor vaccination programs of one population could affect another population. Therefore, in the destination population, we evaluated the influence of effective vaccination rates on prevalence levels under varying conditions of R_0 allowing migration from a source population with unique vaccination rates and R_0 levels (figure 4.1 and table 4.1). The effective vaccination rates in the source population were selected to be 0, 0.75, 1, and 2 yr^{-1} corresponding to no program, suboptimal coverage, complete coverage (100% coverage with no yearly boosting) and intense coverage, respectively. R_0 levels in the source population were chosen to be either the same as the destination population or fixed at 4, 10, and 20 corresponding to low, medium, and high, respectively.

To assess vaccination program success, we constructed a measure incorporating the prevalence levels under a given vaccination rate for varying R_0 conditions. Specifically, we evaluated vaccination effectiveness by measuring the maximum R_0 where a given vaccination rate reduces the population prevalence level below a target value. For the target prevalence level, we selected a conservative cutoff of 1 in a one million where the magnitude of infected individuals would be quite low given a real population size.

To evaluate how migration affects vaccination programs, we focused on the dynamics of the destination population and assumed the source population was at steady state. We conducted the model simulation as follows: 1) we simulated the source population under vaccination until steady state; then 2) we simulated the destination population under migration with no vaccination until steady state; and then 3) we

introduced vaccination into the destination population over a linear implementation period of 2 years until the target vaccination level was reached. Prevalence in the destination population was assessed at two times: 1) at the minimum value induced by initial vaccination; and 2) at the final steady state level.

All modeling was conducted using Python with the lsoda algorithm in the *Numpy* module. Figures were made in R using the *ggplot2* and *lattice* packages.

4.4 Results

4.4.1 Vaccination effectiveness with no migration

Vaccination effectiveness was measured by determining the highest R_0 where a given vaccination rate can achieve a target prevalence of 1 in one million. Specifically, this illustrates the highest transmission conditions where a vaccination policy can achieve the set goal. Vaccination effectiveness, however, may vary over time where initial vaccination can reduce prevalence to very low levels but higher long-term prevalence levels are possible. Figure 4.2 displays both the initial (4.2A) and long-term (4.2B) effectiveness of a vaccination program when there is no migration. Initial effectiveness was determined using the minimum prevalence within 50 years of vaccination implementation and long-term effectiveness was determined using the steady state final prevalence. Divergence between the minimum and final prevalence occurs under high transmission conditions when vaccination does not achieve elimination. Under these conditions, long-term transmission is sustained by reinfection dynamics [86]. However, by achieving low levels of prevalence through initial vaccination, elimination may result from stochastic or probabilistic die-off. In this scenario, divergence in effectiveness highlights conditions where elimination my be fragile. Thus, transmission and vaccination levels that demonstrate effectiveness in the short and long-term demonstrate potential for stable elimination.

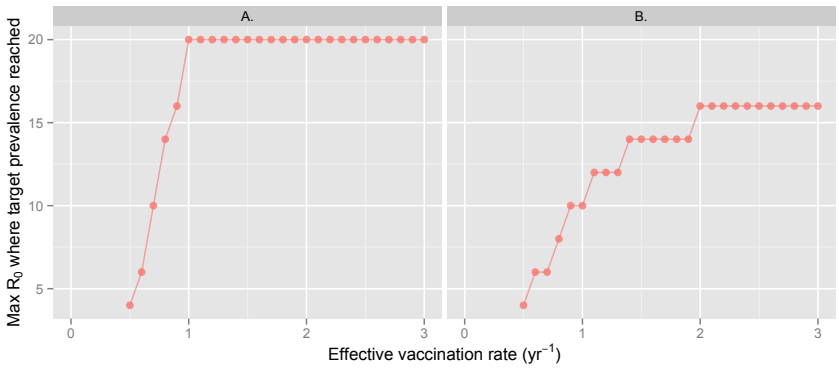

Figure 4.2: **Vaccination effectiveness**. Vaccination program effectiveness for a given effective vaccination rate determined by A.) the minimum prevalence reached within the first 50 years of vaccine implementation and B.) the final prevalence resulting from the vaccination program. Oral polio vaccine (OPV) transmission was set to be 5% as transmissible as wild poliovius (WPV) and waning rates were set such it takes 10 years to reach 50% susceptibility. Vaccination effectiveness was measured, for a given effective vaccination rate, as the maximum R_0 (up to 20) where a target final prevalence of less than 1 in a million was reached. R_0 conditions where the target prevalence is reached initially but not in the long-run illustrate potential fragile elimination conditions.

4.4.2 Vaccination effectiveness depends on vaccination in migrating populations

When migration is introduced, achieving the target prevalence levels depends on the vaccination rate and transmission conditions in the source population (figure 4.3). When there is no vaccination program in the source population, achieving the target prevalence is not possible unless there are low transmission condition and low migration levels. Thus, in regions where migratory populations are an important component of the population, leaving large portions of mobile populations complete unvaccinated is absolutely detrimental to the overall vaccination program.

Both short and long-term vaccination effectiveness in the destination population is reduced due to migration unless there is intense vaccination coverage in the source population. Short-term effectiveness (initial success) describes the immediate impact

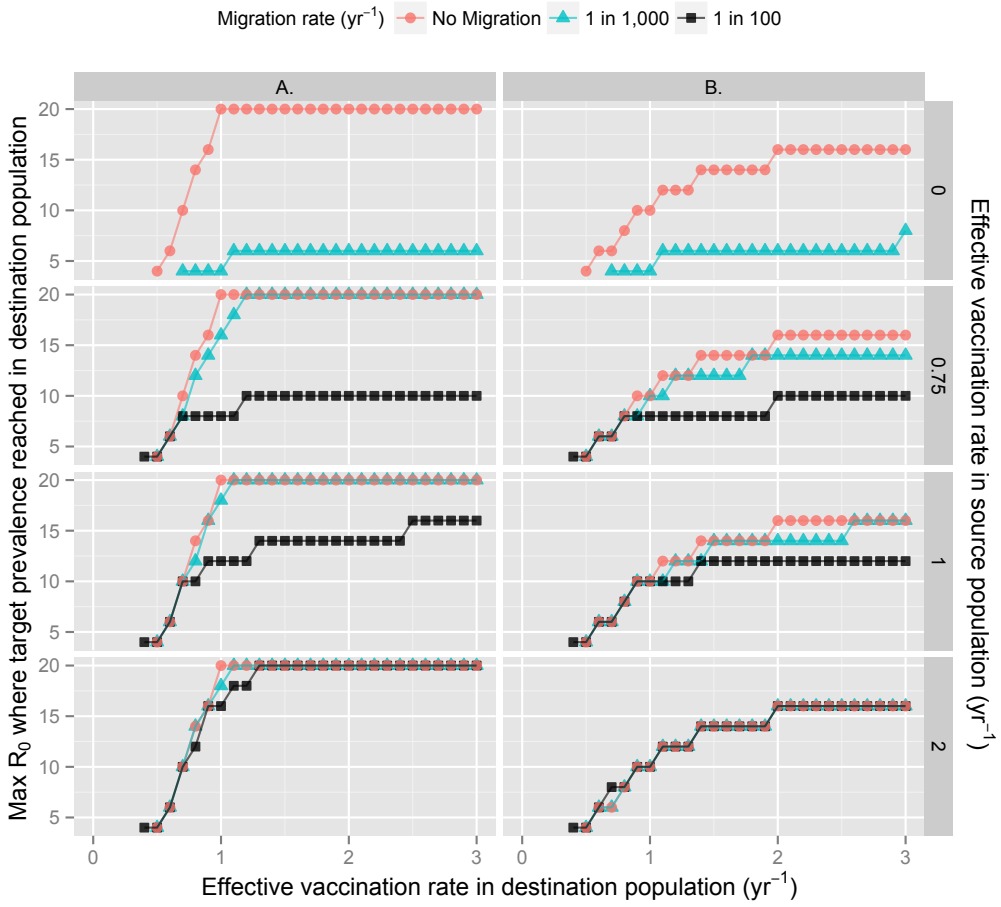

Figure 4.3: **Vaccination effectiveness under migration across similar populations**. Vaccination program effectiveness for a given effective vaccination rate in the destination population across varying vaccination levels in the source population (table 4.1) and migration rates. The source and destination population share the same transmission conditions. Vaccination program effectiveness was determined by column A.) the minimum prevalence reached within the first 50 years of vaccine implementation; and column B.) the final prevalence resulting from the vaccination program. Oral polio vaccine (OPV) transmission was set to be 5% as transmissible as wild poliovius (WPV) and waning rates were set such it takes 10 years to reach 50% susceptibility. The absence of lines indicates that reaching the target prevalence was not possible under the given conditions.

of introducing a vaccination program in the destination populations (column A in figure 4.3) and long-term effectiveness is a measure of whether stable elimination can be expected under the given vaccination program (column B in figure 4.3). In general, compared to the initial success of vaccination implementation, achieving stable elimination is more difficult, particularly in moderate to high transmission conditions (figure 4.2) where source population vaccination is important under migration (figure 4.3). When coverage is complete in the source population, achieving short-term success is possible under moderate transmission conditions but requires much higher vaccinations rate than if there was no migration. Long-term success in moderate transmission conditions requires higher levels of source population vaccination.

When migration reduces vaccination program effectiveness, there is less divergence between short and long-term success. This occurs because achieving the target prevalence, either initially or at equilibrium, is difficult for high transmission conditions when migration occurs from a poorly vaccinated source population. Therefore, under conditions where migration is impeding success, the most useful interventions should focus on overall transmission conditions and vaccinating migratory populations.

In highly mobile regions with similar transmission conditions, the effect of vaccination is sensitive to the coverage in migratory populations. Intense campaigns hoping to quickly reduce prevalence in one region may have less than desirable effects if connected regions are under-vaccinated. Furthermore, while long-term program success is already difficult in moderate and high transmission conditions, it is more difficult under conditions of migration from poorly vaccinated populations. Overall, populations under high transmission conditions with poorly vaccinated incoming migratory populations will experience elimination difficultly without accounting for both problems.

4.4.3 Migration from high transmission conditions may greatly impede vaccination effectiveness

When evaluating vaccination effectiveness in the destination population, increasing the transmission conditions in the source population mitigates the effect of increasing vaccination in the both populations (figure 4.4). When the source population comes from medium transmission conditions (column B. in figure 4.4), less source population coverage is required to achieve an effective program in moderate transmission conditions than when compared to migration from the same or high transmission conditions. When migration occurs from high transmission conditions (column C. in figure 4.4), intense coverage in the source population is critical to vaccination effectiveness in the destination population where high vaccination levels are also required. These results demonstrate that when migratory populations come from high transmission conditions, greater levels of vaccination are necessary in both the source and destination population while effectiveness is reduced. Under these conditions, generally implementing successful vaccination programs becomes much more difficult. It is therefore crucial to not only ensure that migratory populations are well vaccinated but that other strategies to reduce transmission are considered.

4.4.4 Migration from low transmission conditions

When there is migration in the model, the effect of migrating populations from a source population with low R_0 conditions is minimal on vaccination effectiveness in the destination population (figure C.5 in the appendix). Migration has no effect at complete coverage levels in the source population. This indicates that low transmission populations under vaccination programs are not a major hindrance on other populations' elimination efforts.

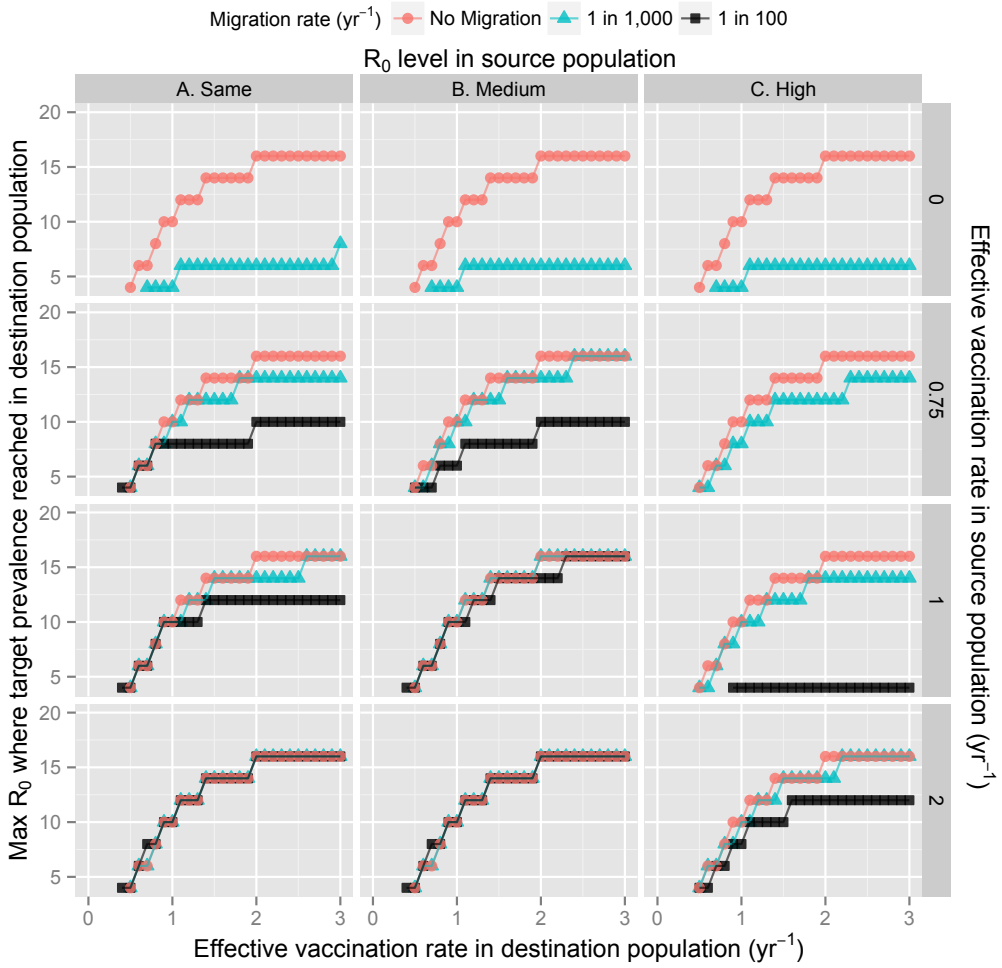

Figure 4.4: **Long-term vaccination effectiveness under migration across populations with different transmission conditions**. Vaccination program effectiveness for a given effective vaccination rate in the destination population across varying vaccination levels and transmission conditions in the source population and migration rates (table 4.1). Transmission conditions in the source population were set to be column A.) the same as the destination population; column B.) medium (R_0=10); or column C.) high (R_0=20). Long-term vaccination effectiveness was measured, for a given effective vaccination rate, as the maximum R_0 (up to 20) where the final (steady state) prevalence in the destination population was less than 1 in a million. Oral polio vaccine (OPV) transmission was set to be 5% as transmissible as wild poliovius (WPV) and waning rates were set such it takes 10 years to reach 50% susceptibility. The absence of lines indicates that reaching the target prevalence was not possible under the given conditions.

4.5 Discussion

4.5.1 Model application to the remaining endemic countries

Achieving polio eradication is a global effort dependent on reaching elimination in the three remaining endemic nations: Afghanistan, Nigeria, and Pakistan. By exploring migration, we contextualized polio transmission dynamics across interdependent populations specifically focusing on how heterogeneous vaccination policies and transmission conditions affect vaccination success. When regions "failure to vaccinate," they may impede campaigns in other regions. Our model illustrates the extent to which this failure impacts regional campaigns due to migration.

Elimination in India has been attributed to implementing high vaccination coverage and switching to monovalent OPV, which induces better immunity against the remaining wild strains [29]. There was specific focus on finding internal migratory populations and ensuring that they were routinely vaccinated. Our model reaffirms the success of this strategy where an increase in effective vaccination rates in both the destination and source populations are crucial to ensuring that prevalence levels are decreased even in high transmission conditions. However, under these transmission conditions, the elimination may be fragile and the region may be capable of sustaining transmission again in the future. Thus it becomes increasingly important to sustain the effort in India while reaching elimination in the remaining endemic nations.

When migratory flows come from high transmission conditions, it becomes more difficult to achieve elimination even with high levels of vaccination. Evidence shows that Pakistan and Afghanistan continually transmit across borders [54] and that Pakistan sustains high transmissions conditions similar to those that India experienced [87]. Furthermore, there are high levels of internal migration in Pakistan [90]. Our analysis indicates that under high transmission conditions, elimination in Pakistan requires that they implement a good vaccination program. Interruption of vaccination

programs due to poor governance or violence may be a serious hindrance in achieving elimination in Pakistan and potentially in border regions of Afghanistan. Lapses in coverage not only make elimination difficult or impossible but also creates conditions where importation to other regions becomes more likely.

Nigeria, the only African nation with endemic polio, periodically seeds outbreaks in neighboring nations [45, 46]. The difficulties in achieving elimination within Nigeria can be attributed to many issues including population aversion to vaccination in northern regions [92], high transmission conditions, poor coverage and immunity levels [87], high levels of combined immigration and emigration [89], and poor vaccination coverage in mobile populations [26]. Recently, Nigeria has worked to increase its vaccination coverage but still remains endemic [46]. In the context of our migration model, Nigeria may comprise a worst-case scenario. Reduced population immunity may indicate poor take-rates (low effective vaccination) or fast waning rates. High population mobility may indicate high migration levels between regions or urban centers potentially comprising source and destination populations with low vaccination rates. Particularly, reaching stable elimination may be difficult, and intense campaigns without blanket coverage may not even achieve initial success. A campaign similar to that of India may find success in Nigeria, but a sustained effort has historically proven difficult. Additional interventions may be desirable to find short-term success including efforts to improve public health in general (*e.g.*, reducing poor sanitation conditions) or adult boosting with IPV. IPV boosting (following previous immunization OPV) may be effective in inducing mucosal immunity [83, 84] and is not a risk for cVDPV, another major concern in Nigeria [45, 46].

4.5.2 Model limitations

The limitations and assumptions of our single population polio transmission model have been previously described [86]. Additional simplifying assumptions were re-

quired to characterize migration in this framework. While migration rates could be independent of polio infection, migration may be age-based or seasonal. In regions with large rates of migration like Afghanistan, families tend to migrate together [93], so age may play a smaller role in determining migration rates. However, because vaccination campaigns target children, age-dependent migration rates may elucidate scenarios for susceptible or infected adults to play an important role in transmission through importation. Because importation outbreaks are rarer, probabilistic events, they are better modeled using a stochastic model.

Our model utilizes unidirectional migration which assumes that connected populations are not fully coupled. In this case, policy and conditions in the destination population cannot affect the source population. This may apply to circumstances where migrants are unlikely to return to their home population (*e.g.*, rural to urban migration). Abstractly, this model can be interpreted such that the source population is a pool of potentially hard to reach migrants thus demonstrating that these poorly vaccinated populations can have detrimental effects on their destination population. A contrasting scenario would be work-based or refugee migration between interconnected regions where people or families may spend a significant time in multiple populations but are likely to return to their home population within a short period of time. Synchrony between fully coupled populations may demonstrate scenarios where migration is beneficial, as demonstrated in an SIR model analysis with vaccination [25]. However, from our analysis, looking at scenarios where the source population has a higher vaccination rates than the destination population (figures 4.3 and 4.4), there are not general conditions where migration is beneficial, particularly for moderate to high transmission conditions in the destination population.

Compared to assessing initial dynamics in the single population model [86], more assumptions were required to define the initial success of vaccination implementation in the migration model. In our approach, we assumed the source population was

already at steady state. This implies that the source population has stable transmission dynamics and that its vaccination implementation does not affect the destination population. An interpretation of this scenario would be that the migratory populations in the destination population are missed by campaigns or routine coverage of the region. Thus, in this context, there are no ramp-ups in coverage in the source population that would affect the destination population. Abstractly, we are assessing how the average population of migrants affects their destination population. We do not make inferences regarding increasing campaigns in both populations but rather focus on the impedance of poorly vaccinated migrating populations on their destination population. The alternatives to this approach are potentially complicated (*e.g.*, partial synchronous coverage increases in both populations) and may be better applied to models that apply to scenarios where there is coupling between the source and destination populations.

We assumed migration was a deterministic, continuous process. Thus our model may not be appropriate for mass migration events or rare migration events. We explored our model over five orders of magnitude of migration rates to assess our results over a wide range of phenomena associated with increasing migration. Based on this sensitivity analysis, migration becomes an important factor between migration rates of 0.1% and 1% per year and so our main results focused on these values. When migration rates were set to 1 in 100,000 yr^{-1}, the effect of migration was entirely lost demonstrating that the continuous nature of the model does not necessarily overstate the effect of slightly connected populations. This model was not designed to predict outbreaks based on sporadic viral importation which should be modeled using a stochastic approach [85].

4.6 Conclusions

The current era of the polio eradication initiative is concurrently triumphant and frustrating. Achieving elimination in India demonstrated that success can be achieved in high transmission conditions among difficult to target populations. The strategy in India illustrates the importance of efforts that address both "vaccine failure" and "failure to vaccinate." The remaining endemic regions, under more varying transmission conditions, have been described by similar difficulty to achieve coverage, particularly with variable governance and cooperation. By highlighting the importance of interconnectedness in polio transmission dynamics, we demonstrated that connected populations require synchronous efforts to ensure broad and complete coverage. Furthermore, achieving elimination is aided substantially by targeting migratory populations that tend to have lower coverage. In high migration and high transmission regions, additional sanitation interventions may substantially increase the likelihood of success. As public health officials act with urgency, ramping up coverage and specifically targeting hard to reach populations in Pakistan and Nigeria potentially holds the final key to eradication success.

CHAPTER V

Conclusions and future work

5.1 Summary

In this work, we developed and analyzed dynamic models of infectious diseases at the host, population, and multiple population level. We assessed host immunity at these levels to demonstrate the importance of host biology in disease modeling. At the host level, differing exposure patterns may elicit different risks of infection due to the innate immune response (chapter II). At the population level, immunity levels affect success of vaccination programs in polio transmission due to reinfection dynamics (chapter III). At the multiple population level of polio transmission, vaccination programs may be impeded by migration from populations with poor vaccination coverage (chapter IV).

5.1.1 Conclusions from Chapter II

In chapter II, we developed a dynamic dose-response model that accounted for differing exposure patterns to assess how the immune response affects the risk of infection. Because infection systems vary with respect to pathogen, host, and contact site, pathogen clearance rates may depend on exposure patterns. We 1) illustrated the versatility of the dynamic dose-response model for risk calculations across varying exposure scenarios; 2) developed a method to fit the model parameters to time-series

data using a survival likelihood; 3) applied the model to the anthrax infection system; 4) showed that infection risk of anthrax is invariant to exposure patterns given the available data; and 5) recommended dose-response experiments that can demonstrate when risks vary by exposure patterns.

The dynamic dose-response model was developed to allow the risk of infection to be sensitive to dose-timing effects. This was accomplished by including dynamic pathogen clearance due to the initial immune response. This framework is an extension of the IAH, the classic assumption for dose-response models that any single pathogen has an independent, non-zero risk of initiating infection. Specifically, while any single pathogen can initiate infection, we allowed the joint pathogen probability of infection to vary depending exposure patterns. The model was also designed to be versatile for contexts when risk is invariant to exposure patterns.

To use the model as a risk assessment tool, we developed a survival analysis approach for fitting the model parameters to time-series data. We applied this approach to anthrax using previously collected time-series data. In this analysis, we demonstrated how to apply the model to imperfect data through the use of censoring intervals, incorporation of biological properties of the pathogen, and profile likelihood techniques. We then identified recommendations for future experiments that can demonstrate when risk depends on exposure patterns. Our dose-response model is ideal to analyze these experiments because it also identifies when risk is invariant to exposure patterns.

Based on our results, risk of anthrax infection is only slightly dependent on exposure patterns. We therefore conclude that risk assessment with respect to anthrax depends more on the total amount of spores released rather than on how it was released. The risk calculations from our model were consistent with past dose-response models of anthrax demonstrating that our model is a viable tool for risk assessment.

5.1.2 Conclusions from Chapter III

In chapter III, we developed a transmission model to assess both successes and failures in polio eradication. To model polio transmission, we developed a model focusing on waning immunity and transmission of OPV. We concluded that 1) short-term success is possible through vaccination implementation; 2) long-term transmission is driven by reinfection dynamics at high vaccination rates when elimination is not achieved; and 3) OPV transmissibility acts as a population booster mitigating the effects of reinfection. Our conclusions imply that additional interventions, such as adult boosting or improvement in sanitary conditions, may enhance eradication efforts.

In this analysis, we explored short-term and long-term outcomes of vaccination implementation. Initial vaccination implementation is capable of reducing prevalence levels to very low levels. This is possible even under high transmission conditions and fast waning immunity through the use of high vaccination rates. However, these regions can still sustain long-term prevalence levels through reinfection transmission.

By varying OPV transmissibility, we demonstrated that population boosting through vaccine transmission attenuates reinfection transmission thus reducing the elimination threshold. This is consistent with the notion that elimination of WPV type 2 was aided heavily by a highly transmissibility vaccine strain. Furthermore, the effectiveness of boosting indicates that expanding vaccination to older population could substantially reduce population transmission capacity.

5.1.3 Conclusions from Chapter IV

In chapter IV, we extended the transmission model in chapter III to include migration. We demonstrated that vaccination effectiveness can be reduced due to migration from populations with variable vaccination policies and transmission conditions. Specifically, we showed that under migration, 1) short and long-term vaccination ef-

fectiveness require adequate vaccination in the migratory populations; 2) migration from high transmission conditions makes vaccination success difficult; and 3) reduction in transmission conditions could substantially aid vaccination success.

We then applied our analysis to explain success in India and failure in the remaining endemic regions; Nigeria, Afghanistan, and Pakistan. In India, recent elimination was achieved by increasing vaccine efficacy and targeting internal migration [29]. Our model analysis demonstrated that these are the key components in achieving elimination under high transmission conditions with high migration rates. Nigeria has demonstrated how poor vaccination coverage can continually prevent achieving elimination. Afghanistan and Pakistan describe connected populations with dissimilar transmission conditions where migration may be impeding vaccination programs [87]. Our model suggests that success in the remaining endemic regions may rely on focusing on hard to reach, migratory populations. In combination with chapter III, intense vaccination campaign or additional intervention efforts may be crucial to reduce polio transmission and achieve eradication.

5.2 Future Work

5.2.1 Applications and extensions of the dynamic dose-response model

The dynamic dose-response model has potential for many future applications. It has been used to design an experiment assessing time-dependent risk of tularemia and analyze the outcome data (data unpublished). In this context, our model is a simple tool for more complicated risk assessments. Specifically, it can be used to both evaluate time-series dose-response data and make risk inferences for scenarios that involve variable exposure patterns.

Further extension of the dynamic dose-response model involves implementation into transmission models. Transmission models generally make simplifying assump-

tions about the risk of transmission. For environmentally mediated transmission systems, exposure and risk are a function of different routes of exposure such as air, fomites, or food contamination. The dynamic dose-response model provides a framework to differentially characterize risk based on varying exposures. Further, transmission model sensitivity to time-dependent risk could be assessed by implementing different parameterizations of the dose-response model.

Lastly, the framework of the model could be extended to include activation of the adaptive immune system. This would have importance in transmission systems were exposures occur continuously over long periods of time (e.g., regions with poor sanitation). Furthermore, transmission risk could be additionally characterized by partial immunity. For vaccination, the extended model with adaptive immunity could be used to assess optimal schedules for vaccination requiring periodic boosting.

5.2.2 Extensions for the polio transmission model

The waning immunity framework implemented in chapters III and IV is a simplistic realization of the actual waning process. One important extension of the modeling framework is to inform experiments to better quantify the waning immunity process. Then the next step would be implementing more complicated immunity structures into the transmission model to assess robustness to immunity assumptions. If immune response varies between WPV and OPV, model inferences may be affected. A better described waning immunity framework may be extended to other pathogens with vaccination and partial immunity, such as measles and pertussis.

The next extension to the polio transmission model includes the relaxation of the continuous, deterministic model framework. To properly assess stochastic die-off, the model needs to be implemented as a discrete, stochastic model where elimination is an outcome from initial prevalence reduction due to vaccination implementation. Furthermore, vaccination was modeled as a continuous, effective rate. Our analysis

demonstrated robustness to a vaccine that induced partial immunity where boosting was required to reach full immune status. However, mass immunization campaigns do not occur continuously and may be best modeled by using vaccination rates and coverage that occurs discretely or as a periodic pulse. At the population level, vaccination does not occur continuously throughout the year and coverage lapses may occur in random pockets of the population. Lastly, the migration model had similar simplifying assumptions where modeling migration as a stochastic process may be a better characterization of movement between populations particularly if migratory populations are small relative to the destination population size.

Combining the work from all of the chapters, the polio transmission model could be extended to include environmental transmission, a reservoir from stable and migratory populations, where risk of infection is calculated using the dynamic dose-response model. Ultimately, using the extended dose-response model with adaptive immunity, risk in environmentally transmitted polio could be characterized by both time-dependent exposure patterns and variable partial immunity levels.

5.3 Public health implications

5.3.1 Dynamic dose-response modeling

Dynamic dose-response models in general have important applications as a public health tools. We have demonstrated the use of the model as a risk assessment through the analysis of anthrax. For epidemiological models, exposure through the environment can elicit differing exposure patterns. Using the dynamic dose-response model can therefore adjust for varying risk from heterogeneous exposures patterns in both transmission models and risk assessments. There is also potential use for the model to study vaccine protocols. For multiple-dose live vaccines, the use of this dynamic dose-response modeling framework could elucidate proper dosing schemes that will

ensure optimized vaccine boosting.

5.3.2 Global polio eradication

Eradicating polio would constitute an major public health triumph. The use of transmission models allows public health officials to characterize the causal processes of transmission and assess intervention efforts. Using our polio transmission model, we assessed the successes and failure of the polio eradication campaign. Particularly, through exploration of waning immunity and transmission of the vaccine, we demonstrated that reinfection dynamics may be the driving component of transmission when vaccination levels do not achieve elimination under high transmission conditions. We further demonstrated, through the migration model, that eradication campaigns are joint efforts and lagging nations may impede efforts in other nations. Using our model analysis, we made public health recommendations focusing on expanded adult vaccination, additional interventions, and targeting mobile populations. While these recommendations were made for polio eradication, they are also applicable to future eradication campaigns.

APPENDICES

APPENDIX A

Additional material for a dynamic dose-response model to account for exposure patterns in risk assessment: a case study in inhalation anthrax

A.1 Functional families for time-dependent dose function

This section aims to mathematically formalize the idea of time-dependence when analyzing dose-response. We examine implications of the time-independence assumption given that the immune system is a dynamic process that affects the risk of infection; i.e., the infection outcome due to one pathogen particle depends on the state of the hosts immune system, which in turn is determined by prior exposure to pathogens. Let F be the candidate function for dose-response that represents the risk of infection for a sequence of n doses, d, inoculated at time intervals Δt. For simplicity, we assume that doses are evenly spaced. Under the condition that the time between inoculations tends to zero, the candidate function F can be represented as

$$F(\{d_{t_0+i\Delta t}\}_{i=0}^{n-1}) = F(\sum_{i=0}^{n-1} d_{t_0+i\Delta t}) \quad \text{when } \Delta t \to 0 \tag{A.1}$$

In this case, the probability of infection is equivalent to the probability of the accumulated dose. Because the time between inoculations is so small, the immune system does not have time to react to the initial doses, and therefore, the infectivity can be characterized as a single accumulated exposure. For large time intervals, the inoculations are so sparse that before a new inoculation arrives the immune system has time to clear out the previous inoculated dose, and therefore, go back to equilibrium. In this case, the probability of infection for the sequence corresponds to the evaluation of n independent events; i.e. the probability of infection of a given dose is independent of the previous doses. This condition is represented as

$$F(\{d_{t_0+i\Delta t}\}_{i=0}^{n-1}) = 1 - \prod_{i=0}^{n-1} (1 - F(d_{t_0+i\Delta t})) \quad \text{when } \Delta t \to \infty \tag{A.2}$$

Finally, we have the non-extreme case, where the time intervals are neither short nor long. This condition is represented as

$$F(\{d_{t_0+i\Delta t}\}_{i=0}^{n-1}) < F(\{d_{t_0+j\Delta t}\}_{j=0}^{n-1}) \quad \text{when } \Delta t_i > \Delta t_j \tag{A.3}$$

The risk of infection decreases as the time between inoculation events increases. Longer intervals between inoculation events imply more time for the immune system to clear out the pathogens from previous doses. When a new dose arrives the immune system is still actively engaging pathogens from the first dose, and the number of remaining pathogens depends on the time interval between inoculations. The longer

the time between inoculations, the fewer pathogens that remain, and consequently, the more likely the immune system is to successfully eliminate the pathogens and prevent infection. The canonical dose-response model used in microbial risk assessment and in environmentally-mediated transmission models is the exponential. In this model, the probability of infection depends solely on the dose, and consequently, the state of the individuals immune system prior to the doses exposure is not considered. Given a dose, D, and risk parameter, k, the risk of infection from a single pathogen is

$$\Pr_{\text{Inf}}(D) = 1 - \mathrm{e}^{-kD} \tag{A.4}$$

The probability of infection is one minus the probability of no infection, which is the probability that none of the D independent trials with a probability, k, are positive. In the exponential model, the probability of infection of a single pathogen, k, is estimated from data of empirical dose-response trials, and by definition, it is independent of previous inoculation events.

To assess whether or not the exponential model is a good candidate for F we demonstrate that the risk of infection predicted by the exponential is the same regardless of the time interval between inoculations. The following example illustrates the implications of this *time-independence*. Two individuals are inoculated with a pathogen following the standard procedure of empirical dosing trials. Subject a is exposed to one pathogen every week for twenty years, which add up to 1040 total pathogens. Subject b receives the same dose, 1040 pathogens, in the course of 5 minutes. If the probability of infection is time-independent, both subjects should have the same probability of becoming infected. This extreme example illustrates the potential problems of not taking time between inoculation and the immune system into account in calculating the risk associated to a dose. One might expect the immune

system to be able to efficiently deal with a single pathogen every week, as opposed to dealing with 1040 pathogens at once. In more realistic examples the timing of inoculation may also have a significant impact on risk estimates. It is unlikely that an inoculation in a real scenario is a singular, isolated event, but rather a sequence of events at different time intervals and different dosage.

One way to capture these dynamics is by using a stochastic process model that accounts for interactions of pathogens and immune particles[10]. However, such a detailed individual-level model is computationally too complex to integrate into population level transmission models. Events in the immune system such as the growth of pathogens and deactivation of pathogens by immune particles occur at faster time scales than the events of the transmission models such as individuals making contact and recovery from infection. Furthermore, a detailed model of the pathogen-immune particle interactions requires a model of the immune system for each individual in the population.

A.2 Closed-form risk and dose calculations when $\alpha = 1$

When $\alpha = 1$, the solution to the integral of $P(t)$ can be described as a closed form solution. Recall from § 2.3.3 that for $\alpha = 1$, the solution to the differential equation (2.1) can be given as an exponential function

$$P(t) = 1 - d\mathrm{e}^{-t\gamma} \tag{A.5}$$

Now consider a sequence of n inoculations given over n time points as discussed in § 2.3.3. To evaluate the total effective dose, we need to integrate our dosing function over the entire exposure course up to a final time point, T. Note that we assume the first dose, d_0, occurs at time, $t_0 = 0$.

$$\int_0^T P(t, \{d_i\}_{i=0}^{n-1})\mathrm{d}t = \int_0^{t_1} d_0 \mathrm{e}^{-\gamma t}\mathrm{d}t + \int_0^{t_2-t_1} d_1' \mathrm{e}^{-\gamma t}\mathrm{d}t + \cdots + \int_0^{T-t_{n-1}} d_{n-1}' \mathrm{e}^{-\gamma t}\mathrm{d}t \tag{A.6}$$

where we define d_i' as the remaining dose plus the current dose at time, t_i, calculated by

$$\begin{aligned}
d_0' &= d_0 \\
d_1' &= d_0 \mathrm{e}^{-\gamma t_1} + d_1 \\
d_2' &= d_0 \mathrm{e}^{-\gamma t_2} + d_1 \mathrm{e}^{-\gamma(t_2-t_1)} + d_2 \\
&\cdots \\
d_{n-1}' &= d_0 \mathrm{e}^{-\gamma t_{n-1}} + d_1 \mathrm{e}^{-\gamma(t_{n-1}-t_1)} + \cdots + d_{n-2} \mathrm{e}^{-\gamma(t_{n-1}-t_{n-2})} + d_{n-1}
\end{aligned}$$

We can simplify these calculations further such that for any given inoculation point, i, when $\alpha = 1$, we can calculate the remaining pathogen level as

$$p_i = \begin{cases} 0, & i = 1 \\ \sum_{j=1}^{i-1} d_j \mathrm{e}^{-\gamma(t_i - t_j)}, & i > 1 \cap \alpha = 1 \end{cases} \tag{A.7}$$

These values have to be described using a recursive formula (equation 2.4) when $\alpha \neq 1$. This closed form solution was calculated by using the relationship that $d_i' = d_i + p_i$.

We see that when the clearance function is exponential, the remaining dose at any time is a linear combination of the inoculations. I.e., the dose at any time can be simply calculated by applying exponential decay to each inoculation independently and summing the results. The decay is only dependent upon γ, a fixed parameter, and the chosen time. When $\alpha < 1$, this property is lost because the decay depends on

both and the previous inoculation sizes, the factor $1/d_i^{\alpha-1}$. By using this derivation we can solve the total effective dose at any given time analytically. It also can be used to find the error associated with assuming that the final time point, T, is equivalent to the extinction time of infinity when $\alpha = 1$. First let us look at the solution to the first, general middle ($i < n-1$), and last integral in equation A.6

$$\int_0^{t_1} d_0 \mathrm{e}^{-\gamma t} \mathrm{d}t = \frac{d_0}{\gamma}(1 - \mathrm{e}^{-\gamma t_1}) \tag{A.8a}$$

$$\int_0^{t_{i+1}-t_i} d_i \mathrm{e}^{-\gamma t} \mathrm{d}t = \frac{d_i'}{\gamma}(1 - \mathrm{e}^{-\gamma(t_{i+1}-t_i)}) = \frac{1}{\gamma}\sum_{j=0}^{i} d_j(\mathrm{e}^{-\gamma(t_i - t_j)} - \mathrm{e}^{-\gamma(t_{i+1}-t_j)}) \tag{A.8b}$$

$$\int_0^{T-t_{n-1}} d_{n-1} \mathrm{e}^{-\gamma t} \mathrm{d}t = \frac{d_{n-1}'}{\gamma}(1 - \mathrm{e}^{-\gamma(T-t_{n-1})}) = \frac{1}{\gamma}\sum_{j=0}^{n-1} d_j(\mathrm{e}^{-\gamma(t_{n-1} - t_j)} - \mathrm{e}^{-\gamma(T-t_j)}) \tag{A.8c}$$

By summing across each piece, we find the following solution to equation (A.6)

$$\int_0^T P(t, \{d_i\}_{i=0}^{n-1}) \mathrm{d}t = \frac{1}{\gamma}\sum_{i=0}^{n-1} d_i(1 - \mathrm{e}^{-\gamma(T-t_i)}). \tag{A.9}$$

Furthermore, if we let $T \to \infty$, we find the total effective dose to be

$$\int_0^{\infty} P(t, \{d_i\}_{i=0}^{n-1}) \mathrm{d}t = \frac{1}{\gamma}\sum_{i=0}^{n-1} d_i \tag{A.10}$$

an independent sum of each inoculation. Thus, if we assume that all doses have cleared (i.e, that $T \to \infty$) when $T < \infty$ we introduce the following error in our effective dose calculation

$$\text{Error} = \frac{1}{\gamma}\sum_{i=0}^{n-1} d_i \mathrm{e}^{-\gamma(T-t_i)}. \tag{A.11}$$

For small inoculations and large γ, this error diminishes very quickly. For other

conditions, a calculation may be necessary to ensure a sizeable pathogen level is not ignored. In our analysis of the Brachman data, the monkeys were observed in a dose-free environment for periods in which the total within host pathogen level was far below 1 (by our parameter estimations) before they were sacrificed.

Now to calculate risk over an entire dosing period until time, T, we make the appropriate substitutions into our survival function and get the following formula

$$\Pr_{\text{Inf}}(T, \{d_i\}_{i=0}^{n-1}) = 1 - \mathrm{e}^{-\frac{s}{\gamma}\sum_{i=0}^{n-1} d_i(1-\mathrm{e}^{-\gamma(T-t_i)})} \tag{A.12}$$

and if we assume that $T \to \infty$ (i.e.,$T \gg t_{n-1}$) we calculate the following risk formula

$$\Pr_{\text{Inf}}(\{d_i\}_{i=0}^{n-1}) = 1 - \mathrm{e}^{-\frac{s}{\gamma}\sum_{i=0}^{n-1} d_i}. \tag{A.13}$$

Note that this resembles the exponential function where $k = s/\gamma$. Further, if we consider each inoculation to extinction independently for a risk calculation, the risk calculation is equivalent. That is, when $\alpha = 1$ under the conditions of dose extinction, our model is equivalent to the exponential model in that risk is independent of exposure patterns and timing. Where the models differ is for evaluating risks at times before assumed within host pathogen extinction by a function of the error term.

A.3 Censoring intervals and lag period

Consider a subject who becomes infected in interval, $(T_{j,l}, T_{j,r})$, bounded by the last observed time before infection and first observed time after infection. The l and r notation denote the left time point and right time point in this censored interval. We can then redefine $f(T_j)$ as follows

$$f(T_j) = S(T_{j,l}) - S(T_{j,r}) \tag{A.14}$$

The problem of potential jump discontinuities would occur in a situation where the interval limits correspond directly to an inoculation time. Recall that the dose function is formulated to be left continuous and thus the inoculations are not counted when approaching from the right. For example, consider a scenario where an infection occurred between days 12 and 13 and inoculations occurred at the start of day 12 and 13. S(12) would not be calculated using the inoculation given at day 12, but S(13) would. However, the inoculation on day 13 would be used by neither (it is assumed not to contribute to the infection likelihood for the given subject). Likelihood equation (2.12) can then be adjusted accordingly by splitting integrands at the interval times, which results in equation (A.15). $T_{j,l}^{+}$ and $T_{j,l}^{-}$ denote the direction of limit approach which acts as the formal notation when inoculation discontinuities might occur as discussed.

$$\begin{aligned} -\sum_j \log L(T_j) = \sum_j \Bigg(& (1-\Delta_j)\big(s \int_0^{T_j} P(t, \{d_i\}_{i=1}^{n_j})\mathrm{d}t\big) + \\ & \Delta_j\big(s \int_0^{T_{j,l}^{+}} P(t, \{d_i\}_{i=1}^{n_j})\mathrm{d}t - \log(1 - \mathrm{e}^{-s\int_{T_{j,l}^{-}}^{T_{j,r}} P(t,\{d_i\}_{i=1}^{n_j})\mathrm{d}t})\big)\Bigg) \end{aligned} \tag{A.15}$$

To implement the τ parameter, we adjusted the final observation time by $T_j = T_j - \tau\Delta_j$. Equation (A.16) illustrates the assignment of T_j based on a j^{th} subjects infection status, given by Δ_j, where $\Delta_j = 1$ when infection occurs and $\Delta_j = 0$ when

no infection is observed.

$$T_j = \begin{cases} T_j, & \Delta_j = 0 \\ T_j - \tau, & \Delta_j = 1 \end{cases} \tag{A.16}$$

Since we have limited information on the lag between infection and death, we do not assess lagged infection times as exact times of infection. Instead we use interval censoring such that we assume that the infection occurred sometime over a given day. For example, if a monkey death occurs on day 15 with lag τ=10 days, then the infection occurred sometime during day 5. This would be evaluated as f(5)=S(5)-S(6) as described in equation (A.14). Previous studies have shown that time between symptoms and death is on the scale of several hours for Cynomogus monkeys[56] so we do not think symptom onset would aid in finding the total lag period.

This lag period, τ, was treated as a population parameter but it is likely probabilistic in nature. Based on prior studies[56] that this lag is variable, a variety of τ values were initially implemented, ranging between 1-13 days. Further review of other anthrax models, specifically Brookmeyer et al.[58], suggested that these lag periods from infection to symptoms are relatively short, less than 4 days on average. This is explained in more detail in the § 2.3.6. We aimed to treat τ as a nuisance and eliminate it from the optimization. This was done statistically by assuming that τ was took potential values of 1, 2, 3, or 4 days with equal probability. Thus we evaluated the likelihood for each of these fixed τ values and then weighted it by their probability ($\Pr(\tau = i) = 25\%$ for i =1, 2, 3, or 4). This was done formally using conditional expectations. Note that the likelihood is represented by the conditional probability of infection given τ.

A.4 Results extension to $\alpha > 1$

As briefly described, it is mathematically possible to allow values in the range $\alpha > 1$. The biological interpretation of this range relies on a priming interpretation. That is, larger inoculation makes the immune system more effective and therefore results in faster clearance, which does not seem biologically plausible. However, another scenario is that immune response is detrimental to clearance, as recruitment occurs over time from prior inoculations, clearance becomes more inefficient. This scenario would seem plausible for pathogens that target the immune response to initiate infection. A problem arises when we consider confidence intervals extending past $\alpha = 1$, and thus conflicting biological assumptions must be statistically considered.

The dynamics of the model when $\alpha > 1$ describe a complete reversal in risk calculations in that large bolus exposures have smaller risks (due to smaller accumulated effective doses) than their evenly distributed counterparts. When $\alpha = 1$, we do not expect any difference in risk between exposure patterns (of same total dose). Delineating between dose timing effects and variability is dependent on the power of our statistics. We thus expect that when α values are close to 1 that the confidence intervals will cover significant ranges of $\alpha < 1$ and $\alpha > 1$ which encompass conflicting biological assumptions about the effectiveness of the immune system. For example, if we unbound α in the Brachman analysis, we extend the upper bound of our CI to 1.48 despite having an MLE $\hat{\alpha}$=0.90. These results are seen in figure A.1.

The MLE values of s and become unstable as $\alpha \to 2$. This is a mathematical phenomenon associated with a singularity of the dose function family at $\alpha = 2$. For these function families, the dose function no longer converges to 0, even as $t \to \infty$. I.e., the total effective dose integrates to infinity. That is, for values that are not arbitrarily large, the risk approaches infinity as t approaches infinity as α approaches 2. These results are not included.

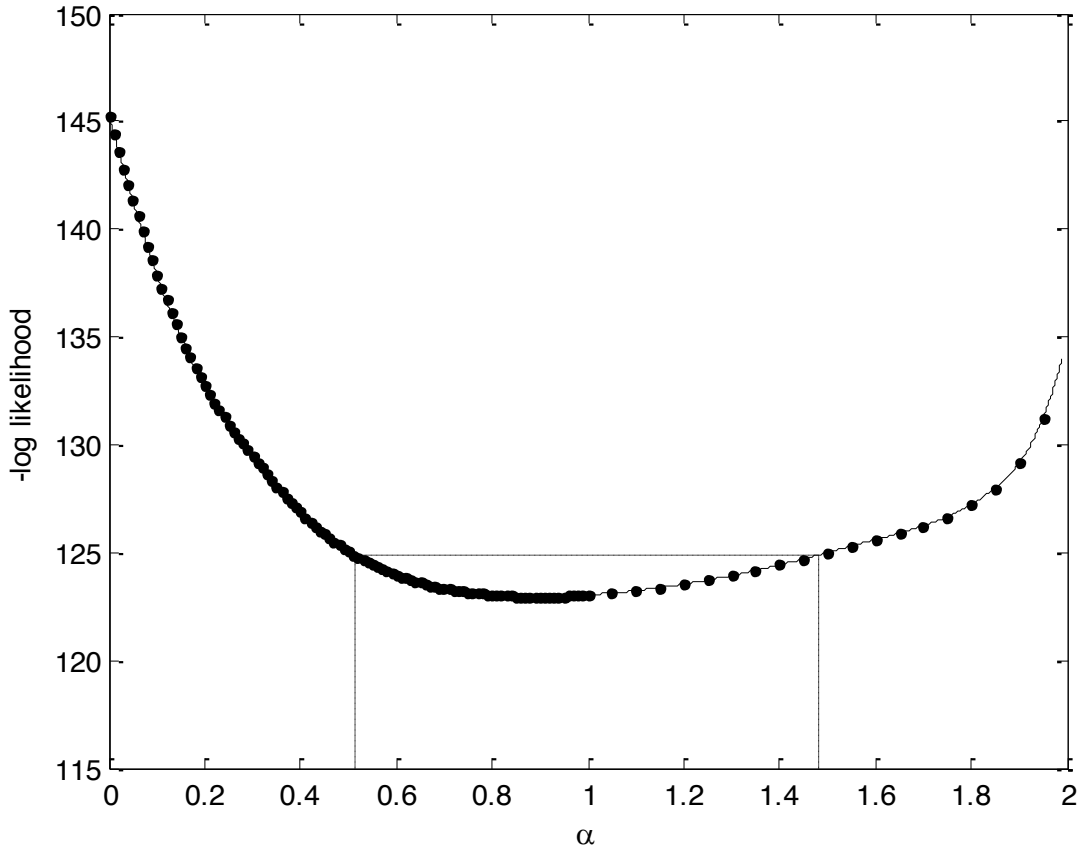

Figure A.1: Results from optimization profile over α with relaxed constraints on α. A spline curve was fit to determine the minimum negative log likelihood (to determine $\hat{\alpha}$ =0.90) and to determine the 95% CI (0.51, 1.48) using the log likelihood ratio test.

APPENDIX B

Additional material for successes and shortcomings of polio eradication: a transmission modeling analysis

B.1 Overview of appendix

This appendix provides details of model equations, assumptions, inputs, and additional results. For background on model development, B.2 describes the formulation of the model and its differential equations with B.3 describing the aging structure and B.4 describing the immunity and waning structure. B.5 includes additional results focusing on waning rates, alternative model structures, expanding vaccination implementation time, model dynamics, and OPV transmission.

B.2 Transmission model structure and equations

The structure of our model is a hybrid of standard SIS and SIRS models. Our model is a deterministic compartmental model with 3 basic states: S (susceptible, i.e. not currently infected with either WPV or OPV), I (infected with WPV), and V

(infected with OPV). We further indexed each of these states by immunity stages, i, and age group, j, so the notation $S_{i,j}$ indicates the uninfected population in immunity stage i and age group j. There are m total age groups (see section B.3) and n total immune stages (see section B.4). Immunity generated from previous infections reduces susceptibility (β_i) to reinfection, and then reduces contagiousness (θ_i) and increases recovery rate (γ_i) for subsequent reinfections. We collapsed the contact rate and infection per contact probability into a single parameter, c, defined as an effective contact rate. In a fully susceptible population, the incidence rate is the product of the susceptible population, the infected population, and the effective contact rate. Reducing contagiousness affects the force of infection, Λ_I and Λ_V, from I and V, respectively, described by the equations

$$\Lambda_I = c \sum_{j=0}^{m-1} \sum_{i=0}^{n-1} \theta_i I_{i,j} \tag{B.1a}$$

$$\Lambda_V = \epsilon c \sum_{j=0}^{m-1} \sum_{i=0}^{n-1} \theta_i V_{i,j}. \tag{B.1b}$$

The force of infection generated by those infected with OPV was attenuated by $\epsilon < 1$, a constant reduction in contagiousness independent of immunity and age.

The following set of ordinary differential equations describes the continuous time evolution of the population in each $S_{i,j}$ compartment. Movement across age groups was modeled as a pure-delay process, i.e., it is instantaneous at fixed time steps described in further detail in section B.3. Death rates, μ_j, and vaccination rates, ϕ_j depended only on age. For concreteness, ϕ_j was taken to be the effective vaccination rate for an individual's age group, which we regarded as being equal to the product of the actual vaccination rate and the average vaccine efficacy in individuals with no previous exposure to either OPV or WPV. Further, the population size, N_0, was normalized to 1 by finding the equilibrium value of birth flow, b, into compartment

$S_{0,0}$, corresponding to the lowest immune level ($i = 0$) and the youngest age group ($j = 0$). The flows into and out of $S_{0,0}$ are described by the following equation

$$\frac{\mathrm{d}S_{0,0}}{\mathrm{d}t} = b - \big(\mu_0 + (\Lambda_I + \Lambda_V + \phi_0)\beta_0\big)S_{0,0}. \tag{B.2}$$

While for other ages ($0 < j < m$) with no immunity ($i = 0$),

$$\frac{\mathrm{d}S_{0,j}}{\mathrm{d}t} = -\big(\mu_j + (\Lambda_I + \Lambda_V + \phi_j)\beta_0\big)S_{0,j}. \tag{B.3}$$

Since the $S_{0,j}$ compartments are characterized by no immunity, they have full susceptibility (i.e., $\beta_0 = 1$). By assumption we did not allow waning back into $S_{0,j}$. However, for $S_{0<i<n-1,j}$, we fixed a duration rate, ω_i, to describe movement across $S_{i,j}$ compartments corresponding to waning immunity (see B.4.2). The general form of these differential equations are

$$\frac{\mathrm{d}S_{i,j}}{\mathrm{d}t} = \omega_{i+1}S_{i+1,j} - \big(\mu_j + \omega_i + (\Lambda_I + \Lambda_V + \phi_j)\beta_i\big)S_{i,j}. \tag{B.4}$$

We then defined an overall recovery rate by age,

$$\Gamma_j = \sum_{i=0}^{n-1} \gamma_i(I_{i,j} + \kappa V_{i,j}). \tag{B.5}$$

We assumed that the entire infected population (I and V) recovers at rate, Γ_j, into the highest state of immunity ($S_{n-1,j}$), where re-infection could not occur. Thus the differential equation for $S_{n-1,j}$ is

$$\frac{\mathrm{d}S_{n-1,j}}{\mathrm{d}t} = \Gamma_j - (\mu_j + \omega_{n-1})S_{n-1,j}, \tag{B.6}$$

Recovery from OPV infection was assumed to occur faster than that of WPV infection

by constant $\kappa > 1$. The relative transmissibility of OPV to WPV is described by ϵ/κ where $0 < \epsilon/\kappa < 1$.

The differential equations for I and V, respectively, are

$$\frac{\mathrm{d}I_{i,j}}{\mathrm{d}t} = \Lambda_I \beta_i S_{i,j} - (\mu_j + \gamma_i) I_{i,j} \tag{B.7a}$$

$$\frac{\mathrm{d}V_{i,j}}{\mathrm{d}t} = (\Lambda_V + \phi_j)\beta_i S_{i,j} - (\mu_j + \kappa\gamma_i) V_{i,j} \tag{B.7b}$$

The R_0 values used in our analysis were calculated as c/γ_0. Table B.1 summarizes the model inputs. The differential equations were solved numerically using Python software set with lsoda method and variable tolerance (absolute and/or relative) ranging from $1\times\mathrm{e}^{-8}$ to $1\times\mathrm{e}^{-12}$.

B.3 Age structure in the model

Three processes depended only on age group, j: the pure delay aging (described below); death, which occurs at a rate μ_j; and vaccination, ϕ_j, which targets a set of age groups. We grouped the population by age into a total of m groups, using 10 half-year compartments for <5-year olds, 10 single-year compartments for 5 to 15-year olds, and 14 five-year compartments for 15-85 year olds ($m = 10 + 10 + 14 = 34$). By this parameterization, an age of 85 is an absorbing state and corresponds to anyone 85 or older. Death rates from these age groups were set consistent with observations from India [94]. We looked at reducing death rates as much as three-fold from India and saw only a small increase in R_0 suggesting that the phenomena described in our results (importance of effects of OPV transmission, waning rates, R_0, and vaccination rates) remain unchanged.

Age-specific vaccination schedules cannot be consistently implemented using a continuous aging process. We modeled aging as a pure-delay process which is consistent with past models of measles and pertussis [81, 82]. Specifically, at a set time,

Description	Symbol	Input Values
Total Immune Stages	n	10
Total Age Groups	m	34. B.3 for further details.
Population Size	N_0	1 (Constant)
Birth Rate	b	0.0249968
Contact Rate	c	40-220
Death rate of population in age compartment j	μ_j	Age-specific Death Rates from India[94]
Vaccination rate for the population in age compartment j	ϕ_j	Varies. Discussed in Text.
Relative contagiousness of OPV compared to WPV	ϵ	Varies. Discussed in Text.
Relative recovery rate from OPV compared to WPV	κ	$1/\epsilon$
Waning rates affecting susceptibility	r_β	Varies, see caption.
Waning rates affecting susceptibility	r_θ, r_γ	$r_\beta/4$.
Minimum Recovery Rate (No Immunity)	γ_{min}	10
Maximum Recovery Rate (Full Immunity)	γ_{max}	40
Rate of Immune State Change	ω_i	$\omega_1 = 0$ $\omega_{2-6} = 0.2$ $\omega_{7-9} = 2$

Table B.1: All rates are per year. r_β is initially set to 0.07/yr (i.e., it takes 10 years to reach 50% susceptibility) in figures 3.2, 3.3 and 3.5 and for results in manuscript unless another waning rate is explicitly stated. In Figure 3.4, $r_\beta = 0.04$/yr and $r_\beta = 0.10$/yr for slow and fast waning, respectively.

populations move across age categories instantaneously. Formally, every 6 months, for $Q_{i,j} \in \{S_{i,j}, I_{i,j}, V_{i,j}\}$, aging occurs as follows

$$Q_{i,j} = \begin{cases} Q_{i,j-1}, & j \in [1,9] \\ Q_{i,9} + Q_{i,10}/2, & j = 10 \\ Q_{i,j-1}/2 + Q_{i,j}/2, & j \in [11,19] \\ Q_{i,19}/2 + 9Q_{i,20}/10, & j = 20 \\ Q_{i,j-1}/10 + 9Q_{i,j}/10, & j \in [21, m-2] \\ Q_{i,m-2}/10 + Q_{i,m-1}, & j = m-1. \end{cases} \tag{B.8}$$

For clearer analysis and presentation, we normalized the population size, N_0, to 1 by finding the equilibrium value of birth flow, b, into compartment $S_{0,0}$.

B.4 Modeling waning immunity

B.4.1 Waning immunity theoretical formulation

We conceptualized infection immunity regarding three aspects of the infection process: 1.) β, susceptibility to infection; 2.) θ, contagiousness when infected; and 3.) γ, recovery rate of illness. To implement the effect of immunity, we allowed these parameters to vary depending on immune status. When an individual has never experienced infection, they are fully susceptible to infection and then, if infected, they are fully contagious with a maximum duration of infection. After an infection, individuals recover into a complete immunity state, where they have no susceptibility. If infection were possible in this stage (that is, ignoring zero susceptiblity), there would be no contagiousness and a maximum recovery rate of illness. We therefore defined β and θ to represent relative levels of susceptibility and contagiousness between these extreme immunity levels, specifically allowing them to range between 0

(no susceptibility or contagiousness) and 1 (full susceptibility and contagiousness). Infection recovery rate, γ, is not defined relatively but it is based on observed ranges of excretion duration [14, 49].

The waning of immunity is a dynamic process that starts at some maximal level of immunity that generally decreases over time until it reaches some minimal level. To allow our infection parameters to vary over time as immunity wanes, we defined them as processes, $\beta(t)$, $\theta(t)$, and $\gamma(t)$, that vary over time, t, the time since infection recovery. Assuming the maximal level of immunity occurs at the time of infection recovery ($t = 0$), waning immunity is depicted as having the minimum susceptibility, contagiousness, and duration assigned when $t = 0$ and then allowing each to increase as time since infection increases. Since we defined β and θ such that they represent relative levels of susceptibility and contagiousness that vary between 0 and 1, we defined $\beta(t)$ and $\theta(t)$ such that at $t = 0$ these parameters are equal to 0 (no susceptibility or contagiousness) and then allow them to approach 1 (full susceptibility and contagiousness) as time since infection increases. We defined $\gamma(t)$ to start at a maximum recovery rate (minimum duration), γ_{max}, when $t = 0$ and approaches a minimum recovery rate (maximum duration), γ_{min}, when time since infection increases. We modeled the change over time in these infection parameters assuming that immunity wanes exponentially with corresponding rate parameters, r_β, r_θ, and r_γ. The following equations describe the exponential function for each parameter

$$\beta(t) = 1 - \mathrm{e}^{-r_\beta t} \tag{B.9a}$$

$$\theta(t) = 1 - \mathrm{e}^{-r_\theta t} \tag{B.9b}$$

$$\gamma(t) = \gamma_{min} + \mathrm{e}^{-r_\gamma t}(\gamma_{max} - \gamma_{min}) \tag{B.9c}$$

Figure B.1 shows curves for varying rates of susceptibility immunity waning and transmissibility, a product of contagiousness and duration. Transmission potential is

an aggregate measure of susceptibility and transmissibility discussed in further detail in section B.5.1.

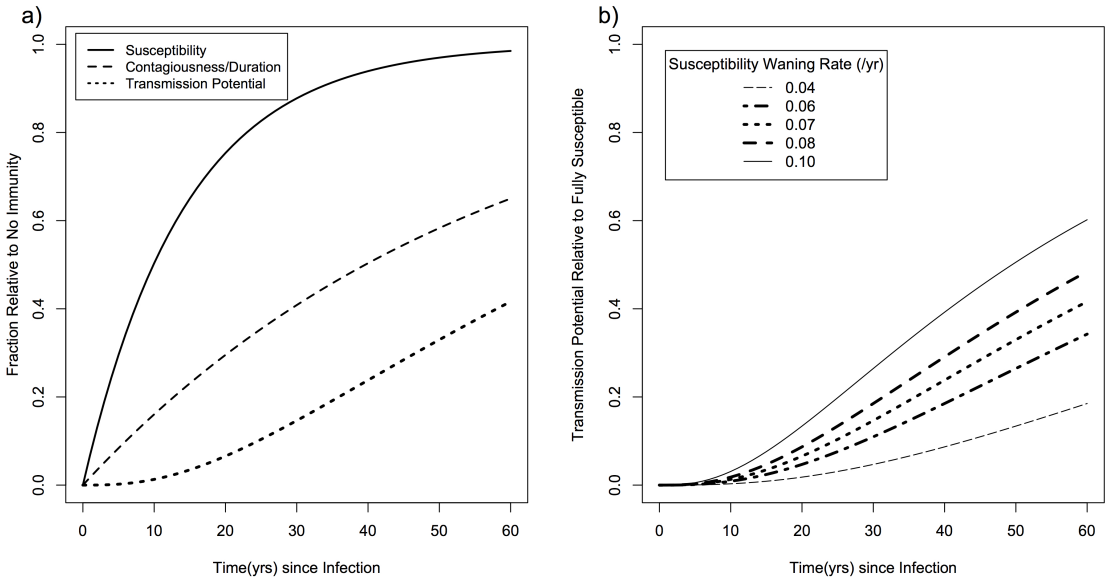

Figure B.1: Immunity levels over time depicted by a) an average immunity profile after infection for a newly infected individual with susceptibility immunity waning rate of 0.07 yr^{-1} and b) transmission potential across varying susceptibility immunity waning rates. Transmissibility is a product of contagiousness and duration. Transmission potential is a product of transmissibility and susceptibility.

B.4.2 Waning immunity model implementation

We conceptualized immunity levels as continuous but for practical computational purposes we grouped the population into n immunity stages where each stage, i, corresponds to a specific time since infection recovery. The immune stages are indexed using integers 0 through $n-1$, where 0 represents no immunity (due to no previous exposure), $n-1$ represents maximum immunity achieved immediately after recovery, and 1 represents the lowest stage to which immunity wanes over a specified time frame. The level of immunity at each waning stage (except for 0) was estimated by a series of times since infection. We did not allow further waning once level 1 is reached

so that we can distinguish the never infected from those with little immunity who were previously infected or vaccinated. Immunity waning only occurred across the susceptible population, S_i. To determine the average duration in each immune state, we selected flow rates, ω_i, between each susceptible compartment. The expected arrival time (i.e., time since infection), t_i, to compartment, S_i, since recovery was calculated as follows

$$t_i = \sum_{k=1+1}^{n-1} 1/\omega_k \quad \text{where } 0 < i < n-1. \tag{B.10}$$

Note that for $i = n-1$, flows into the susceptible compartment do not depend on waning but on the recovery rate from infection so we let $t_{n-1} = 0$. Further, since we assumed there is no waning into or out of S_0, we do not need to consider ω_0 or t_0. The expected arrival times into each S_i compartment that we assigned are illustrated in figure B.2 and table B.1. The model structure is illustrated in figure 3.1 in the main text.

We used the expected arrival times to assign values at each immune stage for each of our infection parameter, β_i, θ_i, and γ_i (susceptibility, contagiousness, and recovery rate, respectively). For populations with no immunity ($i = 0$) we assigned the following values

$$\beta_0 = 1 \tag{B.11a}$$

$$\theta_0 = 1 \tag{B.11b}$$

$$\gamma_0 = \gamma_{min} \tag{B.11c}$$

For other levels of immunity, these parameters were a discrete series of values calculated from our continuous immunity waning functions, equations (B.9a)-(B.9c), using the set of arrival times we calculated in equation (B.10). They are calculated

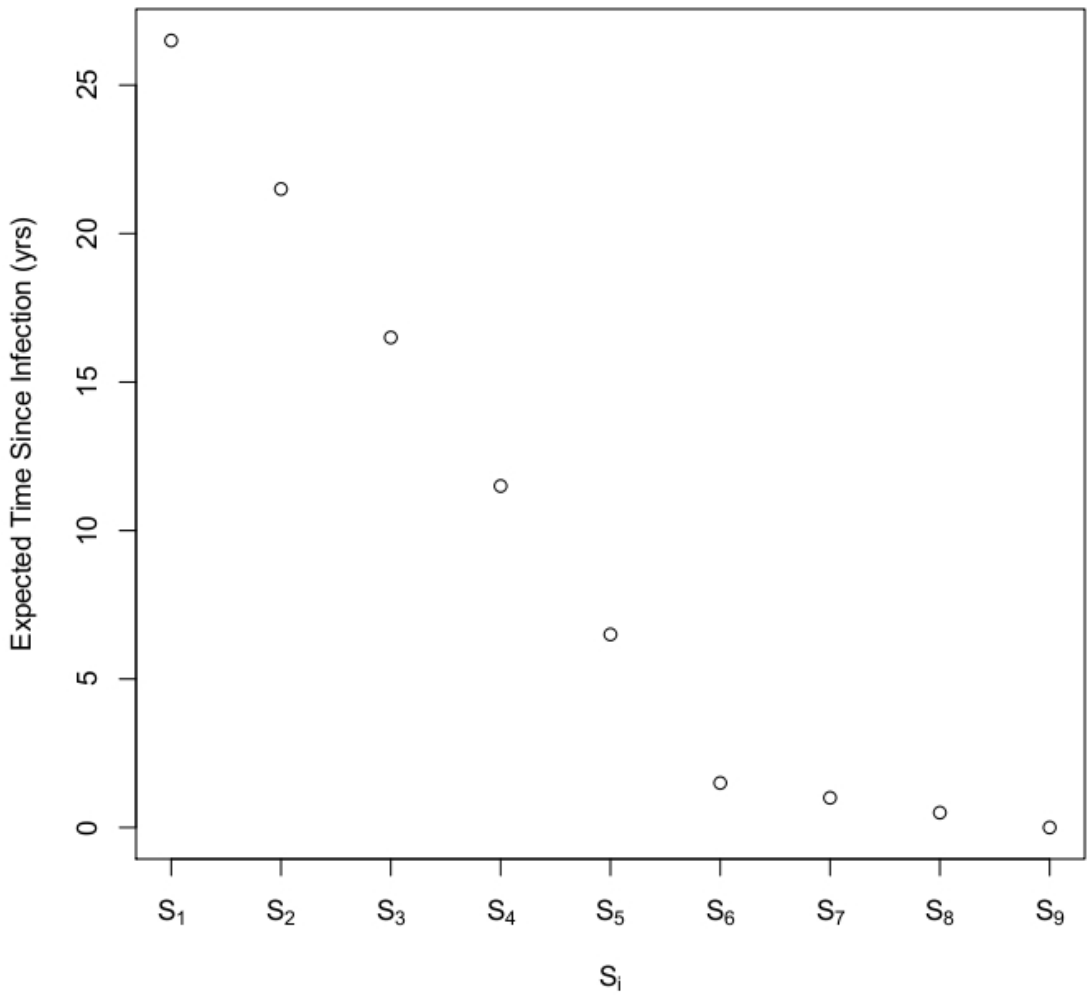

Figure B.2: The expected arrival times into each susceptible compartment. S_0 is not included in this figure because it is not part of the waning process. The duration in each compartment, i.e., distance between each point, was determined by the parameterizations of ω_i (see B.1).

as follows (where $0 < i \leq n - 1$)

$$\beta_i = \beta(t_i) \tag{B.12a}$$

$$\theta_i = \theta(t_i) \tag{B.12b}$$

$$\gamma_i = \gamma(t_i) \tag{B.12c}$$

B.4.3 Waning immunity robustness

Our model of waning immunity was fairly robust to more complicated formulations. We considered using a two rate exponential process (fast waning then slow waning) for each infection parameter, a better match for the actual biological processes. However, the dynamics are robust (results not shown) to either formulation so we used a one parameter exponential function to increase computation speed and clarity of results. We selected ω_i such that the underlying continuous curve would be well represented in our discretized model, as can be seen in figure B.2. The results (not shown) were also robust to increasing the total amount of waning stages.

We also examined a range of maternal immunity formulation options. The shorter the duration or the less effective that maternal immunity is, the greater the potential for intensified childhood vaccinations to eliminate transmission and the higher the level of vaccination of older individuals that is needed to eliminate transmission. To clearly explore the interplay of dynamics of childhood vaccinations levels, reproduction number, OPV transmissibility and waning rates we decided to present the simpler model that does not have maternal immunity.

B.5 Supplemental results

B.5.1 Waning immunity exploration

As a starting point, we fixed waning immunity rates across susceptibility, contagiousness, and duration as follows: susceptibility increases to 50% compared to no immunity after 10 years and reaches 84% after 25 years on average (corresponding to S_1). To simplify this process and characterize it using one parameter, we make the following assumptions about the waning rates of these processes: 1) susceptibility immunity wanes faster than contagiousness and duration immunity because infection and excretion processes are only relevant after infection occurs; and 2) contagiousness and duration have equal waning rates because shedding magnitude and duration are intrinsically tied. We therefore set the exponential rates in which contagiousness and duration increase (r_θ and r_γ, respectively) to be one fourth the rate in which susceptibility increases (r_β). We use one fourth for convenience. Although changing these relative rates may quantitatively affect the role of waning immunity in transmission, it does not qualitatively affect our results. All three factors result in an overall reduction of transmissibility for a re-infected individual. This can be seen in figure B.1. Parameters values for waning are also shown in table B.1.

Figure B.1 illustrates the potential immunity profiles for poliovirus infection we used in our models to assess different levels of waning immunity. Figure B.1a shows loss of immunity over time for one setting of susceptibility immunity waning. Transmissibility is a product of both potential recovery rate and contagiousness. We defined transmission potential as the product of susceptibility and transmissibility. Maximum transmission potential occurs in a susceptible individual who has never experienced infection, and all concurrent transmission potential is relative to this state. In the example of 0.07/year waning rate (figure B.1a), we had a fairly fast increase of susceptibility but these subsequent infections will have a reduced effect on overall transmis-

sion (transmission potential) due to a reduced contagiousness and duration of illness (transmissibility). Figure B.1b illustrates transmission potentials for the range of different susceptibility waning rates we explored (bolded) in our analysis. This shows a wide range of immunity waning from fairly conservative estimates to high estimates without assuming that complete loss of immunity occurs.

B.5.2 Alternative implementation of vaccination

Our model utilized effective vaccination rates instead of real vaccination rates in the model implementation. In reality, OPV vaccination may not always induce an immune response and, if it does take, it may not induce a complete immune response [48, 49]. We assumed an effective vaccination results in full immunity, thus we can still evaluate reduced vaccine take-rates by reducing the effective vaccination rate. For example, one effective vaccination per year compared to 0.75 per year might imply a reduced take-rate. However, our model does not account for induced immunity that is incomplete. It has been shown that it takes 3 or 4 doses of OPV to achieve full immunity in an immunologically naive individual [48]. To explore the sensitivity of our model assumptions to this multiple dosing property, we constructed an alternative model where OPV vaccination (or transmission) does not result in full immunity upon recovery unless there has been a previous infection by WPV or prior multiple OPV doses. Specifically, in the absence of WPV, we assumed that three doses of OPV are required to reach full immunity as depicted in figure B.3.

We ran a similar set of analyses as those presented in the main text utilizing the new model construction. Comparing the results depicted in figure 3.2 in the main text to the results from this model (figure B.4) we see remarkable consistency over a similar scale of vaccination rates. The threshold for elimination is still observed across vaccination rates given an R_0 value but there is a subtle shift in this model requiring slightly higher vaccination rates to reach threshold. Further, while it is difficult to

identify visually, the alternative model formulation shows more robustness of prevalence levels to increases in vaccination for a given R_0. That is, in the main model, we sometimes observe drastic reductions in prevalence (many orders of magnitude) for a tenth increase in the yearly effective vaccination rate, specifically near the threshold for elimination. In the alternative model, reductions in prevalence are constrained to one or two orders of magnitude for a tenth increase in vaccination.

In our model construction, we see that the interruption of WPV transmission due to OPV vaccination and transmission plays a very important role in reaching elimination threshold. In other words, the competition of the two infections without co-infection allows vaccination with poor immunogenesis to still effectively reduce WPV transmission. In reality, the actual vaccination rates are also affected by variable take-rates in certain regions. The alternative vaccination implementation, while giving us a real vaccination rate per year, is still an overestimate of efficacy of vaccination because we have not explicitly included fail rates, i.e., instances where the vaccination fails to take at all. To better implement actual vaccination rates, there would also need to be a fail rate (a proportion reduction in the implemented vaccination rate that actually results in OPV infection). This would translate into a rescaling of the vaccination rate scale for a broader and great range. For example, if we use a take-rate of about 33%, then 9 vaccinations per year would be required, on average, to achieve the results we see in 3/yr in our alternative formulation. It should be noted that this transformation could also be applied to the effective vaccination rates used in the main analysis. While exploring these facets of vaccination may give us a better interpretation of the vaccination rate, they introduce additional complication without changing the inferences we draw from our model concerning the waning of immunity and the transmission of OPV. Specifically, the alternative formulation of the model requiring multiple doses to achieve full immunity does not add any additional information that is not captured by the use of the effective vaccination

rates.

We use effective vaccination rates to reduce complexity regarding vaccine take-rates and incomplete immunity. We can interpret our effective vaccination rate heuristically in several ways. For a 0.5/year effective vaccination rate, the targeted country is achieving 50% immunity (relative to full immunity) in the children population per year. For 2/yr, there is full coverage of the childhood population with an additional booster to full immunity per year. While this is not a direct mapping to the actual vaccination rates, we can loosely categorize countries given their efforts in terms of vaccination coverage (i.e., if they are achieving 100% coverage) and the extent to which they are boosting these populations (e.g., implementation of SIAs).

B.5.3 Effect of vaccination implementation time

Figure B.5 depicts the effect of increasing the vaccination implementation time (to 10 years) on minimum prevalence compared to the vaccination implementation time of 2 years used in the manuscript. Specifically, the left panel of figure B.5 is the same as figure 3.2A in the main text. For increased implementation times, minimum prevalence levels increase for higher R_0 levels with higher vaccination rates. Specifically, this reduces the initial efficacy of vaccination programs in highly transmissive regions even when the eventual target vaccination rates are high. Furthermore, figure B.6 displays how minimum prevalence is affected by differing waning and OPV transmission settings using a 2-year vaccine implementation time. Figure B.7 shows the minimum prevalence for differing waning and OPV transmission settings using a 10-year vaccine implementation time. Comparing figures B.6 and B.7 we see the ability to reduce prevalence to low levels from initial vaccine implementation is highly sensitive to the speed of implementation when immunity wanes more quickly. This effect is magnified when OPV transmissibility is low.

B.5.4 Model dynamics after vaccination

From figure 3.2 in the main manuscript, we observe that the introduction of vaccination can reduce prevalence to low levels (figure 3.2A) that are not necessarily permanent at steady state (figure 3.2B), particularly as we increase levels of R_0. The dynamics that distinguish the high R_0 from the low R_0 situations have complex dependencies upon the level of vaccination, the R_0, the pace at which vaccination is initially ramped up, and the waning dynamics modeled. As discussed in the main manuscript, at high R_0, previously infected individuals are constantly having their immunity boosted by reinfections and the sharp drop in infection levels after vaccination implementation depends upon these high levels of immunity. As immunity wanes, if we have not achieved the threshold of elimination, reinfection dynamics take over the transmission system and we experience rebound epidemics.

At low levels of infection, stochastic events will dominate whether or not infection dies out. If it does die out, then a whole set of issues not included in our deterministic models will determine whether or not infection is reintroduced. But the solutions of the differential equations can provide insights nonetheless. In general, the longer it takes to get a rebound in the deterministic model, the longer the average time to a stochastically determined rebound. That is because the immunity levels of those not getting directly vaccinated are determinants of rebounds in both the deterministic model, whose results we present here, and the more realistic stochastic model, which we do not examine.

Figure B.8 presents the WPV prevalence at the peak of the first rebound epidemic as a function of R_0 and effective vaccination rates. Figure B.9 presents the time after a vaccination program was initiated that the first rebound epidemic occurs. At low R_0 levels the size of the rebound epidemic decreases as the vaccination level is increased, but at higher R_0 levels, the size of the first rebound epidemic may at first go up and then go down as vaccination levels are further increased. Specifically, for higher

R_0 levels, when we compare the minimum prevalence achieved from figure 3.2A with the 5% OPV transmission panel of figure B.8, we observe that the threshold where minimum prevalence begins to reach very low levels (but we do not have elimination at steady state) correspond to the conditions where we also have the highest rebound epidemic prevalence. Furthermore, in conjunction with figure 3.5, we see that the highest rebound peak levels correspond with the transition of transmission burden from first infection to reinfection. In figure B.9, the time until the rebound epidemic peak is fairly invariant for low levels of vaccination (less than 50 years) but slowly takes longer as we increase vaccination and the magnitude of the rebound epidemic diminishes.

If there is a strong rebound, the failure to eradicate will be evident. However, if there is a smaller rebound epidemic, as we see for higher vaccination levels at high R_0 values, then the failure to eradicate may not be so evident. This would indicate that in areas like India, a declaration of elimination should only follow a very extensive search for asymptomatically infected individuals.

B.5.5 Switching to IPV

Lastly, figure B.10 displays the minimum and final prevalence levels when relative OPV transmissibility is 0% (a proxy for an IPV program) for three levels of waning. Compared to figure 3.2a from the manuscript, we see with IPV there is a larger range of R_0 values where it becomes impossible to achieve elimination even for high levels of vaccination coverage. This further emphasizes the importance of OPV transmissibility and reducing transmission conditions in the context of switching to IPV. When R_0 is low, elimination is still possible in our model using IPV assuming a similar efficacy level to OPV.

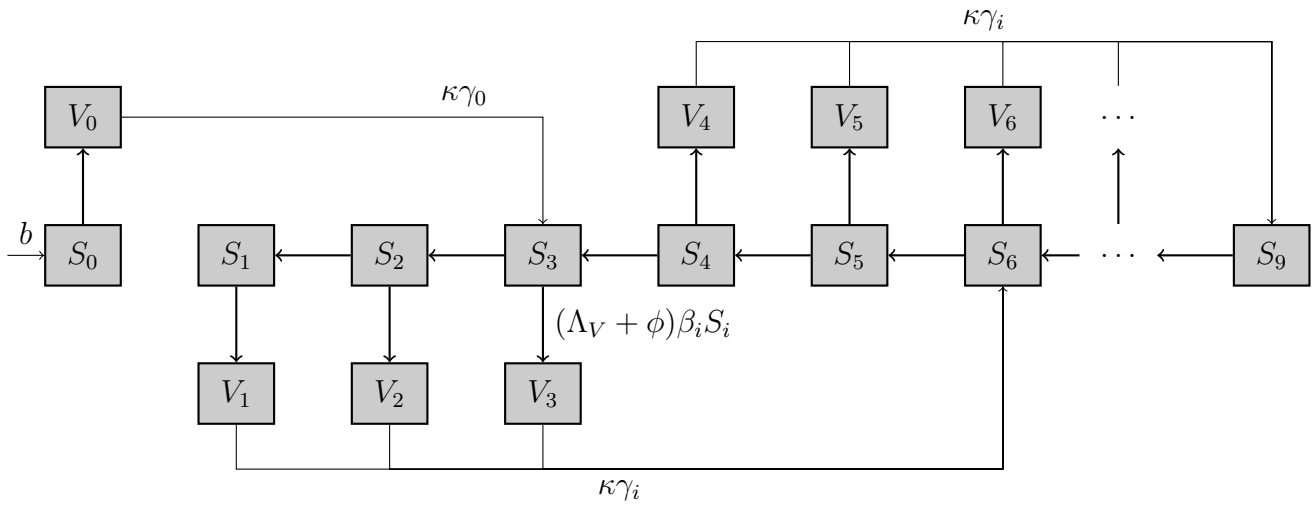

Figure B.3: Alternative formulation of vaccination model for susceptible populations (S_i) and vaccinated populations (V_i). This figure excludes vital dynamics and infection from wild polio virus (WPV), which are included in the simulated transmission model. In the presence of only vaccination rate (ϕ) or force of infection due to oral polio vaccine (OPV) transmission (Λ_V), three vaccinations or infections would be required to reach the highest level of immunity (S_9). Reduced OPV infectious period (γ) relative to WPV infection is denoted by κ. Infection from WPV (not shown) is assumed to result in full immunity prior to waning and thus subsequent OPV exposures act as boosters. Flows between state variables S_i denote waning immunity described in section B.4 and also shown in the main manuscript in figure 3.1 (with WPV infection).

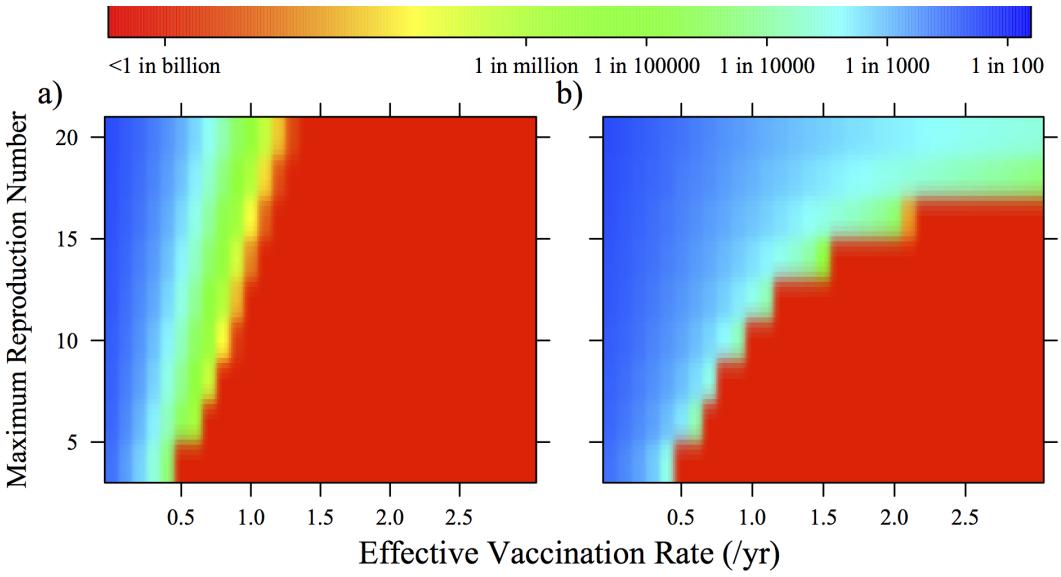

Figure B.4: a) Minimum prevalence and b) final prevalence. Two panels depict prevalence levels across R_0 and vaccination rates under the conditions of 5% relative transmissibility of OPV and waning such that it takes 10 years to reach 50% susceptibility. Panel a) depicts the minimum prevalence reached in the first 50 years due to the initial implementation of a vaccination program, a measure of short-term success. Panel b) shows the final prevalence resulting from a vaccination program, a measure of long-term success. In constrast to the model presented in the main text, this model requires multiple OPV doses to reach full immunity.

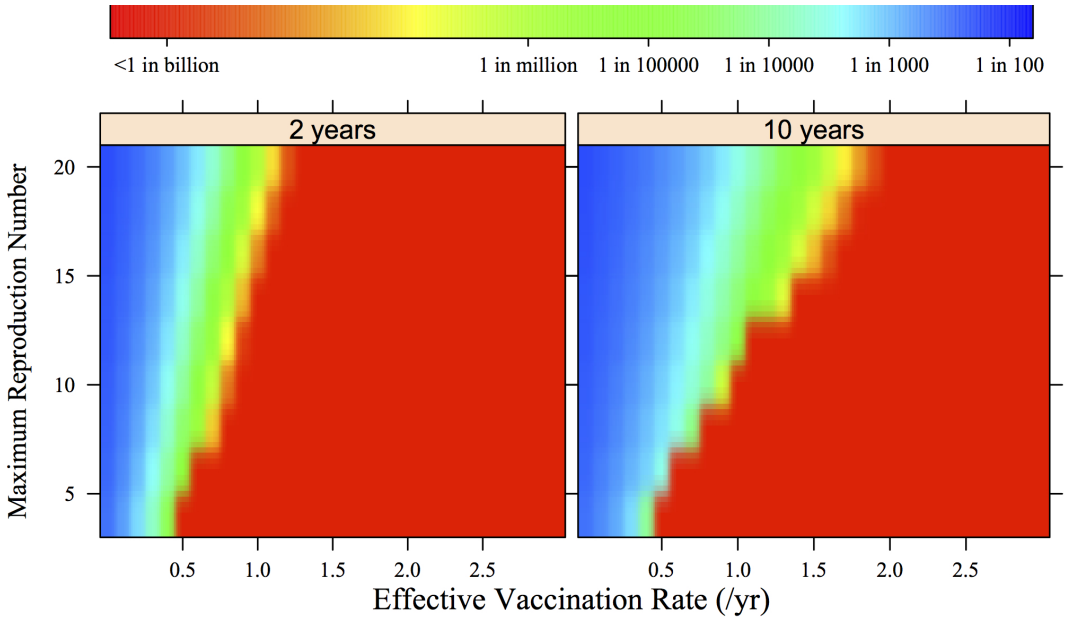

Figure B.5: Two panels depict minimum prevalence levels across R_0 and vaccination rates under the conditions of 5% relative transmissibility of OPV and waning such that it takes 10 years to reach 50% susceptibility specifically comparing 2-year vaccination implementation time (the left panel) to 10-year vaccination implementation time (the right panel). The right panel is presented in the main text in Figure 3.2A. This figure illustrates how vaccination program implementation speed can induce reaching threshold through initial prevalence reduction.

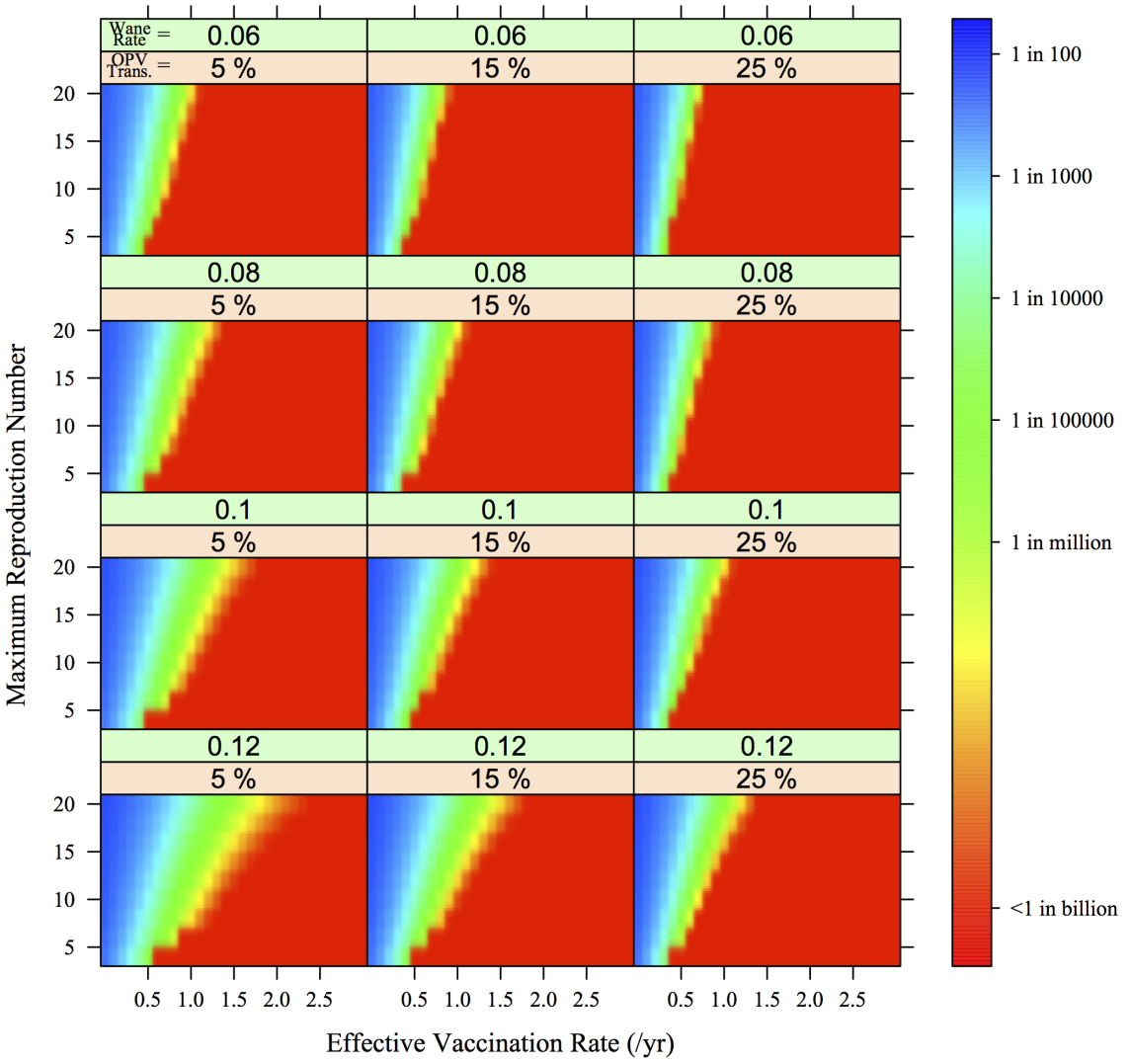

Figure B.6: Sensitivity analysis for minimum prevalence across reproduction numbers and vaccination rates for varying waning rates and OPV transmissibility when vaccination implementation time is equal to 2 years. The top panel label is the susceptibility waning rate (0.07 was used in the manuscript described as 10 years to reach 50% susceptibility). The bottom panel label is relative OPV transmissibility (%) compared to WPV transmissibility. That is, comparing figures horizontally changes OPV transmissibility for a given waning rate and comparing figures vertically changes waning rate for a given relative OPV transmissibility.

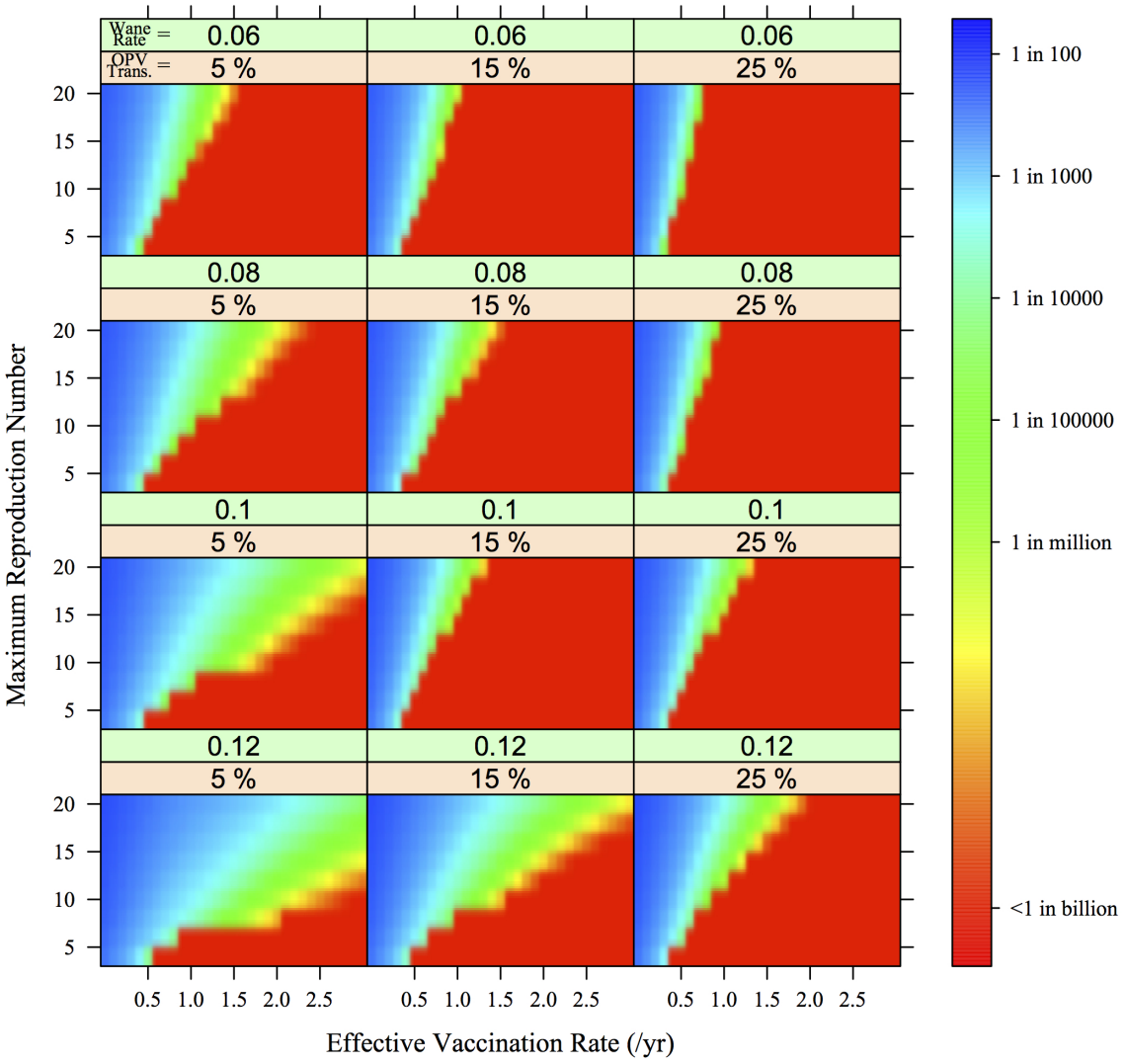

Figure B.7: Sensitivity analysis for minimum prevalence across reproduction numbers and vaccination rates for varying waning rates and OPV transmissibility when vaccination implementation time is equal to 10 years. The top panel label is the susceptibility waning rate (0.07 was used in the manuscript described as 10 years to reach 50% susceptibility). The bottom panel label is relative OPV transmissibility (%) compared to WPV transmissibility. That is, comparing figures horizontally changes OPV transmissibility for a given waning rate and comparing figures vertically changes waning rate for a given relative OPV transmissibility.

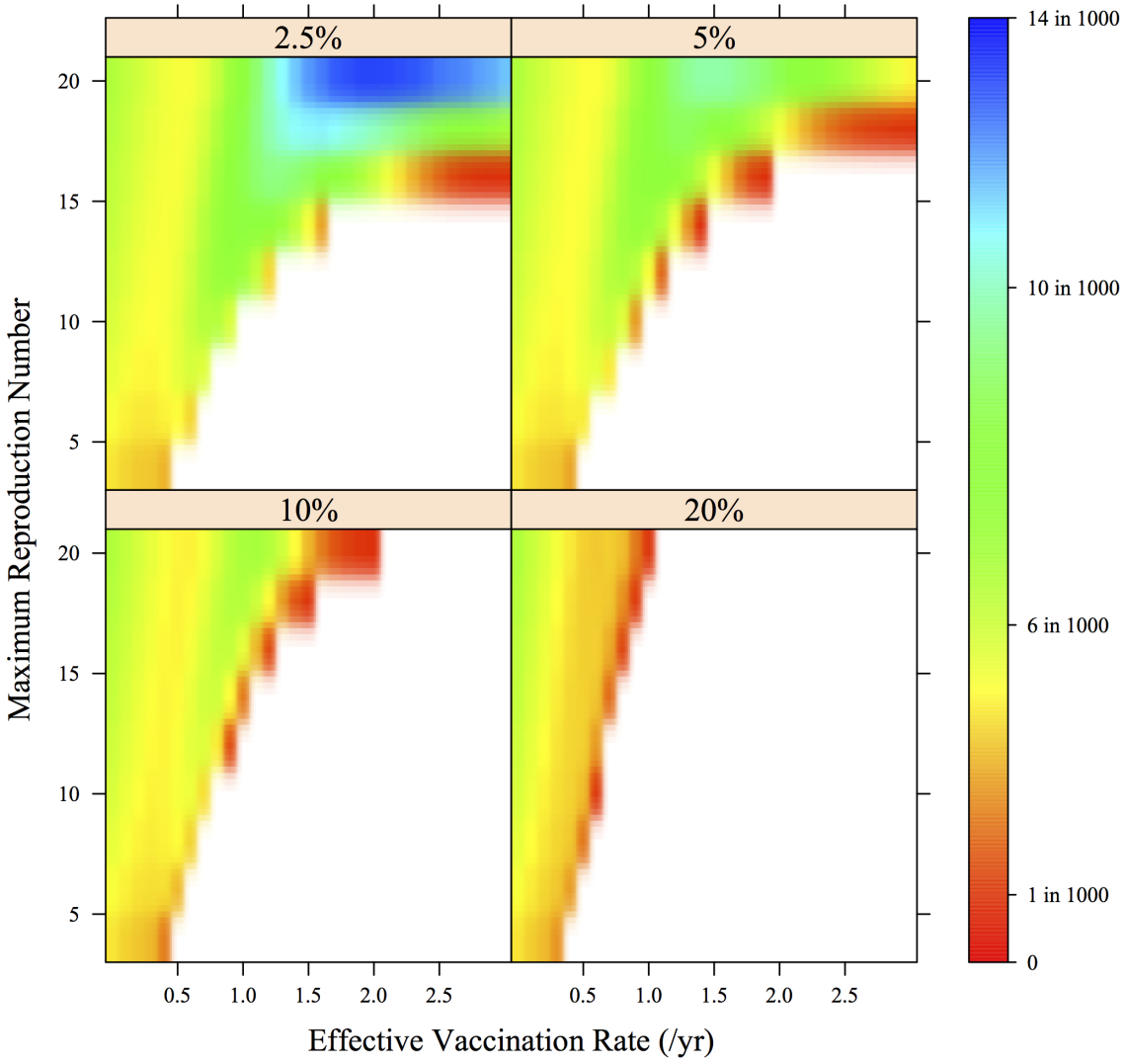

Figure B.8: The size of rebound peak prevalence is presented in heatmap colors as a function of vaccination rate, R_0, and transmissibility of OPV. Waning was set to take an average of 10 years to reach 50% susceptibility. In the white areas of the graph, rebound peaks do not occur.

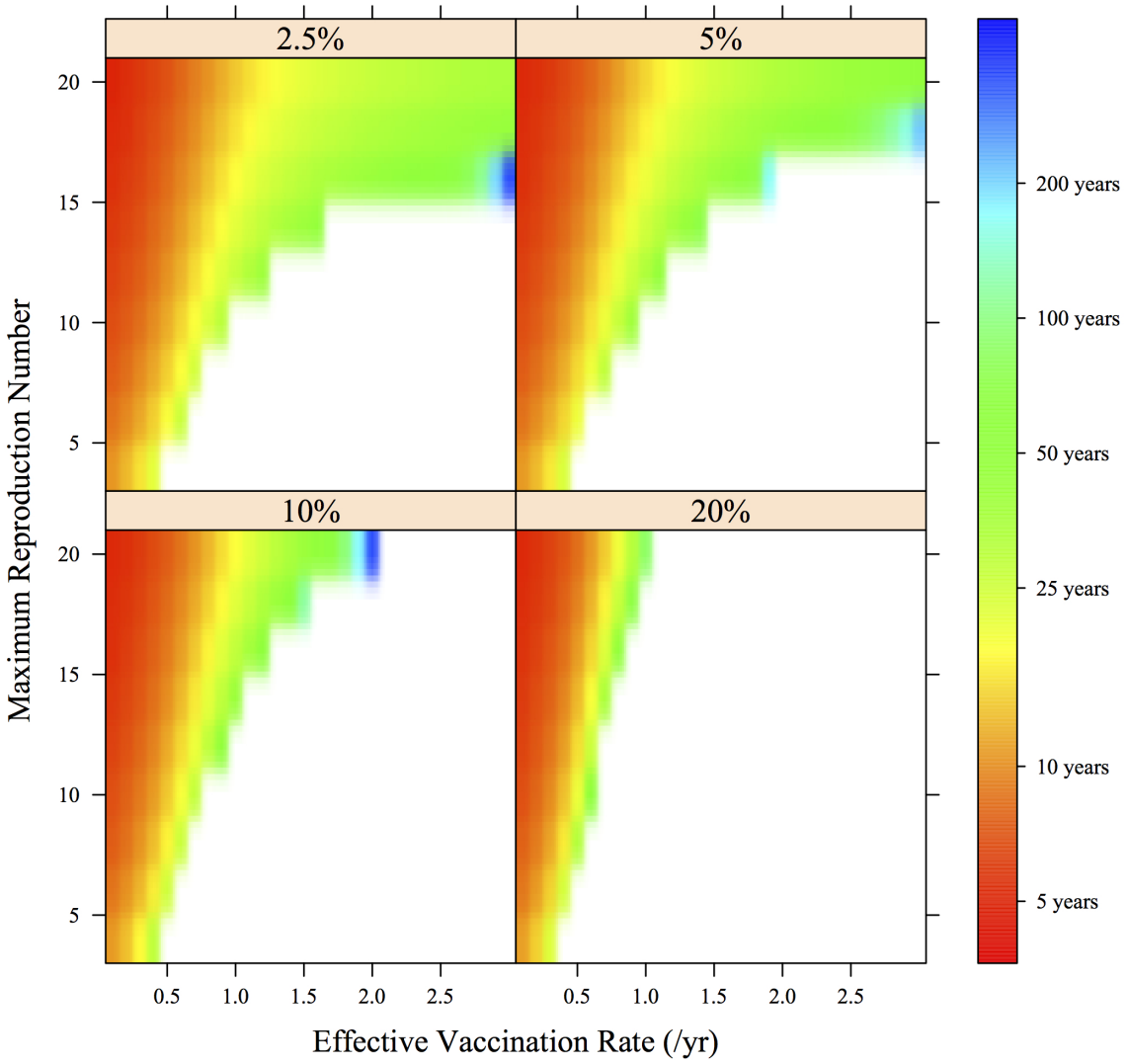

Figure B.9: The time (years) to rebound peak prevalence is presented as heatmap colors as a function of vaccination rate, R_0, and transmissibility of OPV. Waning was set to take an average of 10 years to reach 50% susceptibility. In the white areas of the graph, rebound peaks do not occur.

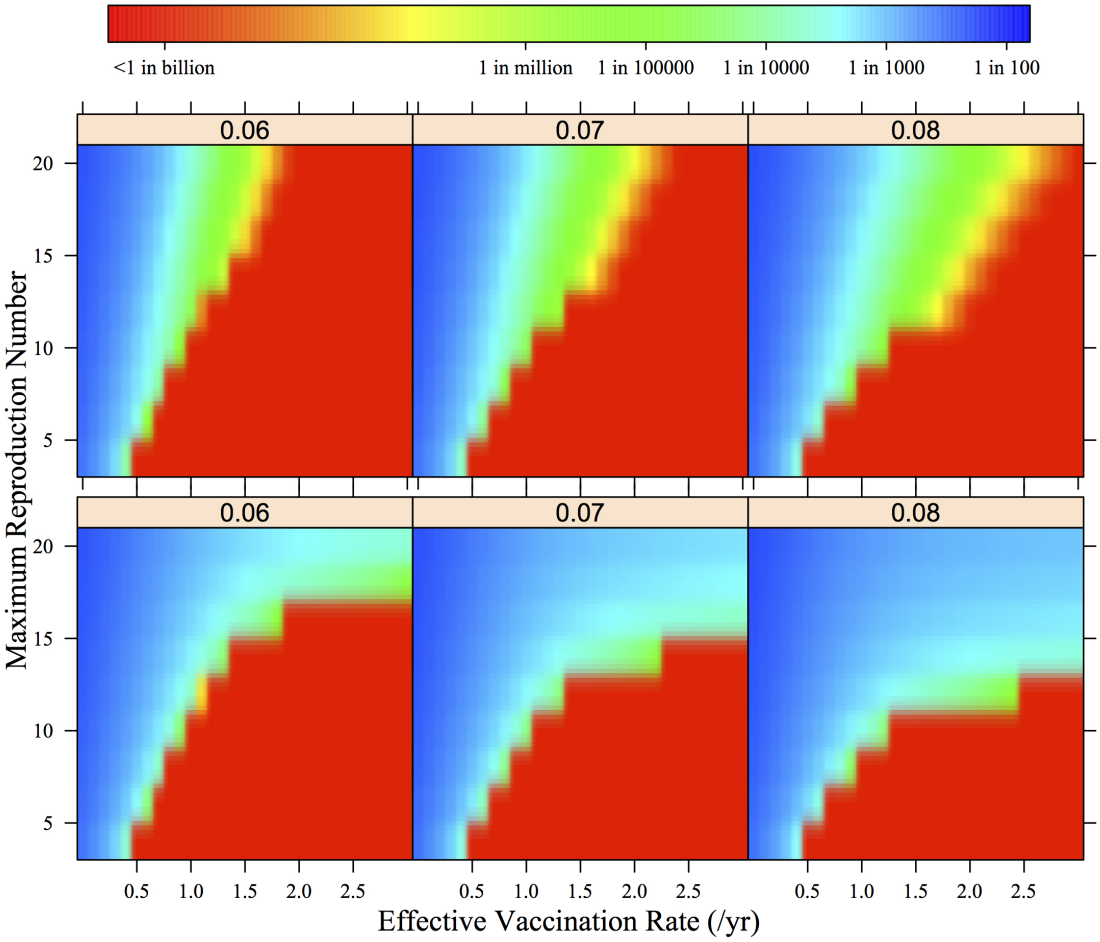

Figure B.10: Panels depict prevalence levels across R_0 and vaccination rates under the conditions of 0% relative transmissibility of OPV and three levels of waning. The top three graphs correspond to minimum prevalence after 2-year implementation of vaccination program. The bottom three graphs display the final prevalence.

APPENDIX C

Additional material for migration and polio eradication

C.1 Model structure and equations

The construction of the this model, including waning immunity and aging, without migration has been previously described in [86]. We extended this model by adding migratory inflows for a separate population. This population is assumed to be in steady state. In the manuscript, model parameters specific to migration are described in table 4.1 and a visual depiction of the model can be seen in Figure 4.1.

The migration rate is denoted by α, the percent change in the population per year. This is implemented in the model equations using the logarithm transformation so the interpretation is a linear change over time rather than exponential (untransformed). We assumed that migration occurs independently of infection and vaccination status so we can group the state variables as follows,

$$Q_{i,j} \in \{S_{i,j}, I_{i,j}, V_{i,j}\} \tag{C.1}$$

where $Q_{i,j}$ is a general state variable in the model for a given immune stage, i, and age group, j. The differential equations for $Q_{i,j}$ have been previously described in chapter III. To describe migration in the model we consider two populations, the source and the destination. The source and destination population vary with respect to vaccination rates, ϕ_j, and contact rates, c. Furthermore, the source population is in steady state. We let $Q^*_{i,j}$ denote the source population. The differential equation for migration in the destination population is therefore

$$\frac{\mathrm{d}Q_{i,j}}{\mathrm{d}t} = \ldots + \log(1+\alpha)Q^*_{i,j} - \log(1+\alpha)Q_{i,j} \tag{C.2}$$

where the unlisted portion of the equation is identical in structure to the model in chapter III. The differential equations were solved numerically using Python software set with lsoda method and variable tolerance (absolute and/or relative) ranging from $1\times\mathrm{e}^{-8}$ to $1\times\mathrm{e}^{-12}$.

C.2 Supplementary results

In sections C.2.1 and C.2.2, we categorize success using prevalence directly. Minimum prevalence reached within 50 yeras of vaccine implementation is an indicator of short-term success. Long-term success can be measured as the final prevalence at steady state. Discrepancies in short and long-term success identify conditions where initial vaccination may be effective but long-term stability may be fragile. For use in sensitivity analyses, actual prevalence levels allow us to make more general inferences about migration under varying parameter conditions.

C.2.1 Migration and varying waning rates

The effect of migration on prevalence levels is generally not differential for different levels of waning immunity rates (figures C.1 and C.2. The general inferences described in the main results sections are robust, specifically that increasing vaccination rates in the source population are important to achieving short and long-term success in moderate to high transmission conditions.

Success, as it depends on waning immunity, is fairly robust to migration rates. Under slow waning conditions (infection and vaccination induce long-lasting immunity), achieving elimination in the short and long-term is achievable under much lower vaccination requirements than when waning is faster. Under conditions of fast waning immunity, reaching low prevalence in high transmission conditions is a result of effectively implementing a vaccination program. Compared to the no migration model, achieving low prevalence requires intense vaccination of the source population as well. While the effects of waning rates do not necessarily depend on migration, waning immunity is still an important component of polio transmission as demonstrated here and in our previous model [86].

C.2.2 Migration and higher OPV transmissibility

In Nigeria, there is circulation of cVDPV of strain similar to WPV type 2 [46]. The type 2 vaccination strain is known to be more transmissible than the other vaccination strains [18] and we previously demonstrated that achieving elimination in short and long-term is much less difficult at higher OPV transmissibility [86]. Thus, cVDPV type 2 in Nigeria may imply that vaccination rates and coverage are very low. To assess how migration affects the transmission system when OPV is more transmissible we allowed OPV to be 20% as transmissible as WPV (figures C.3 and C.4).

For higher OPV transmission, poor vaccination rates in the migratory population can make achieving low prevalence levels in the short and long-term difficult

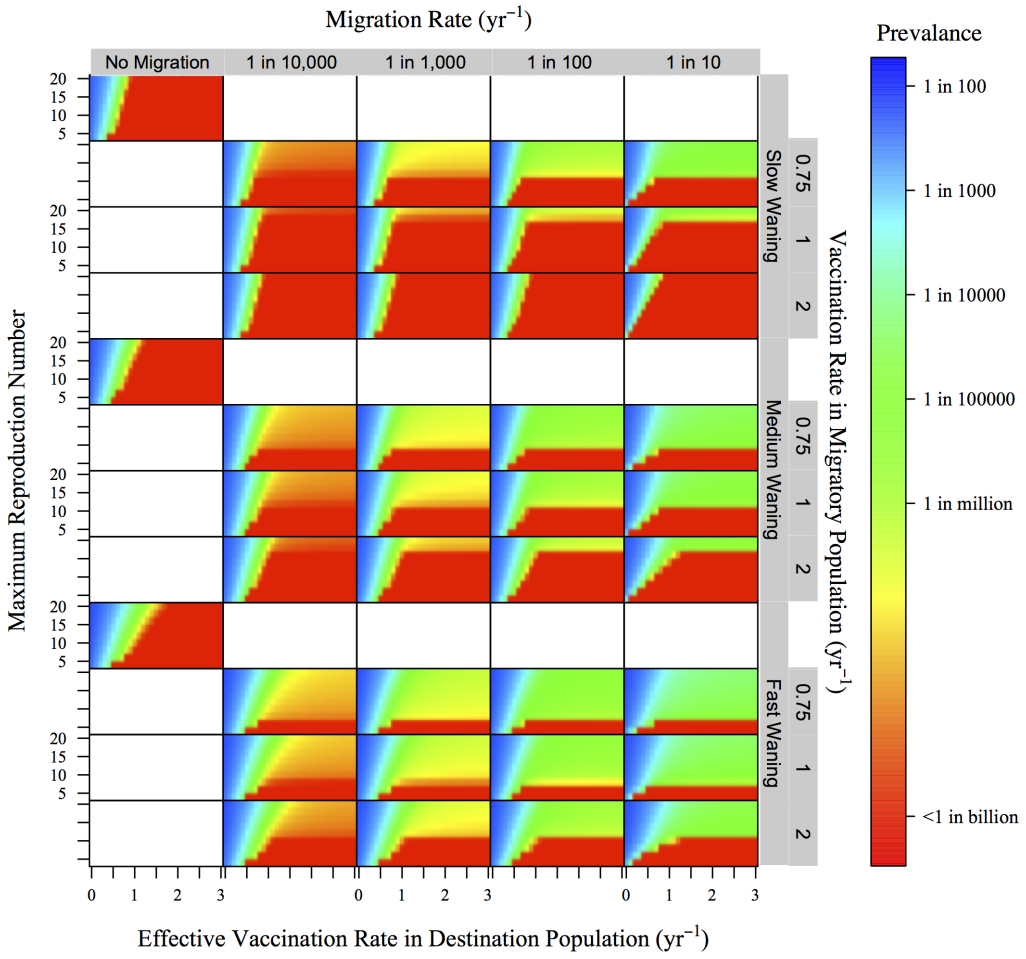

Figure C.1: **Minimum prevalence under migration across similar populations**. Minimum prevalence for two similar populations (same R_0) across vaccination and R_0 in the destination population while varying migration rates and vaccination rates in the migratory population. Waning rates were varied between slow, medium, and fast corresponding to 17, 10, and 7 years to reach 50% susceptibility, respectively.

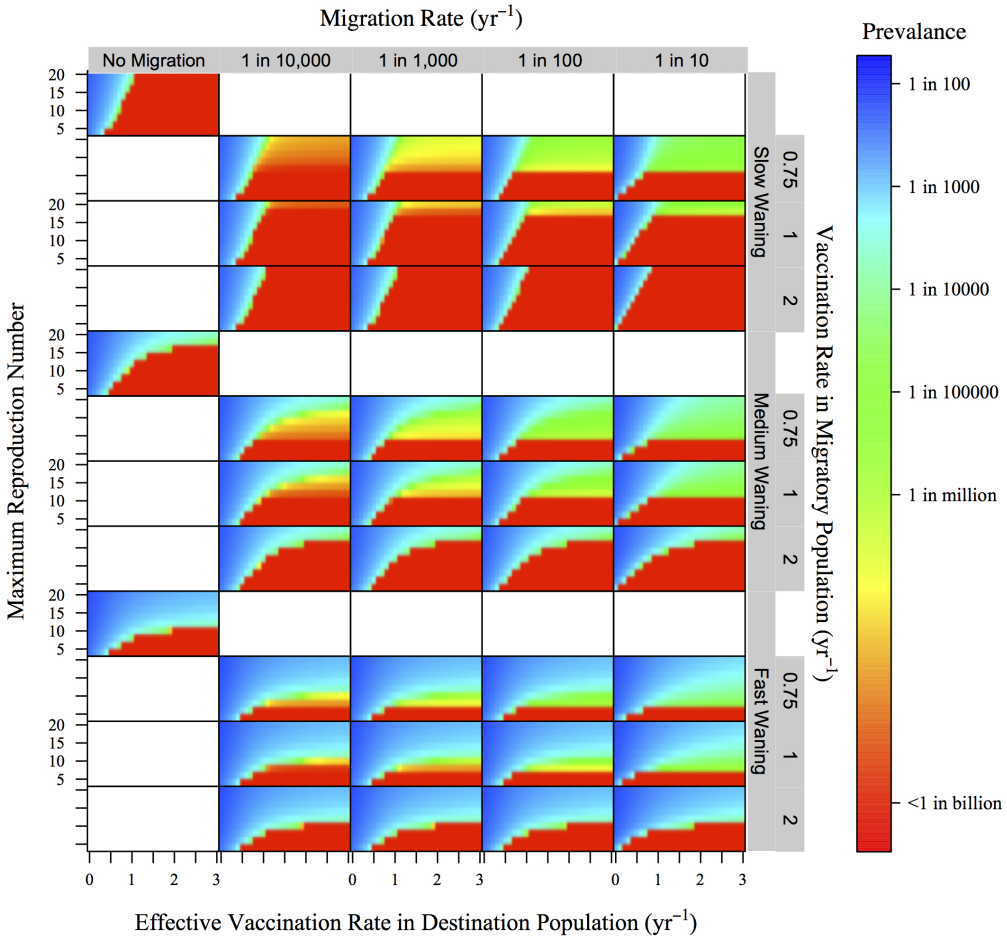

Figure C.2: **Final prevalence under migration across similar populations** Final prevalence for two similar populations (same R_0) across vaccination and R_0 in the destination population while varying migration rates and vaccination rates in the migratory population. Waning rates were varied between slow, medium, and fast corresponding to 17, 10, and 7 years to reach 50% susceptibility, respectively.

when migration rates are high. However, compared to the main analysis when OPV transmissibility was only 5% compared to WPV, this detriment is almost entirely attenuated when vaccination rates in the source population are increased. Even for high migration, short and long-term success is possible at almost all R_0 levels.

In the context of Nigeria, the persistence of cVDPV type 2 implies that there is poor vaccination coverage. Our analysis demonstrated that this is exacerbated when there is high migration. However, because OPV transmissibility is higher for type 2, a general increase in vaccination coverage (rates and targeting) may be who initial success that remains stable. Therefore, achieving eradication of type 2 (vaccine-derived) could be an immediately attainable goal with better implementation in Nigeria and proper cessation of vaccines that includes type 2 (*e.g.*, tOPV).

C.3 Discussion on modeling migration

Afghanistan has a highly mobile population with up 15% of the population displaced (internally or externally)[88]. This could translate into a variety of migration rates into surrounding regions. For example, Pakistan received about half of Afghanistan's migration over the past two decades [93]. However, using the differences in total population size (30m in Afghan to 190m in Pakistan), if 10% of the Afghan population ends up in Pakistan due to displacement, that comprises only about 1.5% of the total Pakistan population. On the other hand, the reverse interpretation shows a small amount of migration from Pakistan could constitute a significant proportion of the Afghanistan population. Current net migration projections are available for Nigeria, Pakistan, and Afghanistan, respectively, at rates of -0.3, -1.4, and 4 per 1000 people per year with Afghanistan's net migration rates are expected to drop to 1.5 over the next few years [91]. For these data, -1.4/1000 person years out of Pakistan corresponds to about 266,000 net people leaving per year, which comprises about 1% of the total Afghanistan population size versus 0.1% of the total

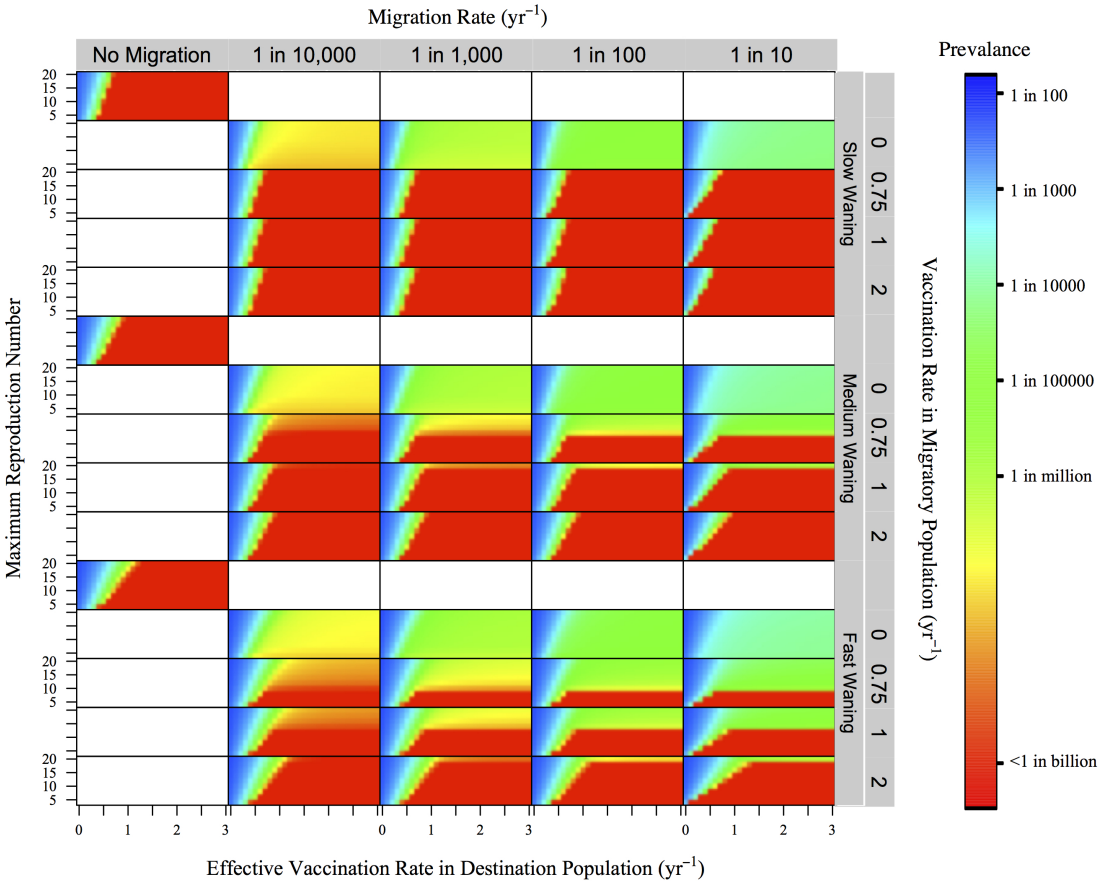

Figure C.3: **Minimum prevalence under migration across similar populations and high OPV transmissibility**. Minimum prevalence for two similar populations (same R_0) across vaccination and R_0 in the destination population while varying migration rates and vaccination rates in the migratory population. Oral polio vaccine (OPV) is 20% as transmissible as wild poliovirus (WPV). Waning rates were varied between slow, medium, and fast corresponding to 17, 10, and 7 years to reach 50% susceptibility, respectively.

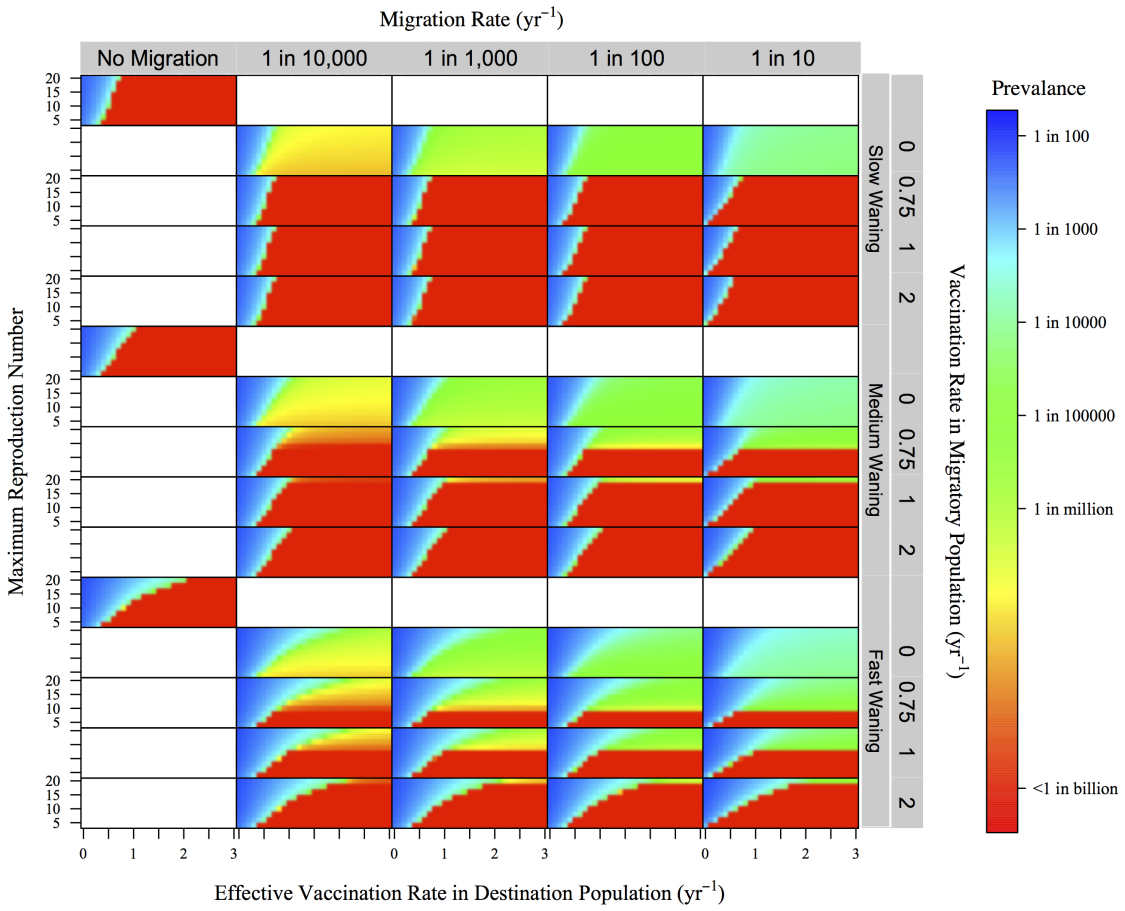

Figure C.4: **Final prevalence under migration across similar populations and high OPV transmissibility**. Final prevalence for two similar populations (same R_0) across vaccination and R_0 in the destination population while varying migration rates and vaccination rates in the migratory population. Oral polio vaccine (OPV) is 20% as transmissible as wild poliovirus (WPV). Waning rates were varied between slow, medium, and fast corresponding to 17, 10, and 7 years to reach 50% susceptibility, respectively.

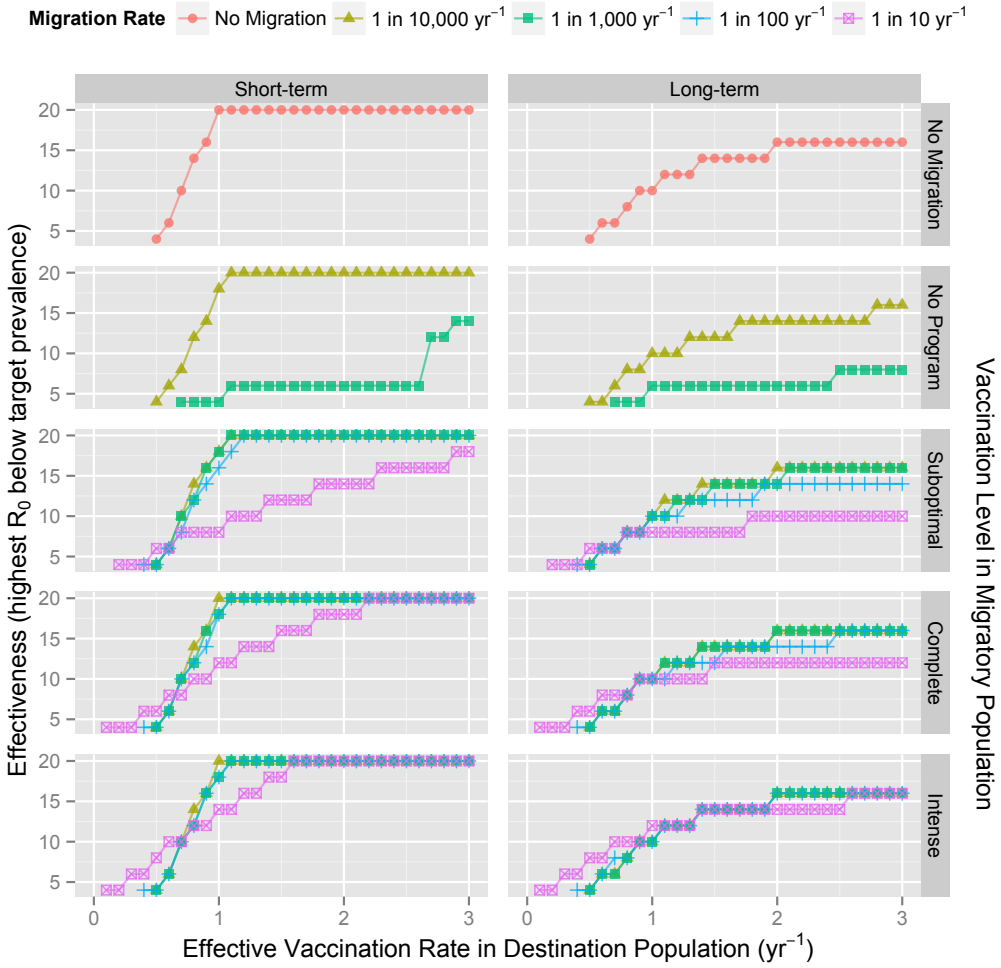

Figure C.5: **Vaccination effectiveness under migration from low transmission conditions**. Short-term (left column) and long-term (right column) vaccination program effectiveness for a given effective vaccination rate in the destination population across varying vaccination levels in the migratory population (table 4.1) and migration rates. The migratory population has a fixed and low R_0 value of 4, oral polio vaccine (OPV) is 5% as transmissible as wild poliovius (WPV), and waning rates were set such it takes 10 years to reach 50% susceptibility. Vaccination effectiveness was measured, for a given effective vaccination rate, as the maximum R_0 (up to 20) where a target prevalence of less than 1 in a million was reached. Initial effectiveness was measured using the minimum prevalence within 50 year of program implementation and long-term effectiveness was measured using the final prevalence. The absence of lines indicates that reaching the target prevalence was not possible under the given conditions.

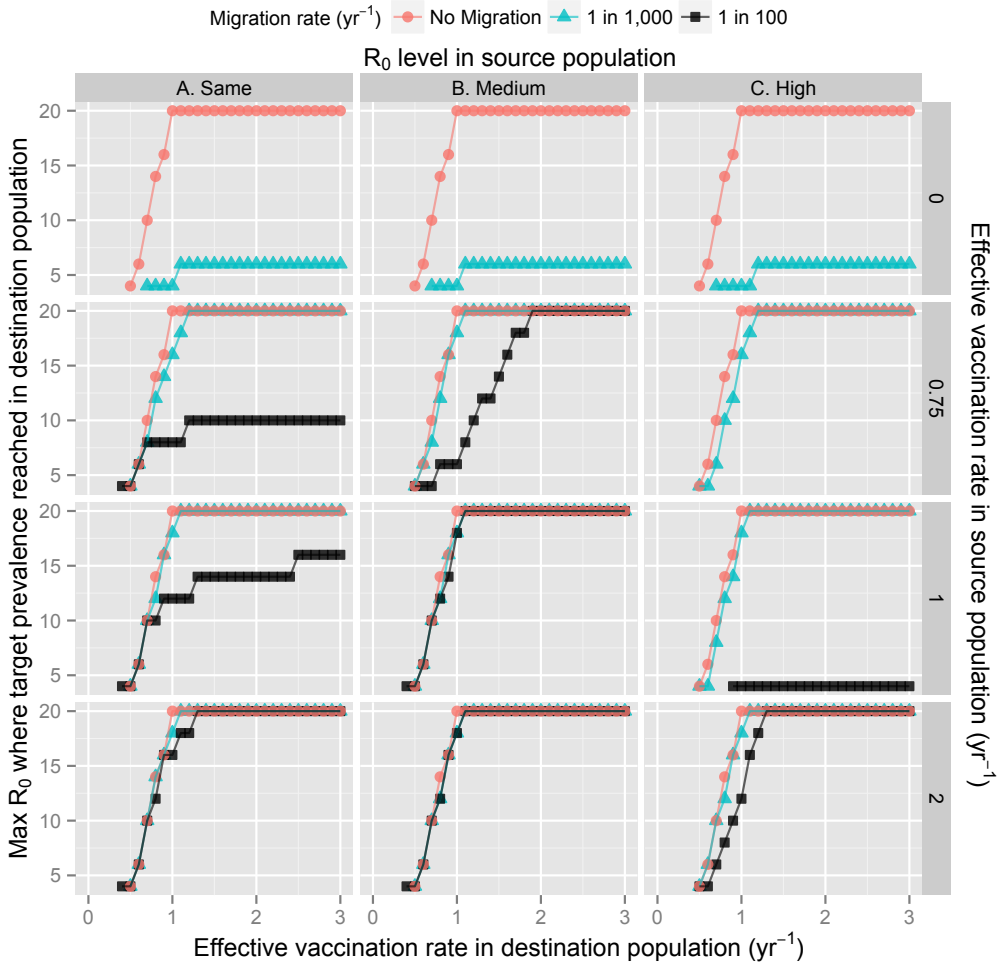

Figure C.6: **Initial vaccination effectiveness under migration across varying transmission conditions**. Vaccination program effectiveness for a given effective vaccination rate in the destination population across varying vaccination levels and transmission conditions in the source population (table 4.1) and migration rates. Initial vaccination effectiveness was measured, for a given effective vaccination rate, as the maximum R_0 (up to 20) where the minimum prevalence (within 50 years) induced by implementation of vaccination in the destination population was less than 1 in a million. Oral polio vaccine (OPV) transmission was set to be 5% as transmissible as wild poliovius (WPV) and waning rates were set such it takes 10 years to reach 50% susceptibility. The absence of lines indicates that reaching the target prevalence was not possible under the given conditions.

Pakistan population size.

There many limitations to quantifying net migration rates and displacement proportions into a transmission model. Net migration rates do not tell a complete story, two nations with net migration rates of zero could have substantially different demographic dynamics where one state may be relatively immobile and another could experience large levels of both immigration and emigration. The total population displaced provides a summary of the proportion of the population that lives outside the nation or are mobile but do not provide appropriate time series data for implementation. For example, Afghanistan immigration occurred steadily over two decades but has experienced major reversal with high levels of repatriation in the last few years [88, 91].

BIBLIOGRAPHY

BIBLIOGRAPHY

[1] C. N. Haas. How to average microbial densities to characterize risk. *Water Research*, 30(4):1036–1038., 1996.

[2] C. N. Haas, J. B. Rose, and C. P. Gerba. *Quantitative microbial risk assessment*. Wiley, New York, 1999.

[3] C. N. Haas. The role of risk analysis in understanding bioterrorism. *Risk Anal*, 22(4):671–7, 2002.

[4] I. H. Spicknall, James S. Koopman, M. Nicas, Josep M. Pujol, S. Li, and J. N. S. Eisenberg. Informing optimal environmental influenza interventions: How the host, agent, and environment alter dominant routes of transmission. *PLoS Comput Biol*, 6(10):e1000969, 10 2010.

[5] C. N. Haas. Estimation of risk due to low doses of microorganisms: a comparison of alternative methodologies. *Am J Epidemiol*, 118(4):573–82, 1983.

[6] A. Srinivasan, J. Foley, R. Ravindran, and S. J. McSorley. Low-dose salmonella infection evades activation of flagellin-specific cd4 t cells. *J Immunol*, 173(6):4091–9, 2004.

[7] A. C. Lowen, S. Mubareka, T. M. Tumpey, A. Garcia-Sastre, and P. Palese. The guinea pig as a transmission model for human influenza viruses. *Proc Natl Acad Sci U S A*, 103(26):9988–92, 2006.

[8] Y. Huang, T. A. Bartrand, C. N. Haas, and M. H. Weir. Incorporating time postinoculation into a dose-response model of yersinia pestis in mice. *J Appl Microbiol*, 107(3):727–35, 2009.

[9] Y. Huang and C. N. Haas. Time-dose-response models for microbial risk assessment. *Risk Anal*, 29(5):648–61, 2009.

[10] J. M. Pujol, J. E. Eisenberg, C. N. Haas, and J. S. Koopman. The effect of ongoing exposure dynamics in dose response relationships. *PLoS Comput Biol*, 5(6):e1000399, 2009.

[11] M. J. Keeling and P. Rohani. *Modeling Infectious Diseases*. Princeton University Press, 2008.

[12] F. Abbink, A. M. Buisman, G. Doornbos, J. Woldman, T. G. Kimman, and M. A. Conyn-van Spaendonck. Poliovirus-specific memory immunity in seronegative elderly people does not protect against virus excretion. *J Infect Dis*, 191(6):990–9, 2005.

[13] I. Grotto, R. Handsher, M. Gdalevich, D. Mimouni, M. Huerta, M. S. Green, E. Mendelson, and O. Shpilberg. Decline in immunity to polio among young adults. *Vaccine*, 19(30):4162–6, 2001.

[14] N. C. Grassly, H. Jafari, S. Bahl, R. Sethi, J. M. Deshpande, C. Wolff, R. W. Sutter, and R. B. Aylward. Waning intestinal immunity after vaccination with oral poliovirus vaccines in india. *Journal of Infectious Diseases*, 205(10):1554–1561, 2012.

[15] M.G.M. Gomes, L.J. White, and G.F. Medley. Infection, reinfection, and vaccination under suboptimal immune protection: epidemiological perspectives. *Journal of theoretical biology*, 228(4):539–549, 2004.

[16] A. Scherer and A. McLean. Mathematical models of vaccination. *British medical bulletin*, 62(1):187–199, 2002.

[17] P. E. Fine. Polio: measuring the protection that matters most. *J Infect Dis*, 200(5):673–5, 2009.

[18] P. E. Fine and I. A. Carneiro. Transmissibility and persistence of oral polio vaccine viruses: implications for the global poliomyelitis eradication initiative. *Am J Epidemiol*, 150(10):1001–21, 1999.

[19] M.J. Keeling and P. Rohani. Estimating spatial coupling in epidemiological systems: a mechanistic approach. *Ecology Letters*, 5(1):20–29, 2002.

[20] M. Jesse, P. Ezanno, S. Davis, and J.A.P. Heesterbeek. A fully coupled, mechanistic model for infectious disease dynamics in a metapopulation: Movement and epidemic duration. *Journal of Theoretical Biology*, 254(2):331 – 338, 2008.

[21] R. M. May and R. M. Anderson. Spatial heterogeneity and the design of immunization programs. *Mathematical Biosciences*, 72(1):83–111, 1984.

[22] C.C. Travis and S.M. Lenhart. Eradication of infectious diseases in heterogeneous populations. *Mathematical biosciences*, 83(2):191–198, 1987.

[23] J.S. Koopman, C.P. Simon, and C.P. Riolo. When to control endemic infections by focusing on high-risk groups. *Epidemiology*, 16(5):621–627, 2005.

[24] B. Grenfell and J. Harwood. (meta) population dynamics of infectious diseases. *Trends in ecology & evolution*, 12(10):395–399, 1997.

[25] J. Burton, L. Billings, D. A. T. Cummings, and I. B. Schwartz. Disease persistence in epidemiological models: The interplay between vaccination and migration. *Mathematical Biosciences*, 239(1):91–96, 2012.

[26] D. Antai. Migration and child immunization in nigeria: individual-and community-level contexts. *BMC public health*, 10(1):116, 2010.

[27] M. Naeem, M. Adil, S.H. Abbas, A. Khan, M.U. Khan, S.M. Naz, et al. Coverage and causes of non immunization in national immunization days for polio; a consumer and provider perspective study in peshawar. *Journal of Postgraduate Medical Institute (Peshawar-Pakistan)*, 26(1), 2011.

[28] L. Roberts. Fighting polio in pakistan. *Science*, 337(6094):517–521, 2012.

[29] T. J. John and V. M. Vashishtha. Path to polio eradication in india: a major milestone. *Indian Pediatr*, 49(2):95–8, 2012.

[30] Y.S. Kusuma, R. Kumari, C.S. Pandav, and S.K. Gupta. Migration and immunization: determinants of childhood immunization uptake among socioeconomically disadvantaged migrants in delhi, india. *Tropical Medicine & International Health*, 15(11):1326–1332, 2010.

[31] J. B. Margolick, R. B. Markham, and A. L. Scott. The immune system and host defense against infections. In K. E. Nelson and C. F. Masters Williams, editors, *Infectious Disease Epidemiology: Theory and Practice*, chapter 10, pages 420–429. Jones and Bartlett Publishers, Massachusettes, 2nd edition, 2007.

[32] C. Sommer. The immune response. In C. M. Porth, editor, *Pathophysiology: Concepts of Altered Health States*, chapter 19, pages 365–386. Philadelphia: Lippincott Williams & Wilkins, 7th edition, 2005.

[33] R. Jayachandran. Anthrax: Biology of bacillus anthracis, 2002.

[34] R. W. Sutter, O. M. Kew, and S. L. Cochi. Poliovirus vaccine - live. In S. A. Plotkin and W. A. Orenstein, editors, *Vaccines*, chapter 25, pages 651–705. Philadelphia: Saunders, Elsevier Inc., 4th edition, 2004.

[35] D. P. Lew. Bacillus anthracis (anthrax). In G. Mandell, J. Bennet, and R. Dolin, editors, *Principles and Practice of Infectious Diseases*, volume 2, chapter 196, pages 2215–2220. Churchhill Livingstone, Philadelphia, 5th edition, 2000.

[36] B. A. Forbes, D. F. Sahm, and A. S. Weissfeld. *Bailey's & Scott's Diagnostic Microbiology*, pages 312–324. Mosby, St. Louis, 11th edition, 2002.

[37] K. E. Nelson. Emerging and new infectious diseases. In K. E. Nelson and C. F. Masters Williams, editors, *Infectious Disease Epidemiology: Theory and Practice*, chapter 13, pages 420–429. Jones and Bartlett Publishers, Massachusettes, 2nd edition, 2007.

[38] J. N. Tournier, A. Quesnel-Hellmann, J. Mathieu, C. Montecucco, W. J. Tang, M. Mock, D. R. Vidal, and P. L. Goossens. Anthrax edema toxin cooperates with lethal toxin to impair cytokine secretion during infection of dendritic cells. *J Immunol*, 174(8):4934–41, 2005.

[39] D. L. Hoover, A. M. Friedlander, L. C. Rogers, I. K. Yoon, R. L. Warren, and A. S. Cross. Anthrax edema toxin differentially regulates lipopolysaccharide-induced monocyte production of tumor necrosis factor alpha and interleukin-6 by increasing intracellular cyclic amp. *Infect Immun*, 62(10):4432–9, 1994.

[40] G. Ruthel, W. J. Ribot, S. Bavari, and T. A. Hoover. Time-lapse confocal imaging of development of bacillus anthracis in macrophages. *J Infect Dis*, 189(7):1313–6, 2004.

[41] R. C. Spencer. Bacillus anthracis. *J Clin Pathol*, 56(3):182–7, 2003.

[42] T. V. Inglesby, T. O'Toole, D. A. Henderson, J. G. Bartlett, M. S. Ascher, E. Eitzen, A. M. Friedlander, J. Gerberding, J. Hauer, J. Hughes, J. McDade, M. T. Osterholm, G. Parker, T. M. Perl, P. K. Russell, and K. Tonat. Anthrax as a biological weapon, 2002: updated recommendations for management. *JAMA*, 287(17):2236–52, 2002.

[43] R. B. Aylward. Poliomyelitis, acute. In D. L. Heymann, editor, *Control of communicable diseases manual : an official report of the American Public Health Association*, pages 484–491. American Public Health Association, 19th edition, 2008.

[44] A. Rzezutka and N. Cook. Survival of human enteric viruses in the environment and food. *FEMS Microbiol Rev*, 28(4):441–53, 2004.

[45] (World Health Organization) W.H.O. Polio global eradication initiative. http://www.polioeradication.org/, 2012.

[46] O. Kew. Reaching the last one per cent: progress and challenges in global polio eradication. *Curr Opin Virol*, 2(2):188–98, 2012.

[47] R. Trivello, G. Farisano, C. Bonello, M. E. Moschen, V. Baldo, S. Majori, G. Moretti, V. Marin, L. Piron, and G. Renzulli. Immunity status to poliovirus in veneto region (north-east italy). a seroepidemiological survey. *Ann Clin Lab Sci*, 24(6):542–7, 1994.

[48] N. C. Grassly, H. Jafari, S. Bahl, S. Durrani, J. Wenger, R. W. Sutter, and R. B. Aylward. Mucosal immunity after vaccination with monovalent and trivalent oral poliovirus vaccine in india. *J Infect Dis*, 200(5):794–801, 2009.

[49] J. L. Henry, E. S. Jaikaran, J. R. Davies, A. J. Tomlinson, P. J. Mason, J. M. Barnes, and A. J. Beale. A study of poliovaccination in infancy: excretion following challenge with live virus by children given killed or living poliovaccine. *J Hyg (Lond)*, 64(1):105–20, 1966.

[50] L. Roberts. The polio emergency. *Science*, 337(6094):514–516, 2012.

[51] H. Yahya. Change in pattern of skin disease in kaduna, north-central nigeria. *Int J Dermatol*, 46(9):936–43, 2007.

[52] S. Wassilak and W. Orenstein. Challenges faced by the global polio eradication initiative. *Expert Rev Vaccines*, 9(5):447–9, 2010.

[53] H. J. Larson and P. Paterson. Eradicating polio: persisting challenges beyond endemic countries. *Expert Rev Vaccines*, 10(12):1635–6, 2011.

[54] M. Angez, S. Shaukat, M. M. Alam, S. Sharif, A. Khurshid, and S. S. Zaidi. Genetic relationships and epidemiological links between wild type 1 poliovirus isolates in pakistan and afghanistan. *Virol J*, 9:51, 2012.

[55] P. S. Brachman, A. F. Kaufman, and F. G. Dalldorf. Industrial inhalation anthrax. *Bacteriol Rev*, 30(3):646–59, 1966.

[56] D. Vasconcelos, R. Barnewall, M. Babin, R. Hunt, J. Estep, C. Nielsen, R. Carnes, and J. Carney. Pathology of inhalation anthrax in cynomolgus monkeys (macaca fascicularis). *Lab Invest*, 83(8):1201–9, 2003.

[57] G. G. Meynell and E. W. Meynell. The growth of micro-organisms in vivo with particular reference to the relation between dose and latent period. *J Hyg (Lond)*, 56(3):323–46, 1958.

[58] R. Brookmeyer, E. Johnson, and S. Barry. Modelling the incubation period of anthrax. *Stat Med*, 24(4):531–42, 2005.

[59] C. Guidi-Rontani. The alveolar macrophage: the trojan horse of bacillus anthracis. *Trends in Microbiology*, 10(9):405 – 409, 2002.

[60] S. N. Radyuk, P. A. Mericko, T. G. Popova, E. Grene, and K. Alibek. In vitro-generated respiratory mucosa: a new tool to study inhalational anthrax. *Biochemical and Biophysical Research Communications*, 305(3):624 – 632, 2003.

[61] D. He, E. L. Ionides, and A. A. King. Plug-and-play inference for disease dynamics: measles in large and small populations as a case study. *J R Soc Interface*, 7(43):271–83, 2010.

[62] C. N. Haas. On the risk of mortality to primates exposed to anthrax spores. *Risk Anal*, 22(2):189–93, 2002. Haas, Charles N United States Risk analysis : an official publication of the Society for Risk Analysis Risk Anal. 2002 Apr;22(2):189-93.

[63] D. A. Wilkening. Sverdlovsk revisited: modeling human inhalation anthrax. *Proc Natl Acad Sci U S A*, 103(20):7589–94, 2006.

[64] T. P. Weber and N. I. Stilianakis. Inactivation of influenza a viruses in the environment and modes of transmission: a critical review. *J Infect*, 57(5):361–73, 2008. Weber, Thomas P Stilianakis, Nikolaos I Review England The Journal of infection J Infect. 2008 Nov;57(5):361-73. Epub 2008 Oct 9.

[65] B. T. Mayer, J. S. Koopman, E. L. Ionides, J. M. Pujol, and J. N. S. Eisenberg. A dynamic dose-response model to account for exposure patterns in risk assessment: a case study in inhalation anthrax. *J R Soc Interface*, 8(57):506–17, 2011.

[66] J. W. Bass, S. B. Halstead, G. W. Fischer, J. K. Podgore, and R. A. Wiebe. Oral polio vaccine. effect of booster vaccination one to 14 years after primary series. *JAMA*, 239(21):2252–5, 1978.

[67] M. A. Conyn-Van Spaendonck, H. E. de Melker, F. Abbink, N. Elzinga-Gholizadea, T. G. Kimman, and T. van Loon. Immunity to poliomyelitis in the netherlands. *Am J Epidemiol*, 153(3):207–14, 2001.

[68] M. S. Green, R. Handsher, D. Cohen, J. L. Melnick, R. Slepon, E. Mendelsohn, and Y. L. Danon. Age differences in immunity against wild and vaccine strains of poliovirus prior to the 1988 outbreak in israel and response to booster immunization. *Vaccine*, 11(1):75–81, 1993.

[69] K. Lapinleimu and M. Stenvik. Experiences with polio vaccination and herd immunity in finland. *Dev Biol Stand*, 47:241–6, 1981.

[70] S. Majori, V. Baldo, A. Poli, M. Riolfatti, F. Alborino, C. Bonello, S. Frau, T. Baldovin, A. Dal Zotto, G. Romano, and R. Trivello. Immunity to poliovirus among children and the elderly in north-east italy. *J Prev Med Hyg*, 47(1):12–5, 2006.

[71] J. R. Murph, C. Grose, P. McAndrew, C. Mickiewicz, S. Mento, F. Cano, L. Radick, M. Ritchey, and M. G. Stout. Sabin inactivated trivalent poliovirus vaccine: first clinical trial and seroimmunity survey. *Pediatr Infect Dis J*, 7(11):760–5, 1988.

[72] O. Nishio, Y. Ishihara, K. Sakae, Y. Nonomura, A. Kuno, S. Yasukawa, H. Inoue, K. Miyamura, and R. Kono. The trend of acquired immunity with live poliovirus vaccine and the effect of revaccination: follow-up of vaccinees for ten years. *J Biol Stand*, 12(1):1–10, 1984.

[73] B. D. Schoub, N. K. Blackburn, and J. M. McAnerney. Seroprevalence to polio in personnel at a virology institute. *J Infect*, 43(2):128–31, 2001.

[74] S. V. Nates, L. C. Martinez, P. A. Barril, L. J. Ferreyra, M. O. Giordano, G. Masachessi, and M. B. Isa. Long-lasting poliovirus-neutralizing antibodies among argentinean population immunized with four or five oral polio vaccine doses 1 month to 19 years previously. *Viral Immunol*, 20(1):3–10, 2007.

[75] W. E. Rousseau, G. R. Noble, G. E. Tegtmeier, M. C. Jordan, and T. D. Chin. Persistence of poliovirus neutralizing antibodies eight years after immunization with live, attenuated-virus vaccine. *N Engl J Med*, 289(25):1357–9, 1973.

[76] R. W. Sutter, A. J. Suleiman, P. Malankar, S. Al-Khusaiby, F. Mehta, G. B. Clements, M. A. Pallansch, and S. E. Robertson. Trial of a supplemental dose of four poliovirus vaccines. *N Engl J Med*, 343(11):767–73, 2000.

[77] J. P. Alexander Jr., H. E. Gary Jr., and M. A. Pallansch. Duration of poliovirus excretion and its implications for acute flaccid paralysis surveillance: a review of the literature. *J Infect Dis*, 175 Suppl 1:S176–82, 1997.

[78] T. A. Swartz, M. S. Green, R. Handscher, D. Sofer, M. Cohen-Dar, T. Shohat, S. Habib, E. Barak, Z. Dror, E. Somekh, T. Peled-Leviathan, R. Yulzari, A. Libling, E. Mendelson, and L. M. Shulman. Intestinal immunity following a combined enhanced inactivated polio vaccine/oral polio vaccine programme in israel. *Vaccine*, 26(8):1083–90, 2008.

[79] A. M. Buisman, F. Abbink, R. M. Schepp, J. A. Sonsma, T. Herremans, and T. G. Kimman. Preexisting poliovirus-specific iga in the circulation correlates with protection against virus excretion in the elderly. *J Infect Dis*, 197(5):698–706, 2008.

[80] N. C. Grassly, H. Jafari, S. Bahl, S. Durrani, J. Wenger, R. W. Sutter, and R. Bruce Aylward. Asymptomatic wild-type poliovirus infection in india among children with previous oral poliovirus vaccination. *J Infect Dis*, 201(10):1535–43, 2010.

[81] D. Schenzle. An age-structured model of pre- and post-vaccination measles transmission. *IMA J Math Appl Med Biol*, 1(2):169–91, 1984.

[82] P. Rohani, X. Zhong, and A. A. King. Contact network structure explains the changing epidemiology of pertussis. *Science*, 330(6006):982–5, 2010.

[83] H. Okayasu, R. W. Sutter, C. Czerkinsky, and P. L. Ogra. Mucosal immunity and poliovirus vaccines: impact on wild poliovirus infection and transmission. *Vaccine*, 29(46):8205–14, 2011.

[84] T.M.P.T. Herremans, J.H.J. Reimerink, A.M. Buisman, T.G. Kimman, and M.P.G. Koopmans. Induction of mucosal immunity by inactivated poliovirus vaccine is dependent on previous mucosal contact with live virus. *The Journal of Immunology*, 162(8):5011–5018, 1999.

[85] R. J. D. Tebbens, M. A. Pallansch, O. M. Kew, V. M. Caceres, R. W. Sutter, and K. M. Thompson. A dynamic model of poliomyelitis outbreaks: Learning from the past to help inform the future. *American Journal of Epidemiology*, 162(4):358–372, 2005.

[86] B. T. Mayer, J. N. S. Eisenberg, C. J. Henry, M. G. M. Gomes, E. L. Ionides, and J. S. Koopman. Successes and shortcomings of polio eradication: A transmission modeling analysis. *Am J Epidemiol*, In Press:DOI:10.1093/aje/kws378, September 2012.

[87] N. Nathanson and O. M. Kew. From emergence to eradication: the epidemiology of poliomyelitis deconstructed. *Am J Epidemiol*, 172(11):1213–29, 2010.

[88] K. Koser. The migration-displacement nexus and security in afghanistan. In Khalid Koser and Susan Martin, editors, *The Migration-Displacement Nexus: Patterns, Processes, and Policies*, volume 32 of *Studies in forced migration*, pages 131–144. Berghahn Books, 2011.

[89] L.O. Ikuteyijo. Illegal migration and policy challenges in nigeria. *Centre for International Governance Innovation (CIGI)*, 2012.

[90] A. Hasan. Migration, small towns and social transformations in pakistan. *Environment and Urbanization*, 22(1):33–50, 2010.

[91] United Nations. World population prospects: The 2010 revision. `http://data.un.org/Data.aspx?d=PopDiv&f=variableID%3A85`, 2011.

[92] J.G. Cooke and F. Tahir. Polio in nigeria: The race to eradication. 2012.

[93] S. S. Issa, G. Desmond, and F. Ross-Sheriff. Pakistan: Refugee history and policies of pakistan: An afghan case study. In Uma A. Segal, Doreen Elliot, and Nazneen S. Mayadas, editors, *Immigration Worldwide: Policies, Practices, and Trends*, pages 171–188. Oxford University Press, Inc., Oxford, 2010.

[94] N. Saikia, D. Jasilionis, F. Ram, and V. M. Shkolnikov. Trends in geographical mortality differentials in india. *MPIDR Working Papers*, (WP-2009-013), 2009.